CONTENTS.

SECTION 1 - KINETICS AND MECHANISM OF HYDROCHLORINATION OF THE SURFACE OF RUBBER LATEX PARTICLES.

ProQuest LLC.
789 East Eisenhower Parkway
P.O. Box 1346
Ann Arbor, MI 48106 – 1346

STUDIES ON THE HYDROCHLORINATION OF RUBBER LATEX.

by Thomas Carbarns B.Sc., A.R.I.C.

Being a thesis submitted to Glasgow University in accordance with the regulations governing the award of the degree of Doctor of Philosophy in the Faculty of Science.

Technical Chemistry Department,
Royal College of Science and Technology,
GLASGOW, C.1.

November, 1956.

SECTION 1. TABLES.

SECTION 2. TABLES.

SECTION 3. TABLES.

SECTION 1. FIGURES.

SECTION 2. FIGURES.

SECTION 3. FIGURES.

---------ooOoo---------

ACKNOWLEDGEMENTS.

The author acknowledges the invaluable guidance of Dr. M. Gordon in matters both practical and theoretical connected with this work, and the assistance of Professor P. D. Ritchie by continual interest and encouragement. Thanks are also due to numerous members of the staff of the Technical Chemistry Department, Royal College of Science and Technology, Glasgow, for services rendered.

PUBLICATION.

Part of the work described in this thesis is published in the Journal of the Chemical Society, 1956, 3298.

SECTION 1.

KINETICS AND MECHANISM OF HYDROCHLORINATION OF THE SURFACE OF RUBBER LATEX PARTICLES.

1a. INTRODUCTION.

The Development of Acid-Stable Rubber Latices. - The preparation of rubber hydrochloride consists in the progressive saturation of individual isoprene units in rubber with HCl:

$$-CH_2.CMe{:}CH.CH_2- \xrightarrow[HCl]{} -CH_2.CMeCl.CH_2.CH_2-$$

The reaction was originally carried out (1, 2) in solution in organic solvents, or by suspending solid rubber in liquid or gaseous HCl. The addition of the reactant to highly dispersed rubber latex was not feasible until the development of suitable stabilising agents, since the colloidal particles are readily coagulated by minimal amounts of acid.

Blow (3) reported the first acid-stable rubber latex, made by using a cationic soap. A similar result was obtained by Hassels (4) using a non-ionic emulsify-

ing agent; and van Veersen (5) announced a fundamentally new process for the manufacture of rubber hydrochloride using these developments. Gaseous HCl passed through the latex, stabilised with a cationic or non-ionic emulsifying agent, is rapidly absorbed into the aqueous serum and becomes available for reaction. The reaction rate is relatively slow (< 4 mole%/hr.) at 1 atm. HCl pressure and normal temperatures, but is increased at higher pressures and lower temperatures. A small intercept on the composition axis of the plot of mole percent conversion against reaction time was not acknowledged until a more accurate experimental technique was introduced.

Kinetics of Hydrochlorination of Rubber. - Using a new micro-technique on acid-stabilised rubber latices, Gordon and Taylor (6) established the form of the kinetic rate curve for hydrochlorination. A number of features are evident: *

(a) A small initial jump (2.5 mole %) corresponding to a rapid hydrochlorination of this percentage of units.

(b) A slow linear (zero-order) portion (slope k_1) followed by a sharp kink.

* for example see Figure 10 of this work.

(c) A fast linear (zero-order) portion (slope K_2) covering 60% of the reaction.

(d) A rapid decrease in reaction rate around 85 mole % hydrochlorination (maximum conversion: 93.5 mole %).

By the experimental method described, the kinetics are reproducible and free from uncontrolled effects.

Fast Bulk Locus Hydrochlorination. - Despite the notable change in substrate from natural to synthetic polyisoprene, nearly identical zero-order rate constants apply to both types. The slow zero-order rate, however, is absent from the synthetic polyisoprene rate curve, and the initial jump (P) is larger (cf. Table 1) and variable from one synthetic latex to another.

It follows that the rate-controlling step in hydrochlorination is independent of the polymer substrate, and that k_2 represents the normal (bulk locus) kinetics of the reaction. The initial jump was identified as a surface reaction controlled by diffusion of the reactant into the (spherical) rubber latex particles.

The constancy of the bulk locus rate k_2 between 20 and 80 % hydrochlorination shows that the rate controlling step remains unaffected by changes in the reaction

medium (particularly in the dielectric constant) as the substrate progressively alters towards the hydrochloride. There is, then, no nett charge on the transition state giving rise to the reactive species.

Reactant concentration and energetic factors suggested that the rate-controlling step is the formation of an uncharged, but not covalent, form of HCl, which is immediately captured by neighbouring unreacted isoprenic double bonds. The evidence indicated the creation of an "ion pair" from solvated ions:

$$(H_2Cl)^+ + Cl^- \longrightarrow (H_2Cl^+ . Cl^-) \quad .... 1$$

This species is familiar in media of low dielectric constant.

Slow Bulk Locus Hydrochlorination. - Kinetic evidence (7) shows that an unidentified trace substance, occuring in natural latex particles only, retards the hydrochlorination reaction k_1, before the full rate k_2 is attained. The retarder deactivates a constant weight of ion pair $(H_2Cl^+ . Cl^-)$ irrespective of temperature, HCl pressure, or reaction rate. In six kinetic runs, in which these factors were varied, the fast bulk locus (k_2) extrapolated

to the composition axis at a constant value (-27 ± 3 mole %). The total retardation (k_1) is, therefore, equivalent to a fixed proportion (27 %) of the isoprene units present.

Surface Locus Hydrochlorination. - In the aqueous phase surrounding the rubber particles (synthetic and natural), ion pairs are at a much higher concentration than inside. Penetration of the species at the particle surface accounts for the rapid hydrochlorination which is reflected as an initial jump (P) in the rate curve.

Crampsey, Gordon, and Sharpe (8) have compared P with measurements on the electron microscope of the average particle diameter D (unshadowed) or D' (shadowed):

Table 1.

Latex	P	D, Å	D', Å	τ, Å	τ', Å
Natural	2.0	4500	-	15.0	-
Latex I	6.25	1175	1400	12.5	14.7
Latex II	20.0	467	700	17.0	24.9
Latex III	15.0	670	-	15.0	-
Latex V	22.0	460	-	17.4	-

The particle diameter D is averaged thus:

$$D = \left[\left(\sum_i D_i^2 \right) / n \right]^{\frac{1}{2}} \quad \ldots\ 2$$

The thickness τ of the outer shell of a sphere of diameter D, comprising P% by volume of the sphere, is given by:

$$\tau = D \left[1 - 0.2155(100 - P)^{1/3} \right] /2 \quad \ldots\ 3$$

The measurements (Table 1) confirm that electron microscope values of D require correction by a constant amount because of aberration effects when using gold/palladium alloy for shadow-casting:

$$D' = D + 230 \text{ Å} \quad \ldots\ 4$$

Values of are constant at 15 ± 2.5 Å, confirming that P represents the reaction of isoprene units privileged by their nearness to the particle surface.

The surface locus reaction in Latices III and V was isolated kinetically (9) at low (0.33 atm. or less) HCl pressure. The kinetic curve is of high reaction order and the reaction becomes immeasurably slow after P% hydrochlorination. Since polyisoprene chains, pictured as lying parallel to the particle surface, are spaced at 5 Å intervals (10), the surface reaction is equivalent to about three molecular layers.

1b. SUMMARY.

A technique described by earlier workers (6) is used to follow the kinetics of hydrochlorination of several natural and synthetic polyisoprene latices by means of density measurements. The main purpose is to study the mechanism of the particle surface locus reaction involving an outer skin of about three molecular layers of polymer. A theoretical mechanism proposed by Gordon (11) is successfully fitted to the experimental data. The mechanism treats the double bonds of the polymer as fixed on a pseudo-lattice, and considers a reactive species such as a solvated ion pair ($H_2Cl^+ . Cl^-$) to diffuse inwards across the particle surface to react with these bonds.

The reagent has an exceedingly low equilibrium concentration in the aqueous phase surrounding the polymer particle ($\sim 10^{-13}$ mole/l.); inside the non-polar polymer it has a short life-time ($\sim 10^{-19}$ sec.) after which it

reverts to inactive covalent HCl, unless it finds a double bond as reaction partner or diffuses back into the aqueous phase.

This generalised Hill-Hermans mechanism of diffusion-reaction accomodates well the kinetic effects observed when the pressure of HCl, the temperature, or the particle size of the latex are varied. A specially fine synthetic polyisoprene latex (Latex V1) of average particle diameter ~180 Å was prepared for these studies, in which half the particle mass was accessible to the surface locus mechanism. The small effect on the surface and bulk locus rates of admixture of sulphuric acid with the aqueous phase has been investigated. The study of bulk locus kinetics has been extended to include runs at $1\frac{1}{2}$ and $2\frac{1}{2}$ atm. HCl pressure on natural latex.

-----oOo-----

1c. EXPERIMENTAL.

Previous work (12) has shown that synthetic polyisoprene latices can be smoothly prepared from monomeric isoprene (b.p. 34.5-35.5°C), ammonium persulphate (catalyst), Vulcastab LW * (emulsifier), and distilled water as dispersion medium. Reaction conditions, favourable to the preparation of fine particles in emulsion polymerisation (13, 14), were adopted here to produce a new synthetic latex (cf. Table 2, Latex VI). As a comparison, the reaction conditions for the four synthetic polyisoprene latices recorded to date are included in Table 2. The present work has shown that a balance must be struck between the desired particle size and the reaction temperature, since overheating (above about 65°C) leads to flocculation.

* A non-ionic emulsion stabiliser of the ethylene oxide condensation type.

Table 2.

Preparation of Synthetic Polyisoprene Latices.

Latex	Monomer g.	Catalyst g.	Vulcastab LW* ml.	Water g.	Time hr.	Temp. °C	D
I	3.5	0.075	1.5	1.5	19.0	60	1400 Å
II	4.0	0.085	1.5	5.0	4.5	57	700
V	10.0	0.250	4.0	15.0	9.5	49	460
VI	1.4	0.050	4.0	20.0	2.0	60	180

* As a 20% aqueous solution.

A considerable reduction in particle size (50% from Latex V to Latex VI) was obtained by:

(a) High catalyst concentration.

(b) Short reaction time.

(c) High temperature.

(d) High emulsifier concentration.

(e) Rapid stirring.

The decrease in average particle diameter D is accompanied by a progressive change in the appearance of the latex, from white and opaque to bluish and translucent. Polystyrene latices (D = 1300-3000 Å) prepared by Harkins (14)

were of the former type.

The reaction mixture (Latex VI, Table 2) was sealed under CO_2 in a Pyrex glass ampoule and agitated at 60°C by continuous revolution. After the stated time, the ampoule was broken and further polymerisation arrested by removal of excess monomer in a stream of CO_2 under slight vacuum and gentle heat (40°C). Under similar conditions the volume was reduced by half by removal of water. A small quantity of rubbery coagulum was removed by filtration through fine glass cloth. Further purification was deemed unnecessary (12).

Preparation of Acid-Stable Natural Rubber Latices. - Dunlop 60% natural rubber latex (100 ml.) was freed from ammonia by bubbling with nitrogen (4 hr.) from a cylinder. The total solids content rose to 64%; and on this basis the following acid-stable (20% H_2SO_4) latex was prepared:

Latex 8	Ammonia-free (64%) latex	....	50.0 g.
	20% Vulcastab LW soln.	....	1.0 ml.
	Sulphuric acid (98%)	....	4.9 g.

The ingredients were mixed in the order given, with rapid stirring to avoid coagulation by localised concentration

of acid. Latices 4 and 9 were prepared similarly, using 54 ml. of concentrated hydrochloric acid (i.e. equal volumes of acid and latex) in place of sulphuric acid.

Micro-Reactor for Hydrochlorination of Acid-Stable Rubber Latices. - The apparatus (Fig. 1) and procedure adopted for kinetic measurements on synthetic Latices V and Vl and natural Latices 4, 8, and 9 were those originally developed by Gordon and Taylor (6). The characteristics of the method are: (a) rapid starting and stopping of the reaction, (b) avoidance of frothing, and (c) elimination of zero-time uncertainties.

The pressure of HCl gas is accurately governed by the mercury head in the manometer (A) which is interconnected with the trident (B) and the generator (C) (at a-a, b-b, etc.) by thick-walled Polythene tubing which is unaffected by the reactant. Pressure-tight seals are provided by glass/fused Polythene joints. Stop-cocks and ground glass joints are greased with Diapiezon. The generation of HCl gas (from H_2SO_4 + NaCl) is controlled by the stop-cock in C.

20-40 mg. of latex are introduced into the reaction

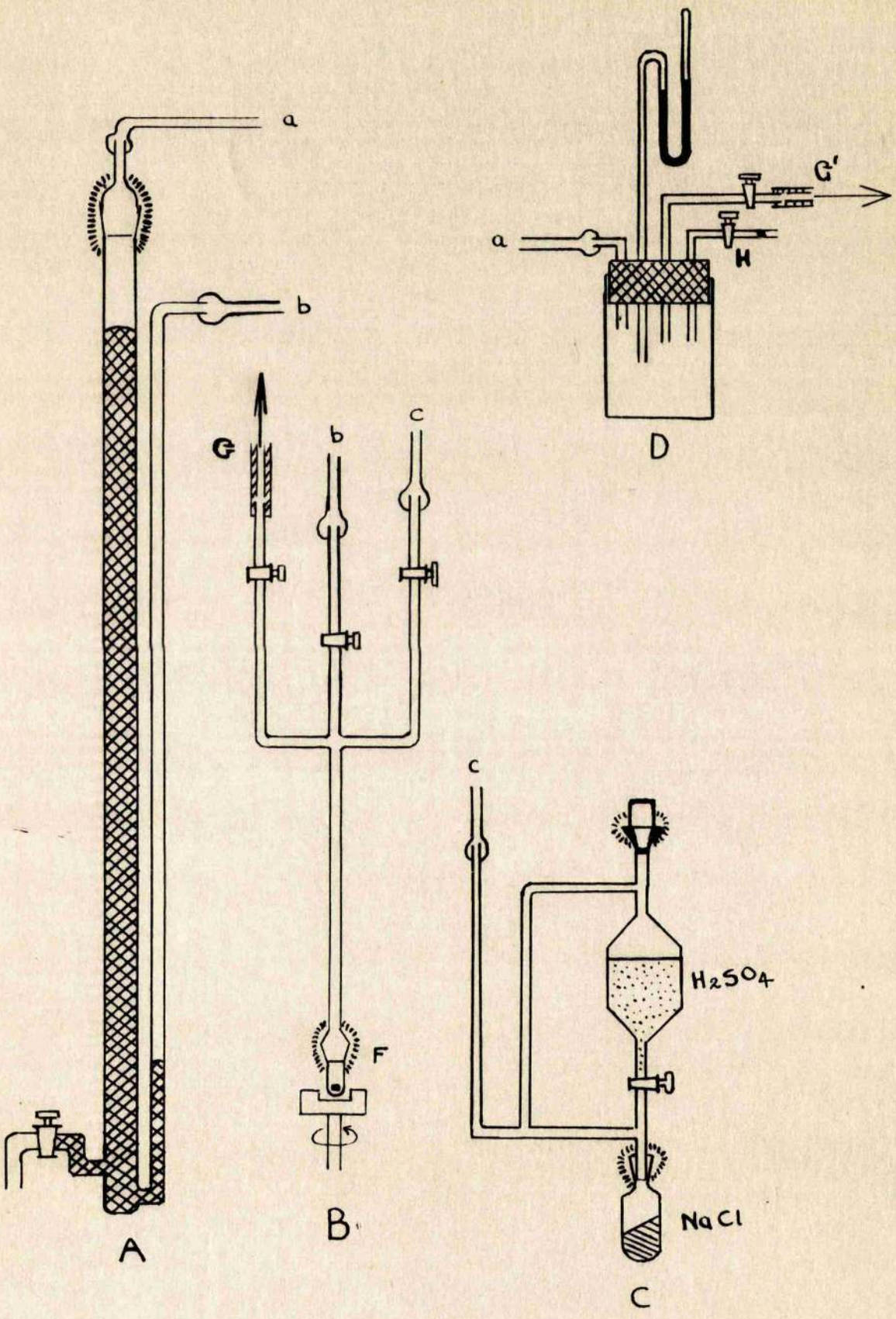

Fig. 1 - Micro-reactor.

flask (F) which is fitted with a glass-sheathed soft-iron stirrer rotated by an external magnet. The latex sample is frozen at -70°C (acetone/Drikold) to prevent solution of HCl; and the whole system is evacuated through G. The stop-cock G is then closed and the apparatus filled with HCl gas to atmospheric pressure and again evacuated. The required pressure (1, 1½, 2, or 2½ atm.) is then generated by building up the mercury level in A. Excess of reactant bubbles away through the manometer, and gas evolution is kept at a slow steady rate to avoid undue disturbance of the mercury column.

The reaction is started by immersing the trident B in the thermostat. The latex melts, is stirred, and becomes saturated with HCl to equilibrium in a few seconds. At the required time, the reaction is stopped by releasing the pressure at G. The latex froths gently in the flask as HCl escapes, and is then transferred by a dropper to 20 ml. of boiling 25/75 acetone/water mixture for immediate flocculation. The polymer is filtered off (Whatman No.1, 1 cm.) and washed 20 times with distilled water. After this purification, the polymer is dried by storage (overnight) under high vacuum in preparation for

density measurement.

For runs with HCl pressure below atmospheric, a refinement (D, Fig. 1) is employed. A fixed quantity (say 5 cm.) of mercury is placed in A for all runs at the same pressure. At the final generation of HCl, the stop-cock G is closed and the pump transferred to D. The pressure inside the flask D, measured on the small manometer, is adjusted by the stop-cock at H which controls the intake of air through a sintered glass plug until:

Working Pressure = Pressure in D + Fixed Height in A

The overall pressure is adjusted roughly at A and finely at D by varying the air intake.

Certain precautions attending the use of the apparatus at 2.5 atm. are outlined in Section 2c.

Composition of Rubber/Rubber Hydrochloride Copolymers. - Gordon and Taylor (6) have shown that density measurements on rubber/rubber hydrochloride copolymers is suitable for the determination of composition. The overall density ranges for maximum conversion are:

(a) Natural rubber (m_2 = 0 to 0.935), d = 0.9040-1.1400.

(b) Latex VI (m_2 = 0 to 1), d = 0.9018-1.1328.

where m_2 = mole fraction of hydrochloride.

Calibration plots (cf. Fig.2) for both the natural and the synthetic copolymers (6, 12) have been used for the present work. The initial density of natural rubber from two separate batches was constant at 0.9040 g./ml. Copolymer composition (wt.% hydrochlorination W) was interpolated in the "natural" line of Fig.2, which follows the relationship:

$$V = 1.106 - 0.0023W \quad \ldots\ 5$$

where V = specific volume of copolymer. Beyond W = 65 there is a deviation due to crystallisation of the hydrochloride.(12, 15).

In contrast, the initial densities of the present series of synthetic polyisoprenes vary over relatively wide limits (cf. Table 3).

Table 3.

Initial Densities of Synthetic Polyisoprenes.

Latex	I	II	V	VI
Initial density	0.9042	0.9105	0.9057	0.9018
Specific volume	1.1059	1.0983	1.1041	1.1089

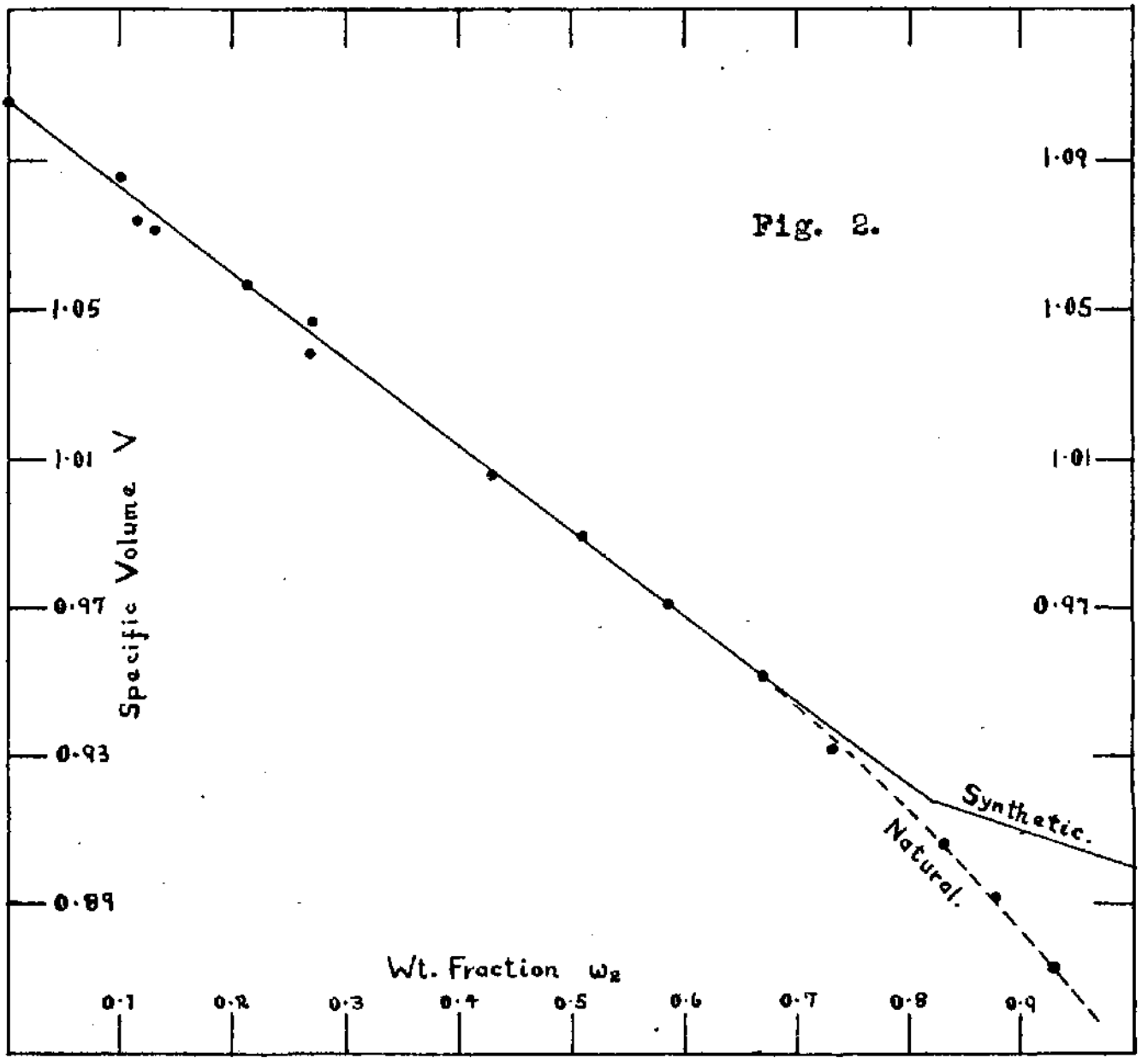

Fig. 2 - Calibration plots for natural and synthetic polyisoprene. Data taken from Gordon and Taylor (6, 12).

• - Natural.
——— - Synthetic.
- - - - - - Natural (divergence due to crystallisation).

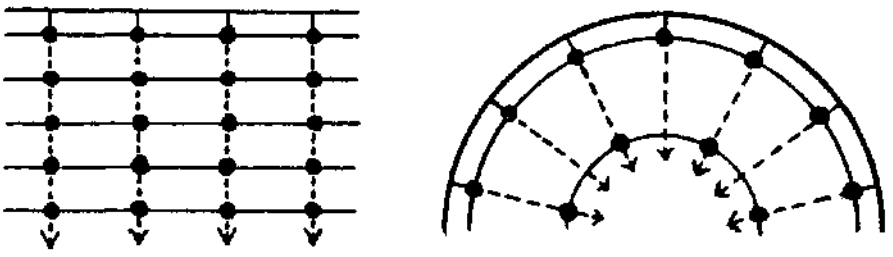

Fig. 11a - Convergence of flow lines.

The main linear portion of the calibration plot for synthetic polyisoprenes (Fig.2) is based on Latex I and is almost identical to that for natural rubber:

$$V = 1.106 - 0.00226W \quad \ldots\ 6$$

Since the change in density for complete hydrochlorination of synthetic Latices I, II, V, and VI is constant, equation 6 is written more generally thus:

$$V = V_i - 0.00226W \quad \ldots\ 7$$

where V_i = initial specific volume (cf. Table 3).

Copolymer compositions falling along the second linear portion of the calibration plot can be found from the following general equation:

$$V = (1.021 - dV_i) - 0.00124W \quad \ldots\ 8$$

where $dV_i = 1.106 - V_i$.

The point of coincidence of the two linear portions of this plot is a characteristic of the calibration temperature (here 26.7°C) and is fully explained in Section 3a.

Using the density gradient technique described below, copolymer densities are measurable to 0.001 g./ml. or better (i.e. to 0.3% reaction or less).

Density-Gradient Tube Method for Determination of Copolymer Densities. - Complete coverage of the density ranges involved (cf. page 14) was provided by four dumb-bell shaped density-gradient tubes (6). Bulbs (diam. 8 cm.) act as density buffers thus stabilising the gradient of density formed by interdiffusion of two aqueous solutions in the connecting tube (length 30 cm.; diam. $1\frac{1}{2}$ cm.). Suitable aqueous solutions are available throughout the density range (cf. Table 4).

Table 4.

Composition of Gradient Solutions.

Tube	I	II	III	IV
Range	0.89-0.97	0.97-1.03	1.03-1.11	1.11-1.16
Solute(s)	EtOH	EtOH/ Lactic acid	$Na_2S_2O_3$/ KCl	$Na_2S_2O_3$/ KCl

18 small Pyrex floats * (16) (diam. 2-3 mm.) calibrated to 0.0001 g./ml. were used as density standards (cf. Appendix 1).

* The author's thanks are due to Drs. Gordon and Taylor for the loan of this apparatus.

A sample of dried purified polymer is pressed in steam between two clean microscope slides for $2\frac{1}{2}$ min. A transparent gas-free film is formed and is allowed to cool. Unpressed edges or sections are cut away with a sharp blade and discarded. The remainder is cut into about ten 2-mm. squares and wetted with EtOH or Teepol. In the thermostated (26.7°C) gradient tube, the samples settle in a layer where their density coincides with that of the surrounding solution. An average density is determined by accurately measuring the heights of films and floats with a cathetometer and interpolating as shown by the following example (cf. also Fig.3):

Float*	Density	Height	Film heights.	
II(2)	0.9882	22.68	12.02 12.05	
			12.07 12.15	density: 1.0343
II(3)	1.0006	19.55	12.15 12.17	V = 0.9668
			12.17 12.18	W (from equn. 7)
II(4)	1.0232	14.51	12.21 12.23	= 51.95%
			12.23 12.32	
III(1)	1.0416	10.75	12.32 12.35	
			12.37 12.42	
			Average 12.21	

* cf. Appendix 1.

Example: Latex VI, containing 17.4% H_2SO_4, 249 partial pressure HCl (26.7°C) (cf. Appendix 2d).

The accuracy of the method (0.001 g./ml.) is confirmed

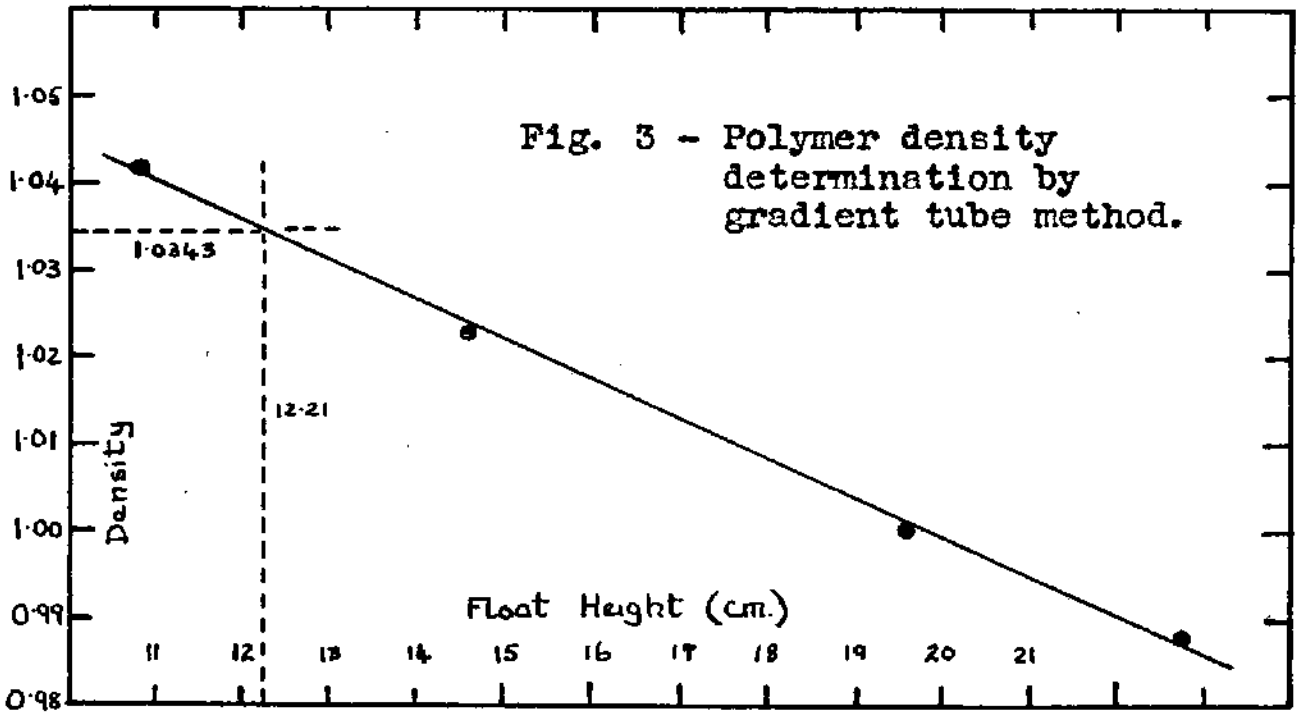

Fig. 3 - Polymer density determination by gradient tube method.

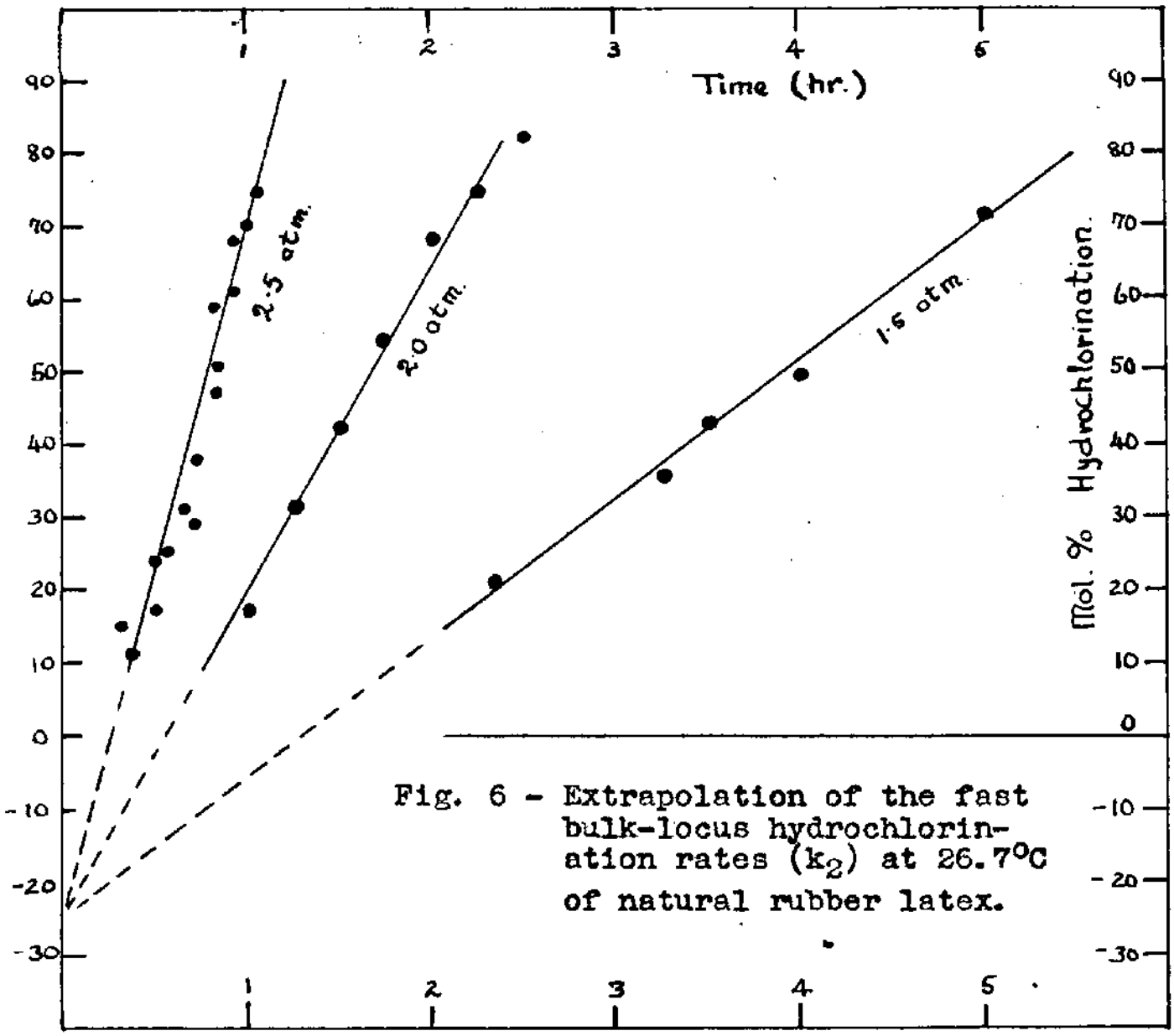

Fig. 6 - Extrapolation of the fast bulk-locus hydrochlorination rates (k_2) at 26.7°C of natural rubber latex.

both by the smoothness of the plot of height versus density (Fig.3) and by the narrow scatter of the film layer.

Kinetic Measurements of Bulk Locus Hydrochlorination in Natural and Synthetic Polyisoprene. - Measurable reaction rates of bulk locus hydrochlorination are associated with HCl pressures of 1 atm. or greater (6). Figure 4 illustrates the bulk hydrochlorination kinetics of one natural and three synthetic (I, II, and VI) latices at 2 atm. (26.7°C) reported to date (cf. Table 5).

Table 5.

Hydrochlorination (2 atm.; 26.7°C) of Latices in Fig.4.

Latex	Reaction rate k_2 mole%/hr.	Initial jump P
I	49.0	6.3
II	56.0	22.0
VI*	54.0	48.5
Natural	15 (retarded)	2.5

* This work.

Fig. 4 - Rate curves for the hydrochlorination of polyisoprene latices at 26.7°C and 2 atm. HCl.

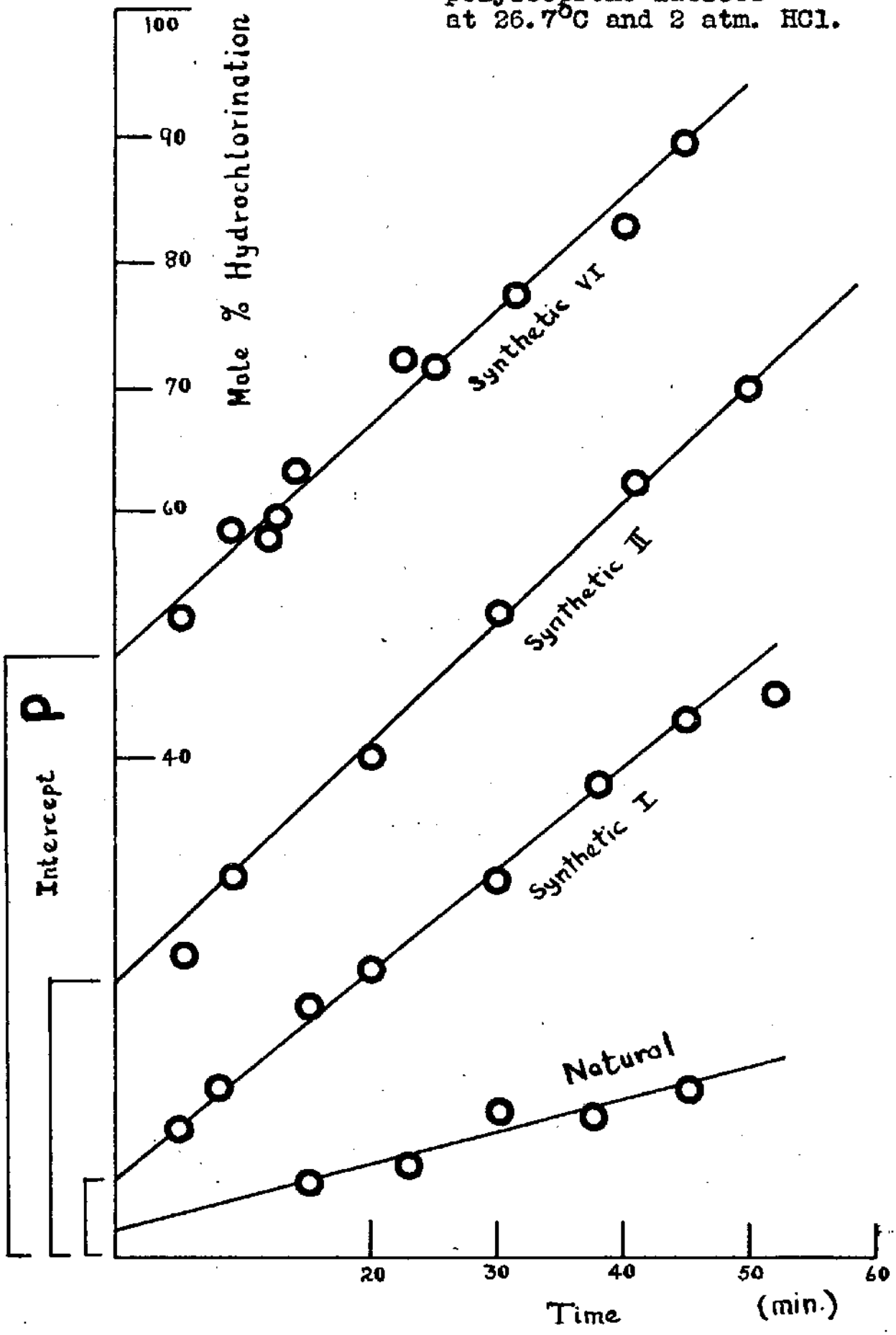

In Figure 5 a comparison is drawn between the bulk locus kinetics (2 atm.; 26.7°C) of natural rubber latex reported by Gordon and Taylor (6) and Latex 8, containing 20% H_2SO_4. on the water + acid content (cf. Table 6 and Appendices 3a and 3b).

Table 6.

Hydrochlorination of Natural Latices in Fig.5.

Latex	k_1 mole%/hr.	k_2 mole%/hr.	P	$M_{max.}$	Extrapol$^{n.}$ of k_2
Natural	15	45.5	2.5	93.5	} -27 mole%
Latex 8*	15	37.5	2.5	86.0	

* This work.

The effect of HCl pressure on the fast bulk locus hydrochlorination rate (k_2) of natural rubber latex at $1\frac{1}{2}$, 2, and $2\frac{1}{2}$ atm. (26.7°C) is illustrated in Fig.6. A plot at 1 atm. (listed in Table 7) is omitted for clarity. Details of the experimental results for Latices 4 and 9 are carried in Appendices 4 and 5.

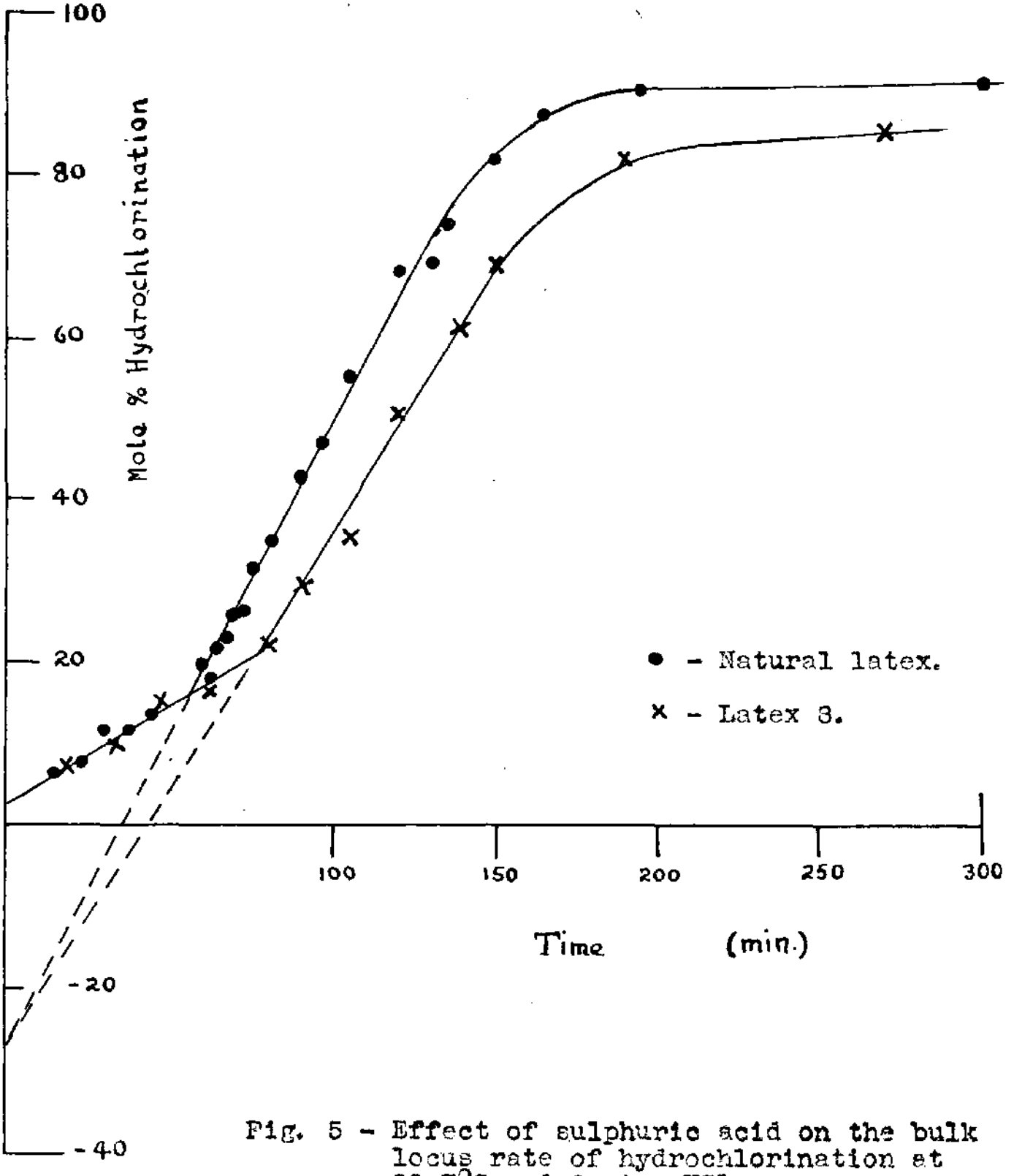

Fig. 5 - Effect of sulphuric acid on the bulk locus rate of hydrochlorination at 26.7°C and 2 atm. HCl.

Table 7.

Unretarded Bulk Hydrochlorination Rates (k_2) of Natural Rubber Latices at 26.7°C (Fig.6).

Latex	k_2 mole%/hr.	Extrapolation	HCl pressure p_1
Natural	5.24		1.0 atm.
Latex 4*	19.50	-27 mole%	1.5
Natural	45.90	± 2.5	2.0
Latex 9*	176.50		2.5

* This work.

The experimental results in Table 7 for two latices (at 1 and 2 atm.) are taken from the work of Gordon and Taylor (6).

Maximum Attainable Conversion. - Using equation 8 the maximum hydrochlorination obtained in the case of Latex VI (2 atm.; 26.7°C; 75 min., cf. Appendix 2e) is calculated as 100.5 mole% (d = 1.1123). This figure represents complete stoichiometric conversion (experimental accuracy 0.5%) and confirms similar observations by Crampsey, Gordon, and Taylor (12) on Latices I and II.

Kinetic Measurements of Surface Locus Hydrochlorination.

A number of kinetic runs have been carried out on samples of Latices V and VI (cf. Appendices 2 and 6) at HCl pressures below 0.33 atm., where the surface locus hydrochlorination rate becomes measurable (9). The refinement to the micro-reactor (D, Fig. 1) was used. The resulting experimental data have been compared in various ways, to be discussed later, in Figs. 7-11. Relevant measurements are contained in Table 8, which also lists results for Latex V (p_1 = 163 mm. and 249 mm. at 26.7°C) found by earlier workers (9):

Table 8.

Hydrochlorination of Latices V and VI (Figs. 7-11).

Latex	HCl pressure p_1	Reaction temp.	Flux rate /m $min.^{-1}$
V	163 mm.	26.7°C	0.30
V	249	26.7	0.67
V*	167	69.9	0.30
VI*	249	26.7	0.67
VI*	57	26.7	0.074
VI*	249 +	26.7	-
VI*	229	44.2	

* This work. + Contains 17.4% H_2SO_4.

Fig. 7 - Theoretical surface locus rate curves (eq. 10) for various reagent stabilities (s).

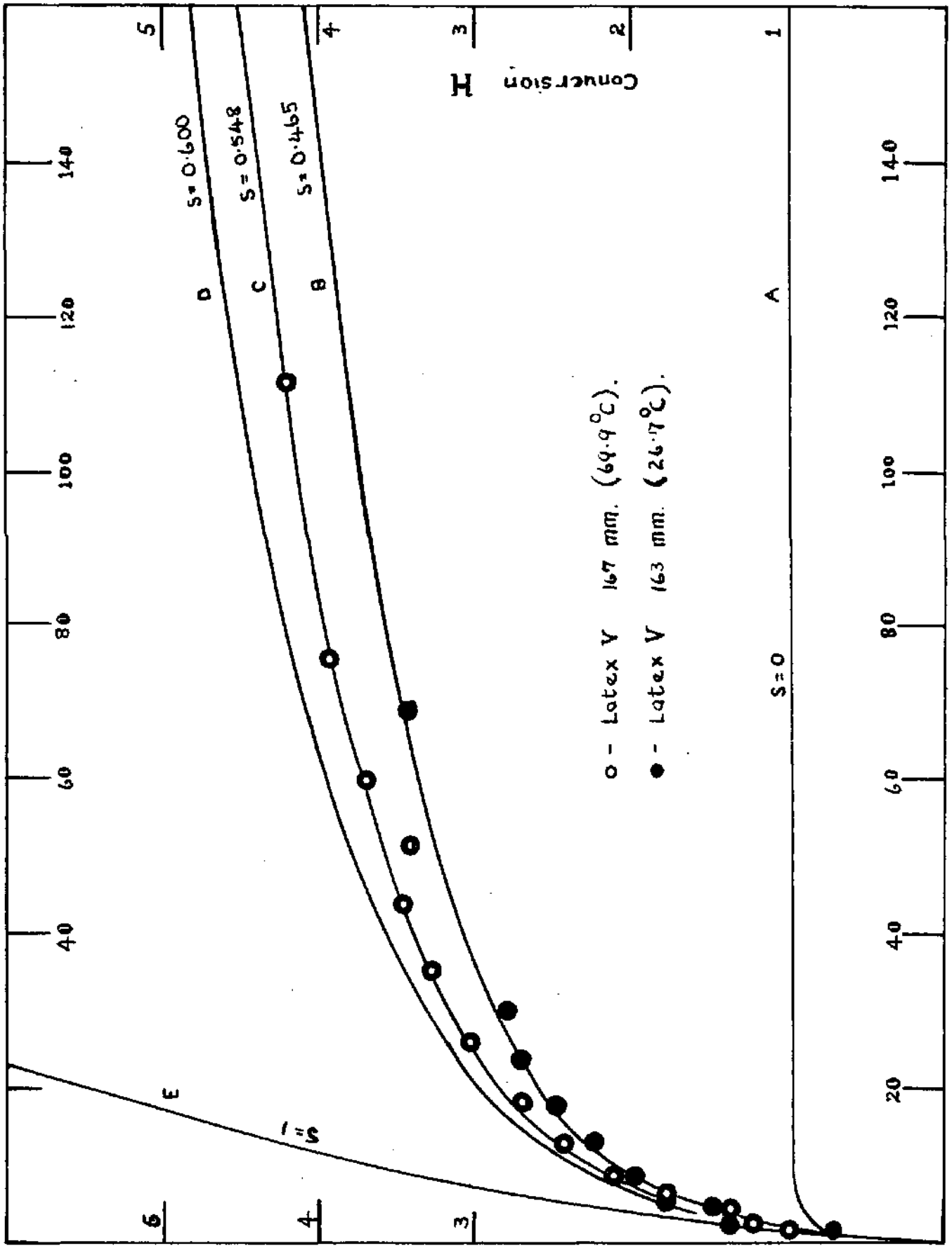

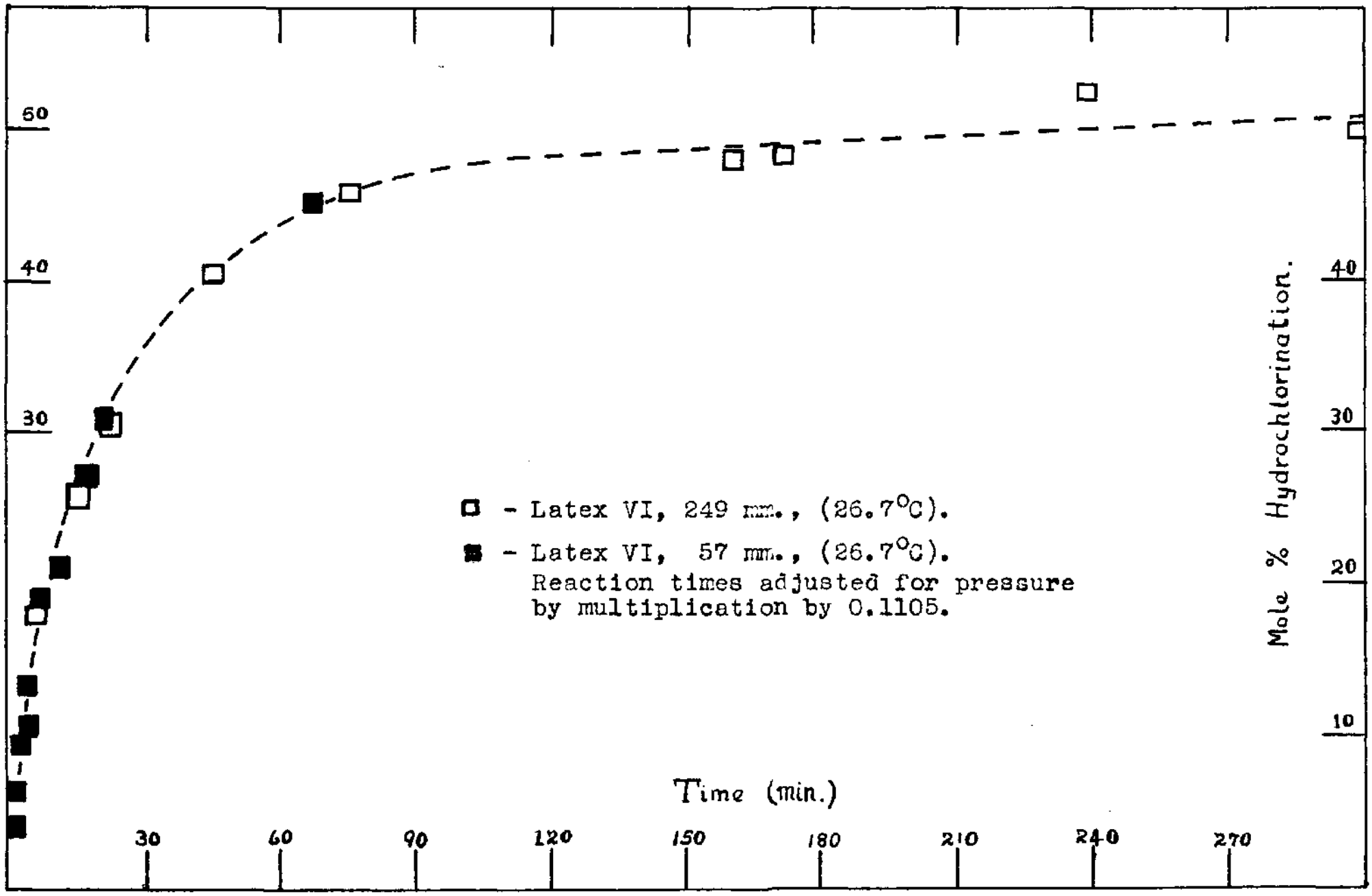

Fig. 8 - Invariance of the shape of the surface locus rate curve with a change in HCl pressure.

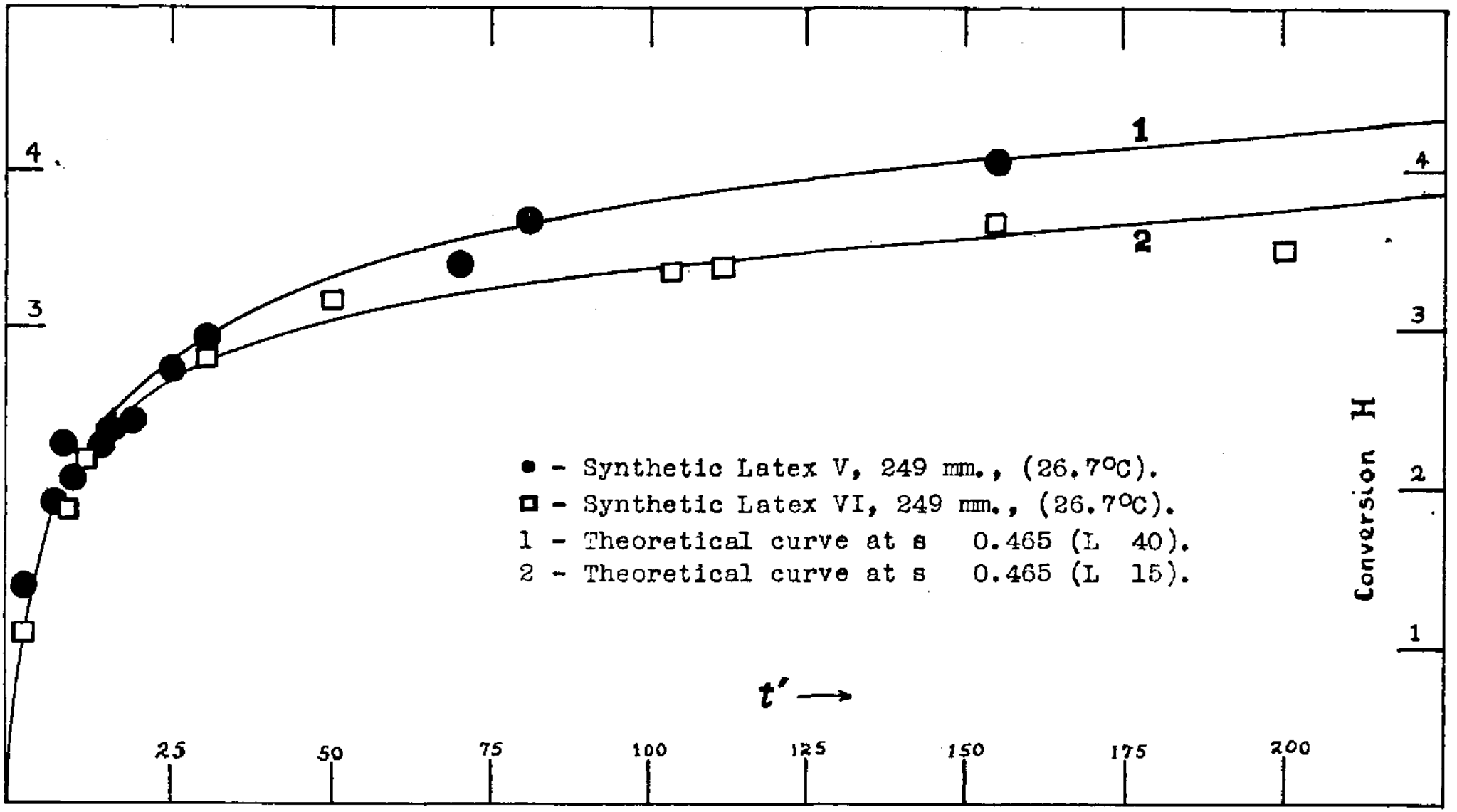

Fig. 9 - Effect of particle curvature on the surface locus rate curve.

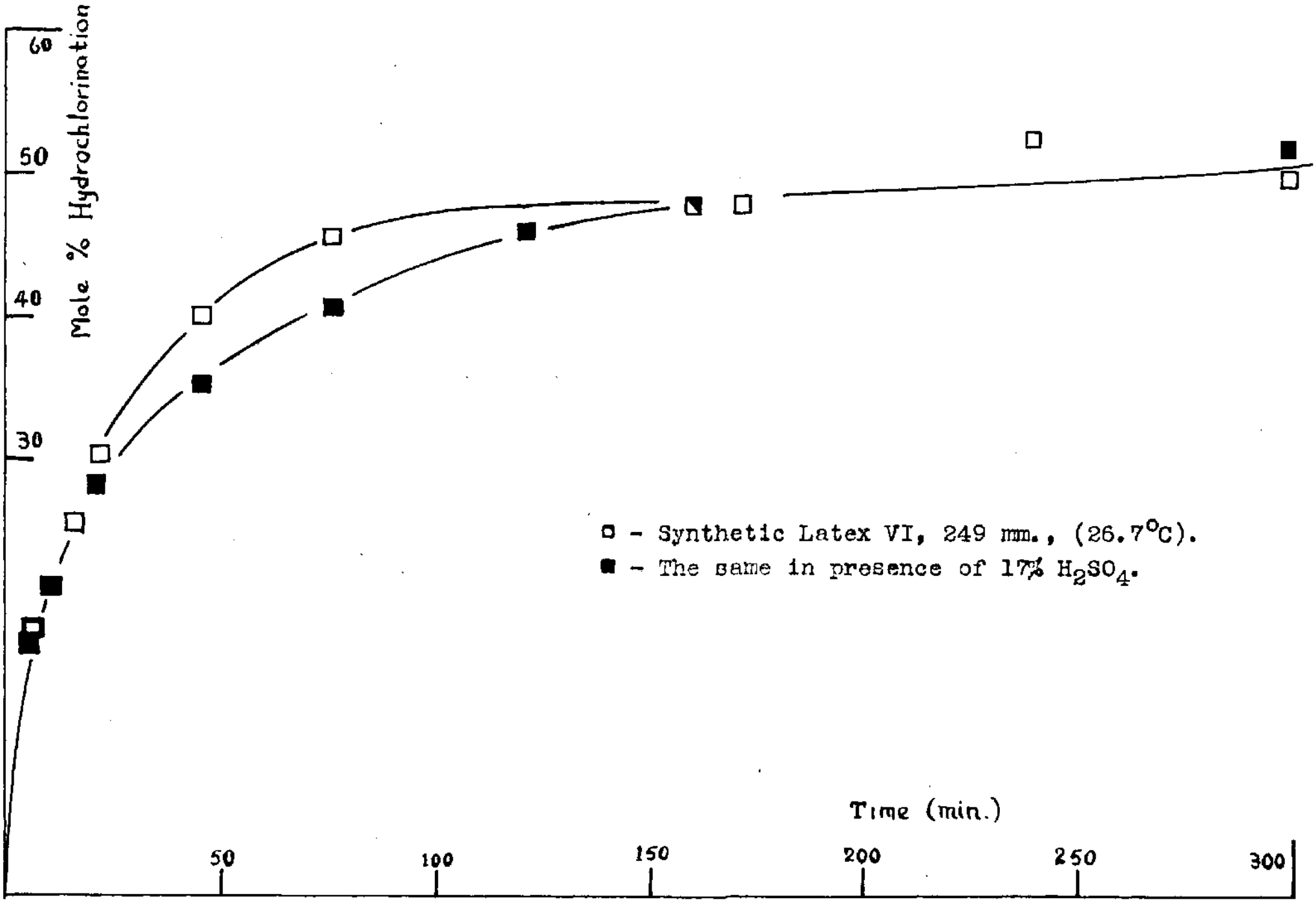

Fig. : 10 - Effect of sulphuric acid on the surface locus hydrochlorination rate.

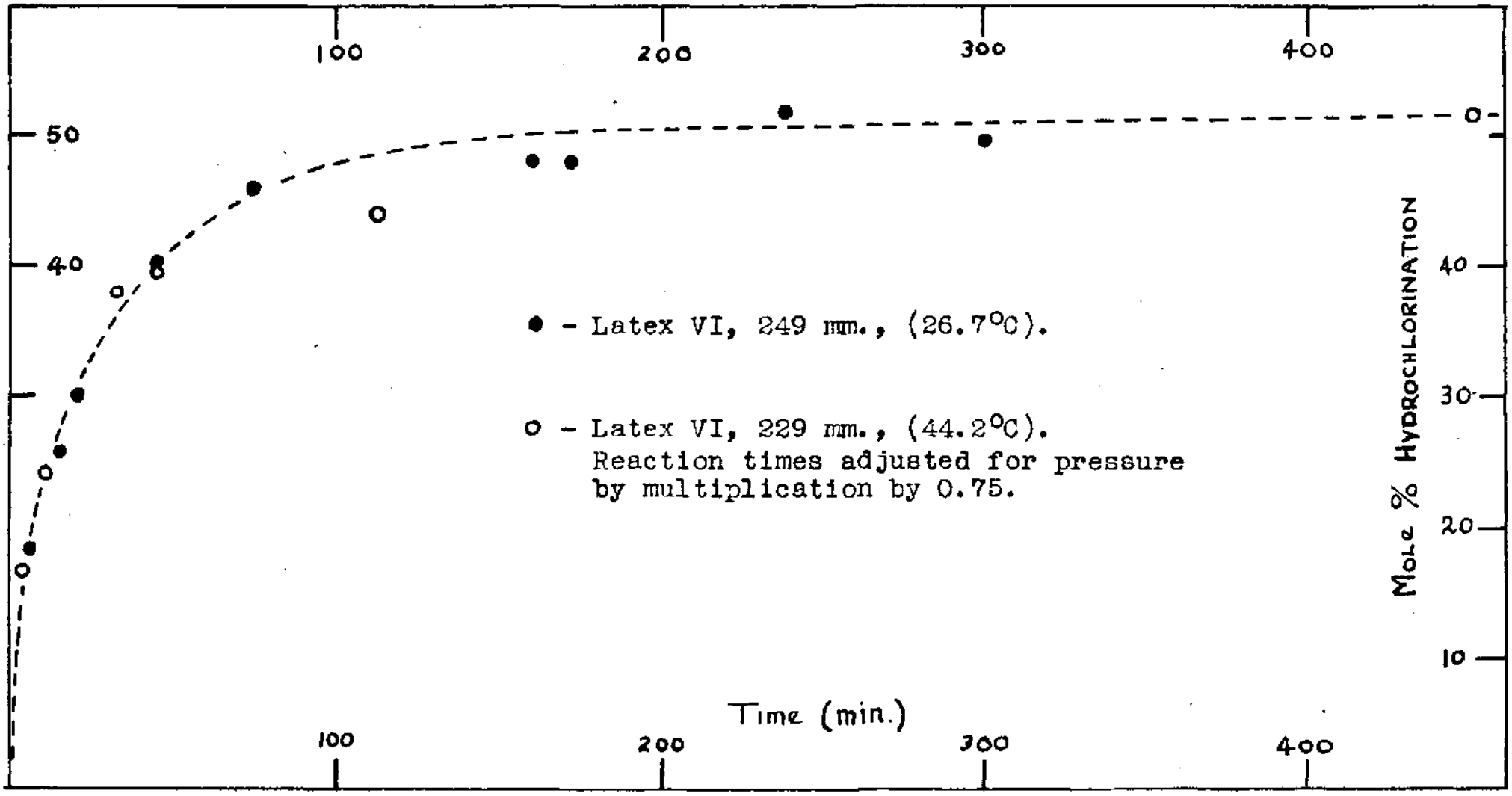

Fig. 11 - Invariance of the shape of the surface locus rate curve with a change in HCl pressure.

Partial Pressures of HCl gas in Kinetic Runs. - The overall vapour pressure (p) recorded on the manometer (A, Fig. 1) is composed of two partial pressures (p_1 and p_2) of HCl gas and water vapour respectively, the contribution from mercury being negligible. For convenience, values of p are normally regulated to multiples of 1 atm. (760 mm. Hg). Variations in barometric pressure are readily accomodated by small adjustments to the manometer level. Accurate values of p_1 are required for comparisons among the foregoing kinetic runs. These have been derived from published data (17) on aqueous solutions of HCl for the reaction temperatures 0, 26.7, 44.2 and 69.9°C (cf. Table 9, p. 24). A sample determination is shown in Appendix 7.

Compatibility of Rubber and Rubber Hydrochloride. - The incompatibility of rubber and its hydrochloride was confirmed by the following observations:

0.5 ml. of synthetic Latex VI were divided into two approximately equal portions. One half (d = 0.9018) was weighed (0.224 g.) and laid aside, while the other was fully hydrochlorinated (2 atm.; 26.7°C; 2 hr.). Both halfs were thoroughly mixed and the weight of

Table 9.

Partial Pressures of HCl in Aqueous Solutions.

$p = p_1 + p_2$ mm. Hg	Reaction temp.	Partial pressure of HCl p_1
65 mm.	26.7°C	57 mm.
170	26.7	167
255	26.7	249
255	44.2	229
255	69.9	163
760 (1 atm.)	0.0	760
760	26.7	759
1140 ($1\frac{1}{2}$ atm.)	26.7	1138
1520 (2 atm.)	0.0	1520
1520	26.7	1517
1900 ($2\frac{1}{2}$ atm.)	0.0	1900
1900	26.7	1900

the hydrochlorinated portion (0.245 g.) obtained by difference. The mixture was flocculated, purified, and dried in the normal way.

Blending in the latex condition ensured a thorough intermixing of the two substrates which is otherwise unobtain-

able. The average density of the combined samples (d = 0.9018) represents 49.2 mole% hydrochlorination. Unlike pure polyisoprene, the flocculate failed to form a translucent brown mass but was white, opaque and non-adhesive. On pressing, a bright orange film was produced, which reverted to the opaque condition during storage (two months).

Determination of Particle Size of Latex VI by Electron Microscopy. - For investigation on the electron microscope, rubber latex particles are too soft to resist the stresses of high vacuum and readily collapse into immeasurable forms. Stiffening may be affected by a number of saturation reactions such as bromination (18) and hydrochlorination (8). The former method, although rapid, causes undue increase in particle volume, whereas hydrochlorination is more suitable for particle size determination while slower and narrower in application.

A fully hydrochlorinated example of Latex VI was prepared for examination on the electron microscope by diluting with distilled water (100:1). One drop of this dispersion on a collodion specimen grid was dried

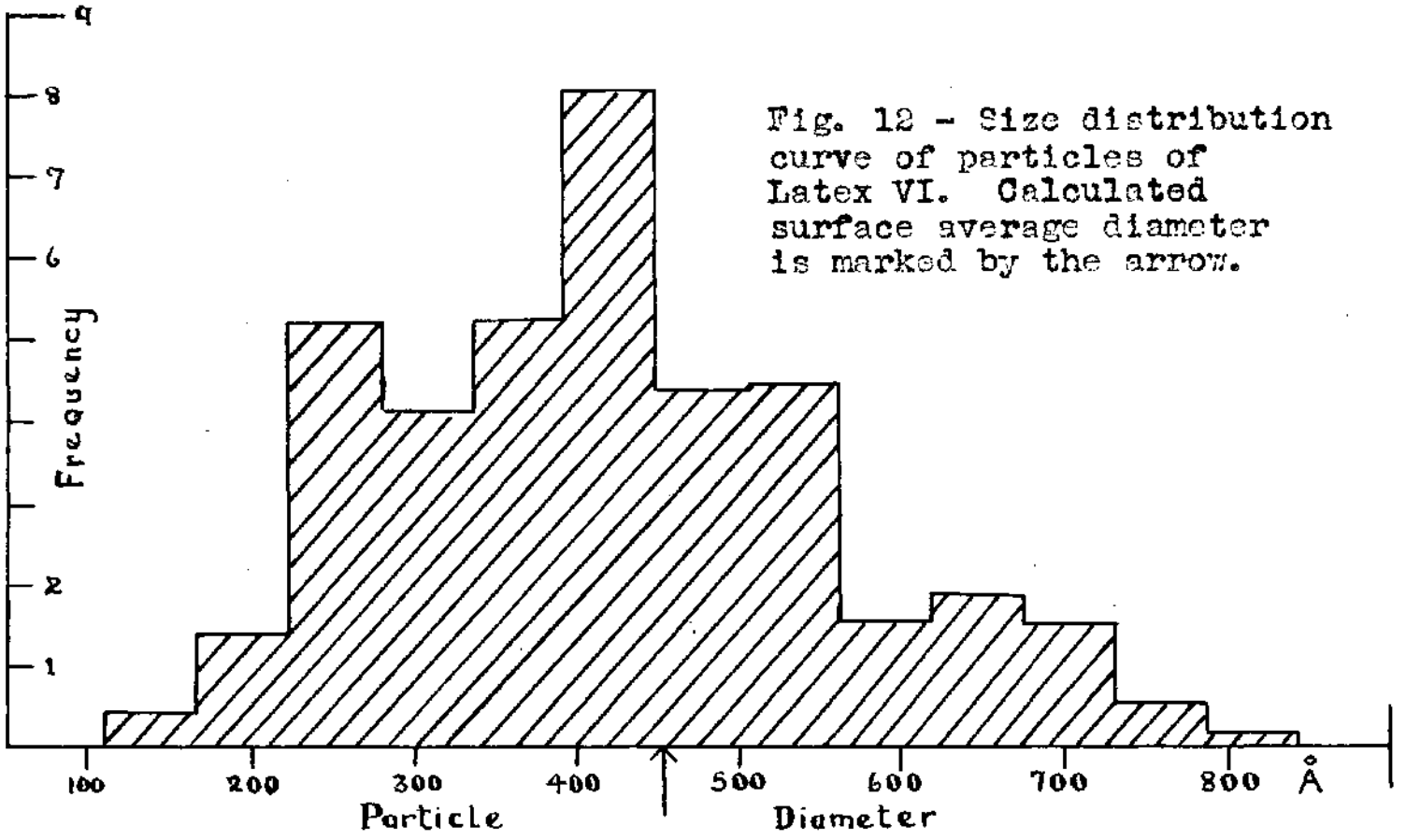

Fig. 12 - Size distribution curve of particles of Latex VI. Calculated surface average diameter is marked by the arrow.

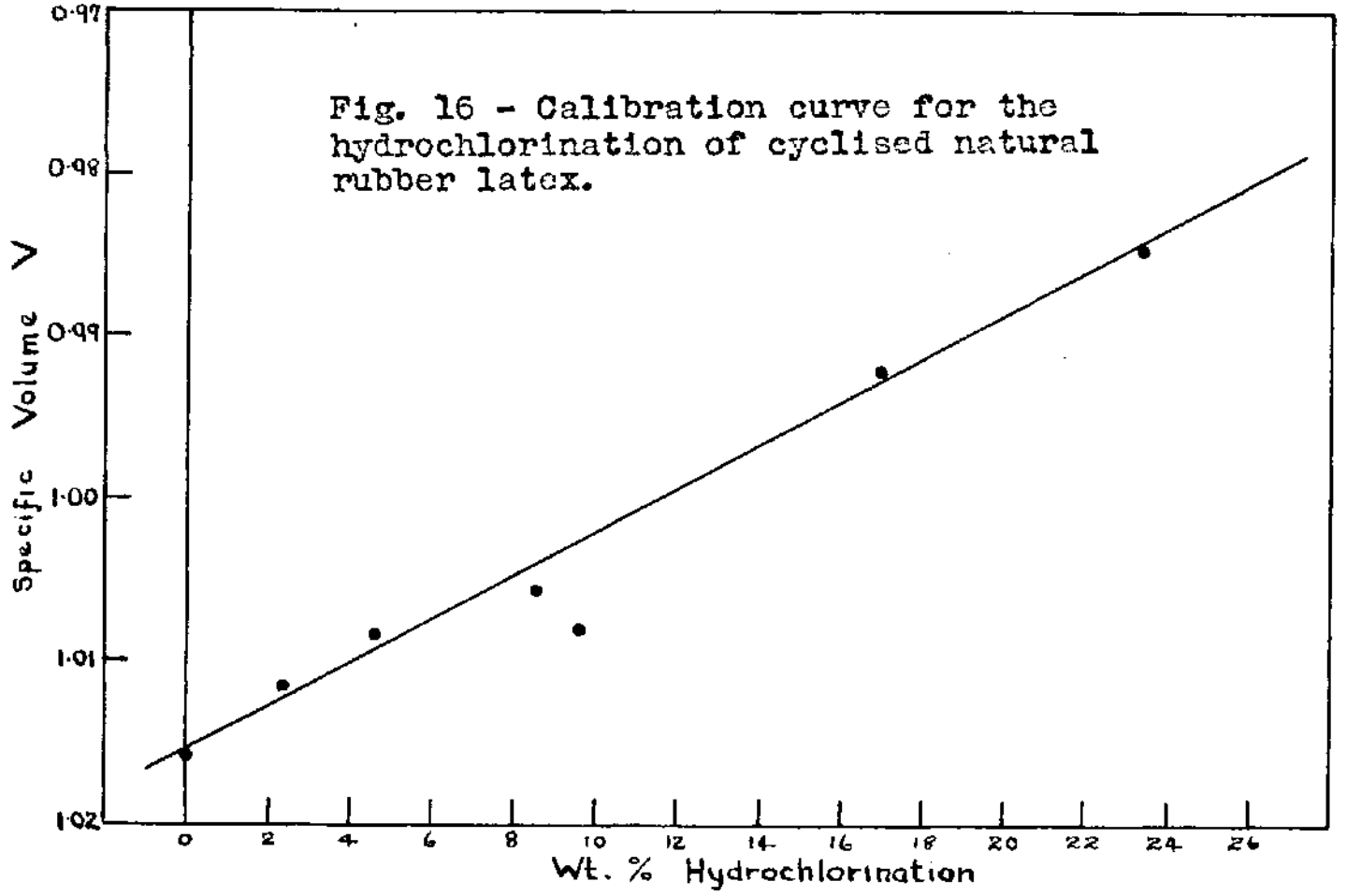

Fig. 16 - Calibration curve for the hydrochlorination of cyclised natural rubber latex.

in vacuum and shadowcast with gold/palladium alloy to enhance contrast. The sizes of 791 particles on a micrograph (12,400X) were measured by projection on a photographic enlarger (5.74X) to give the average particle diameter D, using equations 2 and 4:

	Max.	Min.	Av.	
Latex VI	950	110	452Å	D = 222Å

The distribution curve (Fig. 12) shows a particle size distribution somewhat wider than that for synthetic Latices I and II (8) (cf. Appendix 8).

Acknowledgment is due to Mr. J. W. Sharpe for taking the electron micrograph described in this section.

-----oOo-----

1d. DISCUSSION.

The two reaction loci involved in the hydrochlorination of both natural and synthetic polyisoprene latices were established to be: (a) the surface locus, affecting about 15Å (three molecular layers) on the outside, and (b) the bulk locus comprising the inside of the particles. Although both react simultaneously at all HCl pressures, they may be isolated kinetically for separate study because, at pressures below 0.33 atm., the bulk locus is too slow to be measurable, and above 1 atm. the surface locus rate is fast enough to become manifest simply as a positive intercept (P) when the linear (zero-order) bulk locus rate is extrapolated to the composition axis. The intercept (P) is thus a

measure of the integrated total of the surface locus (i.e. of the amount of rubber accessible to the surface mechanism). For particles of sufficiently large radius ($r > 200\text{Å}$), P is proportional to the specific surface of the particles, or inversely to r.

The hydrochlorination rates of the two isolated loci vary approximately as powers of the pressure p_1 of HCl. The bulk locus rate varies as $p_1^{3.9}$ according to the slope of the logarithmic plot II in Fig. 13 over the range $760 \leqslant p_1 \leqslant 1900$. The co-ordinates of this plot are derived from Table 7 as shown in Table 10:

Table 10.

Dependence of Bulk Locus Rate on HCl Pressure p_1.

p_1	log p_1	Reaction rate R mole%/hr.	log R
760 mm.	1.881	5.24	0.719
1140	2.057	19.5	1.290
1520	2.182	45.9	1.662
1900	2.279	176.5	2.247

The plot refers to measurements on natural (Hevea) latex alone, but synthetic polyisoprene gives results

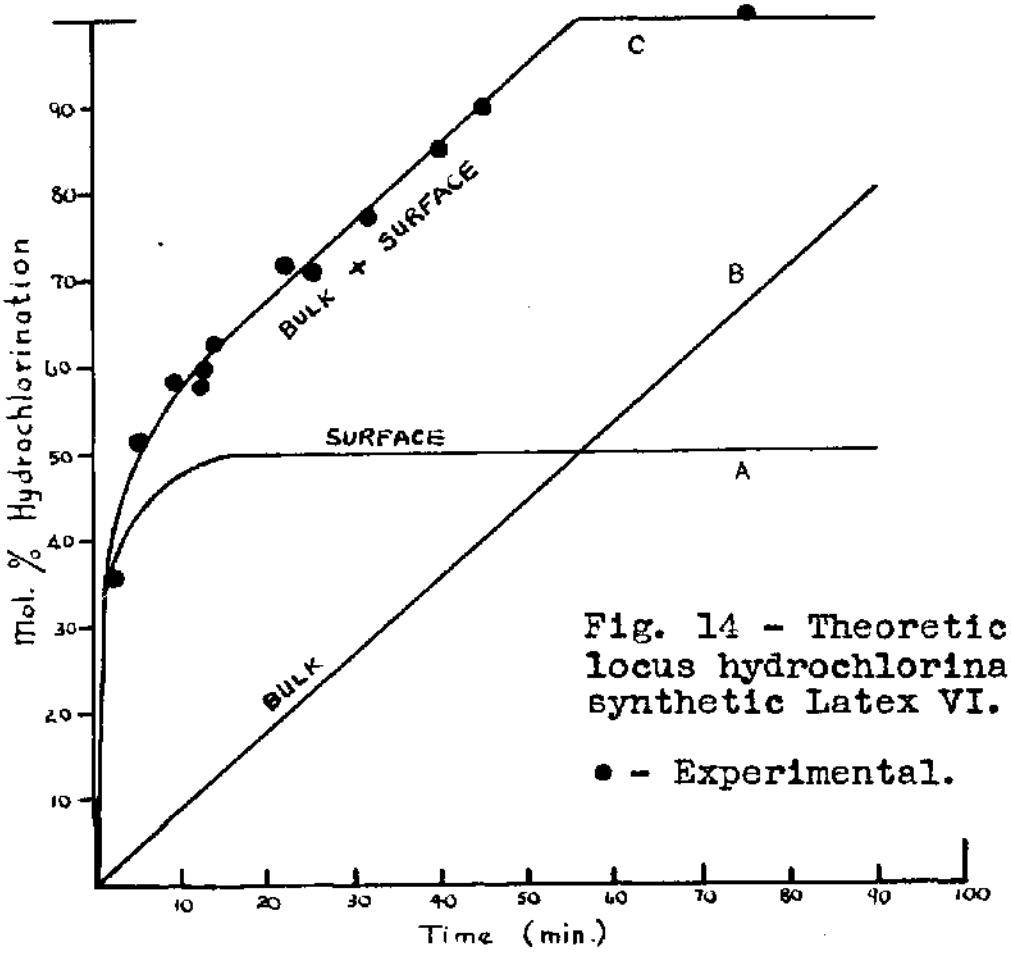

Fig. 14 - Theoretical bulk locus hydrochlorination of synthetic Latex VI.

● - Experimental.

Fig. 13 - Pressure dependence of surface and bulk locus rates.

I Initial surface locus rate (100 ϕ/m, hr.$^{-1}$)
II Unretarded zero-order bulk locus rate.

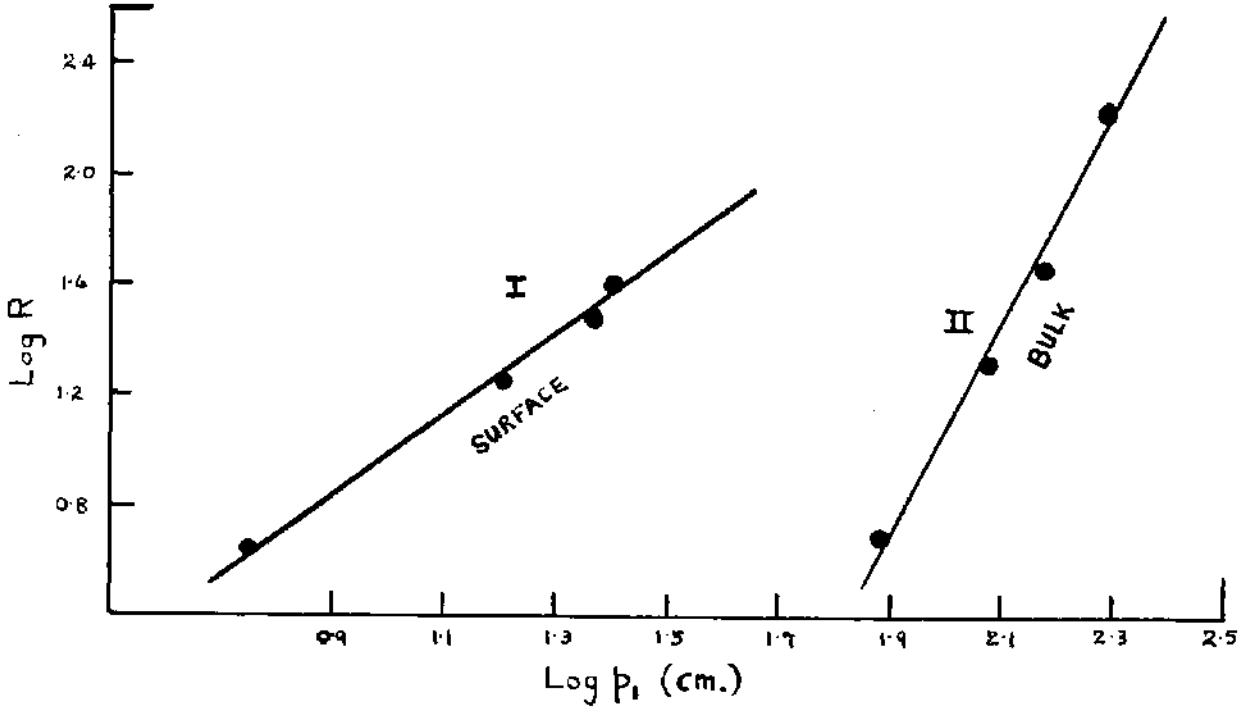

in good agreement (12) (cf. Table 5).

The rate-controlling step, which must take place inside the rubber phase, was previously suggested (cf. page 4) to be:

$$2HCl \longrightarrow (H_2Cl^+.Cl^-) \qquad \ldots. 1$$

The idealised rate-determining step suggested below for the surface reaction is the passage of an ion pair $(H_2Cl^+.Cl^-)$ through the water/rubber interface, leaving its hydration shell behind. A dependence of the hydrochlorination rate on p_1^2 would be predicted if the diffusion flux ϕ is assumed to be strictly proportional to the activity of the reactive ion pair. Since this assumption is only approximate, the observed proportionality to about $p_1^{1.6}$ over the range $57 \leq p_1 \leq 249$ is acceptable (plot I, Fig. 13).

The validity of the foregoing conclusions is confirmed by the following observations, which come to light through the introduction of fine-particle synthetic polyisoprene Latex VI.

(a) Plot II, Fig.13, extrapolates to a negligible bulk rate (i.e. $<$ 1 mole%/hr.) at a pressure p_1 = 500 mm.

Any influence of the bulk rate, then, upon the surface locus curves reproduced in Figs. 7-11 may be disregarded since p_1 is always less than 260 mm.

(b) Using the fine Latex VI, the rate measurements are sufficiently sensitive to confirm the simultaneous operation of the surface and bulk loci at 1517 mm. and 26.7°C. Thus plot C, Fig. 14, is the theoretical combination of both loci, and is seen to fit the experimental points well (cf. Appendix 2e). The composite plot is the sum of plot A for the theoretical surface rate and plot B for the theoretical bulk rate. Plot A is obtained by reducing the time-scale of the experimental plot at 249 mm. and 26.7°C (Appendix 2a). The scale factor used is 1/13.75 which is derived from plot II, Fig. 13, by extrapolation to 1517 mm. Plot B represents the asymptote to fit the measurements in plot C.

Mechanism of Surface Hydrochlorination. - A molecular mechanism, which has been discussed in theoretical terms by Gordon (11) is here to be fitted to the surface rate curves (Figs. 7-11). This is intended not only to strengthen our understanding of the hydrochlorination of rubber, but to emphasise a new treatment of a wider

class of surface reactions.

Kinetic analysis of the mechanism of the bulk locus in the hydrochlorination (6, 12) and cyclisation (19) reactions shows that diffusion is not a controlling factor in typical rubber latex reactions. Diffusion of the relevant reagents (e.g. $H_3SO_4^+$) from the aqueous phase to the particle centre is too fast to have a bearing on the mechanism. In the surface hydrochlorination rate curves, a number of factors point to the relevance of diffusion phenomena, especially the high reaction order and the low (or even zero) activation energy discussed below. The surface locus reaction operates equally well in natural and synthetic polyisoprene latices, although the two substrates are chemically different (12); the structure of the hydrocarbon is therefore not an essential factor. Accordingly, if only an outer skin of about 15Å is accessible to a fast surface reaction, this must inevitably be due to some failure in 'transport' (i.e. to diffusion).

Polymer reactions controlled by diffusion across an interface have been widely studied in terms of a basic mechanism associated with the names of Hill

(20) and Hermans (21). This concerns the diffusion, from an aqueous bath into a polymer (muscle, resin, fibre, hide, gel, etc.), of reagent molecules which are instantaneously captured at a suitable site by chemical action. The site is thereby inactivated as regards any reagent arriving subsequently. Such a process would set up a diffusion wave travelling into the polymer with a rather sharp boundary between the reacted and unreacted layers of polymer sites. In the reaction now under discussion, the reagent is some species derived from hydrochloric acid, and the polymer sites are provided by the double bonds in polyisoprene.

Contribution to the reaction rate by segmental diffusion of polymer sites to meet the incoming reagent has been discussed (21), but the kinetic analysis given below shows that such co-operation by the polymer is negligible in the present case.

The <u>initial</u> rate of the surface hydrochlorination reaction (i.e. the initial slopes of Figs. 7-11) is very slow relative to other Hill-Hermans reactions. This observation can be satisfactorily aligned with the mechanism just described provided the concentration of

the reagent species in the aqueous phase, and hence its diffusion flux into the polymer, is sufficiently small. However, the subsequent rapid decline in the reaction rate (i.e. the high reaction order) is totally irreconcilable with the shape of the curve predicted by the theory (Fig. 7) unless some radically new factor is introduced to account for the rapid deceleration of the diffusion wave-front on its way into the polymer.

If the molecular structure of the polymer is represented by layers of polymer chains, the new factor decelerating the wave, on its course perpendicularly through the layers, must take the form of a decrease in specific reaction rate constants of successive layers starting at the interface. A general kinetic treatment has been derived (11) for any law fixing the relative constants of successive layers; which treatment duly degenerates into ordinary (non-decelerated) Hill-Hermans diffusion for the particular law appropriate to it.

The physical cause for the deceleration in surface hydrochlorination is taken to be the <u>instability</u> of the diffusing reagent. The more distant a layer is from the source of reagent (i.e. the aqueous phase) the

greater is the chance of complete deactivation of the reagent by some specific mishap, which makes it 'disappear' before arrival at the layer. More exactly, the reagent is assumed to have an equal chance of deactivation in any equal time interval. The correct law determining the relative rate constantsfor the i^{th} layer from the interface, on this assumption, was shown by Gordon (11) to be:

$$k_{i,s} = \sinh (\operatorname{sech}^{-1} s) / \sinh (i \operatorname{sech}^{-1} s) \quad \ldots\ 9$$

where s is the stability constant, namely the chance of the reagent molecule surviving without deactivation the diffusion jump from one layer to the next.

Justification for ascribing the observed deceleration to this specific cause of reagent instability rests on several arguments. Firstly, the rate curves can be fitted within the small experimental error on this basis, although this point loses some of its significance since s requires adjustment as an independent parameter. Secondly, a plausible mechanism for the deactivation reaction of the reagent can be proposed, which should have a very low activation energy, in agreement with

observation. Thirdly, it is theoretically to be expected that reagents, originating in a highly polar aqueous medium and thenceforward diffusing into a hydrocarbon, should be susceptible to deactivation, decomposition, or neutralisation reactions.

Finally, conclusive evidence has been provided by Gordon and Taylor (9) that a surface locus reaction affecting only two layers of polymer is observed when latex is vulcanised under certain conditions. A surface locus reaction of considerable range of penetration has been held responsible for an initial fast reaction in the cyclisation of rubber latex (8) which was independently observed by Bloomfield. The fact that surface reactions of varying range of penetration occur in the three different latex reactions studied supports the deduction that they are decelerated by reagent instability; for on this hypothesis the range of the surface reaction is determined by the stability constant s, which should vary from one reagent to another. Fig. 7 illustrates this with theiretical sample rate curves for Hill-Hermans diffusion decelerated by reagent instability. According to the value of s chosen, in the range

$0 \leqslant s \leqslant 0.6$, the curves are seen to level off sharply after the equivalent of between one and four polymer layers has reacted.

For a plane surface, the Hill-Hermans rate equation underlying these plots has been obtained (11) in the following form:

$$H = \sum_{i=1}^{\infty} \left(\sum_{a=1}^{\infty} C_{a,i,s} \right) \left[1 - \exp(-k_{i,s} \cdot t') \right] \quad .... \quad 10$$

As shown below, all but one of the latices studied (Latex VI) were composed of particles so large that they can be treated by this plane body law. However, it must be remembered that H is the amount of reaction measured in multiples of complete reaction of the surface layer. Experimentally, the fractional conversion c of the particle as a whole is measured. For spherical particles of radius r, and a spacing of 5Å between the molecular layers of rubber, the two kinds of unit are measured thus:

$$H = cr/15 \quad .... \quad 11$$

When a distribution of particle sizes is present in a latex, the surface average radius $\bar{r}$ replaces r in equation 11. This average radius may be deduced from

the intercept P of the bulk rate plot (Fig. 4) using equation 3 (cf. page 6). The thickness Υ of the reactable surface layer was determined (8) to be 15Å by electron microscopic calibration of $\bar{r}$, and this value is used here.

The constants $C_{a,i,s}$ in equation 10 are given by:

$$C_{a,i,s} = \sum_{j=1}^{a} k_{j,s} / (k_{j,s} - k_{i,s}) \qquad \ldots\ 12$$

where $C_{1,1,s} = 1$ and $j \neq i$.

For diffusion decelerated by reagent instability, the reaction constant $k_{i,s}$ of the i^{th} layer is given by equation 9 in terms of the stability constant s, which is an adjustable parameter.

The time unit t' is a dimensionless measure of reaction progress. It is related to the experimental time t (in seconds) through the unknown gross flux ϕ (in moles of reagent per $cm.^2$ of surface), and to the number m_1 (moles) measuring the unsaturation per $cm.^2$ in the surface layer, as follows:

$$t' = t\phi/m_1 \qquad \ldots\ 13$$

Since the flux is unknown, the scaling of the time axis

of the present experimental plots is subject to an adjustable factor (Φ/m_1).

Because of the two adjustable parameters (underlined), the fit in Figs. 7, 8, and 9 with the experimental data, though excellent, cannot be held to prove the mechanism underlying equation 10 without independent support. Such support has been found in studies of competition for surface unsaturation by pre-vulcanisation (9). Additional support, by the present work, is derived below from the effects of HCl pressure, of admixture of H_2SO_4, of temperature, and of particle size.

Note on the Calculation of the Rate Equation 10 at Different Values of s. - A sample application of equation 10 (at s = 0.548) is included in Table 11. Values of $k_{i,s}$, in the first instant, are directly available in the range $1 \leq i \leq 12$ from tables of trigonometric functions using equation 9. A preliminary triangular table is set up listing the differences $k_{a,s} - k_{i,s}$ from a = 1 to a = 11, and hence the analogous table of constants $C_{a,i,s}$ from equation 12 (cf. Table 11, page 39).

Table 11.

Evaluation of Rate Equation 10 from Equations 9 and 12.

$k_{a,s}$	a	$C_{a,1}$	$C_{a,2}$	$C_{a,3}$	$C_{a,4}$	$C_{a,5}$	etc.
1.0000	1	+1.0000	-	-	-	-	
0.2734	2	-0.3763	+1.3763	-	-	-	
0.0818	3	+0.0335	-0.5871	+1.5536	-	-	
0.0241	4	-0.0008	+0.0568	-0.6498	+1.5939	-	
0.0072	5	+0.0000	-0.0015	+0.0627	-0.6771	+1.6160	
0.0021	6	-	+0.0000	-0.0017	+0.0661	-0.6867	
0.0006	7	-	-	+0.0000	-0.0018	+0.0670	
0.0002	8	-	-	-	+0.0000	-0.0018	etc.
Summation of Columns		+0.6564	+0.8444	+0.9647	+0.9810	+0.9945	etc.

Tabulation starts with the value $C_{1,1,s} = 1$; and vertical values of $C_{a,i,s}$ are derived consecutively from the one immediately above down the first column, until further terms are not required for sufficient accuracy (only four significant figures are used in Table 11 for the sake of economy, but this is normally

carried to six). The starting value from the second column ($C_{a,2}$) is obtained from $C_{2,1}$ thus:

$$C_{2,2,s} = 1 - C_{1,1,s} \qquad \ldots\ 14$$

The remaining terms in all columns are derived similarly. Tabulation is continued until the value of $C_{12,12,s}$ has been entered, and the columns are summed to give

$$\sum_{a=1}^{\infty} C_{a,i,s} \quad .$$

Values of $1 - \exp(-k_{i,s}.t')$ from i = 1 to i = 12 are derived from tables of the exponential function (e) correct to six figures. The product

$$(\sum_{a=1}^{\infty} C_{a,i,s})(1 - \exp(-k_{i,s};t')$$

is obtained by multiplication at the corresponding values of i, and equation 10 evaluated by summation. The final form at s = 0.548 is:

$$H = 0.6564(1 - e^{-t'}) + 0.8444(1 - e^{-0.2734t'}) + 0.9647(1 - e^{-0.0818t'}) + 0.9810(1 - e^{-0.0241t'}) + 0.9945(1 - e^{-0.0072t'}) * \ldots\ldots\ldots \qquad \ldots\ 15$$

Smooth theoretical curves may be drawn (cf. Figs. 7,8,

and 9) using values of t' = 1, 10, 25, 50, 75, 100, 150, and 200.

The derivation of plots A and E in Fig. 7 is somewhat different. Gordon (11) has shown that, at s = 1, to a close approximation:

$$H = (t'/2\pi)^{\frac{1}{2}} \int_0^{t'} 1 - e^{-u}/u^{3/2}.du \quad .... \ 16$$

where u = t'/i. Hence:

$$H(2\pi)^{\frac{1}{2}} = 2t' - t'^2/3 + t'^3/15 - t'^4/84 + \cdots \quad .... \ 17$$

Equation 17 may be used to evaluate points on the plot of s = 1 as far as t' = 5, beyond which the series converges slowly (Table 12).

Table 12.

Evaluation of Equation 17.

t'	$\frac{1}{4}$	$\frac{1}{2}$	1	2	3	4	5
H	0.191	0.369	0.687	1.220	1.658	2.032	2.364
$H(2\pi)^{\frac{1}{2}}$	0.480	0.925	1.722	3.056	4.152	5.093	5.925
$t'^{\frac{1}{2}}$	0.500	0.707	1.000	1.414	1.733	2.000	2.236

Values of H, in the range $7.5 \leq t' \leq 25$, may be extrapolated on the linear plot of $H(2\pi)^{\frac{1}{2}}$ versus $t'^{\frac{1}{2}}$ (cf. Appendix 9).

For the plot at s = 0, the constants $k_{a,s}$ are all zero, except $k_{1,s} = 1$. $\sum_{a=1}^{\infty} C_{a,i,s}$ equals unity throughout and equation 10 reduces to:

$$H = 1 - e^{-t'} \qquad \ldots\ldots 18$$

which is asymptotic to the line H = 1 at high values of t' (cf. Appendix 9a).

Throughout the theoretical interpretation the absorbed layer of non-ionic stabiliser (Vulcastab LW) has been ignored, since variations in the nature and concentration of the stabiliser have been shown (6) to leave the kinetics of latex reactions unaffected.

Independent Support for the Mechanism Underlying Equation 10.

Effect of Pressure. - An increase in the pressure of HCl will be reflected in an increase of the equilibrium concentration C of the reagent species in the aqueous phase. According to the proposed mechanism, this has only one simple effect on the rate curve, viz. a shortening of the time-scale. Thus the flux ϕ is related to C by Collins's equation (22):

$$\phi = DC\alpha/l \qquad \ldots\ 19$$

where D is the diffusion coefficient of the reagent in the aqueous phase, and l the length of one diffusion jump. The 'accomodation coefficient' (α) may be taken as unity, on the assumption of perfect absorption at the particle surface without reflection of reagent species back into the water. An increase in C should effect a proportional increase in ϕ, and thus in the time t' (equation 13). Experimental tests of this prediction, which leave nothing to be desired, are presented in Figs. 8 and 9 for two latices (V and VI) of different particle size and for a pair of pressure values (cf. Appendices 2 and 6). In each case the experimental

curve at the lower pressure has been adjusted (cf. Table 8, page 22) by multiplication with a suitable factor of all the experimental time values, so that the kinetic curve is brought into coincidence with that obtained at the higher pressure. The scaling factor is equal to the ratio of the flux rates.

This finding provides valuable confirmation of the irrelevance of the diffusion of rubber segments to the interface. Flux of the reagent species into the rubber is alone seen to control the nature of the rate curve; and the assumption, in the model underlying equation 10, of stationary rubber sites (double bonds) is therefore vindicated. The adequacy of the assumption is, at first sight, surprising. Some mixing by segmental diffusion of reacted rubber hydrochloride with the original polymer might be expected to occur over the period of minutes or hours involved in the rate curves. The success of the theory of stationary polymer sites is probably due to the incompatibility (immiscibility) of rubber hydrochloride with unreacted rubber chains. Independent observations (cf. page 23) confirm the incompatibility of the two polymers at the reaction temperatures.

Effect of Admixture of Sulphuric Acid. - The form of dependence of the rate curve on HCl pressure, discussed in the last section, suggests an investigation of the equilibrium concentration of the reagent in the aqueous phase surrounding the rubber particle, while leaving the equilibrium pressure constant. Reductions of overall solubility of HCl in water can be acheived by admixture of sulphuric acid, an acid somewhat stronger than hydrochloric at equal percentage concentration. However, if the medium is made too concentrated in H_2SO_4, incursion of the acid-catalysed cyclisation reaction (cf. Section 2) of rubber as a side reaction is to be feared, whose rate (in the absence of HCl) becomes measurable above about 60% H_2SO_4 in the aqueous phase (19). A compromise has therefore been sought by studying the effect on the hydrochlorination kinetics of an aqueous phase composed of 17.4 parts of H_2SO_4 to 82.6 parts of water by weight;

Latex VI (8% solids, incl. stabiliser)- 4.2429 g.

Sulphuric Acid (98%) - 0.8428 g.

As shown in Fig. 10, this appreciable change in the acidity of the original aqueous medium produces very little change in the surface hydrochlorination rate. The initial rate is unchanged within the small experimental error. Indeed, the only alteration in the rate

curve due to the addition of H_2SO_4 is a moderate variation which appears in the middle range and remains unexplained.

The conclusion is drawn that the equilibrium concentration of the reagent, and hence the flux responsible for surface hydrochlorination, depends only on the activity (vapour pressure) of HCl, and not on the activity of water which must be expected to vary considerably on the addition of the above amount of sulphuric acid. Consequently, the reagent is merely formed from an integral number (n) of HCl units,

$$n\ HCl \rightarrow \text{reagent} \qquad \ldots\ 20$$

and thus carries no nett ionic charge. In the bulk locus reaction, the same absence of nett charge was deduced (12) for the reagent involved there, which is formed from precursors within the rubber particle rather than supplied ready-made from the aqueous phase. For the surface locus, it is unlikely that n = 1 or 2; hence the most probable form of the reagent is generated thus:

$$n\ HCl \rightarrow (H_2Cl^+.Cl^-) \qquad \ldots\ 1$$

The reactive ion pair then adds HCl to the double bond with great facility. Every collision with an unsaturated

unit is taken as effective, as an essential assumption in the model underlying the derevation of equation 20. The molecule of HCl, solvating the proton in the reactive ion pair, would merely be liberated as covalent (unreactive) HCl at the moment of saturation of the double bond.

Effect of Temperature. - At constant pressure, the bulk locus hydrochlorination reaction has an apparent negative activation energy of -6 Kcal. In contrast, the surface hydrochlorination rate dH/dt' is found to be virtually independent of temperature, as well as of added sulphuric acid. The initial rate does not vary measurably at the three temperatures (26.7°C, 44.2°C, and 69.9°C) over the 43C° range studied, and the estimated accuracy of these measurements leads to the limits

$$\Delta E = 0 \pm 1.5 \text{ Kcal./mol.}$$

for the activation energy using the Arrhenius equation:

$$\log k_2/k_1 = E/2.303R(T_2 - T_1/T_2T_1)$$

where $k_2/k_1 \not> 1.4$ between 0°C and 69.9°C. The shape of the curve does change slightly, but definitely, in a manner which is excellently accomodated by the theory (see below).

According to the postulated Hill-Hermans

mechanism, the transition state of the surface locus reaction consists in the passing of a reagent such as ($H_2Cl^+.Cl^-$) through the water/rubber interface. This follows since the rate of hydrochlorination depends on the flux across the interface, and because the reagent, once entered into the rubber, reacts with a double bond on the first collision, i.e. without energy requirement.

While HCl dissolves in concentrated hydrochloric acid with considerable evolution of heat (about 10 Kcal. per mole) due to the hydration of its constituent ions, it appears that this energy requires to be returned when the ion pair reagent is pushed out of the water and through the rubber surface. The absence of an activation energy indicates that the energy state of the reagent passing through the rubber surface is on a level with the corresponding number of covalent molecules of HCl in the gas phase. A detailed heat balance of the transition state would require to account for the energy of charge separation in the ion pair, its heat of condensation, etc. Broadly speaking, however, the absence of activation energy may be taken to indicate that the reagent, when entering the rubber, is practically stripped of its hydration shell, in agreement with the

conclusion already reached that water does not enter into its composition.

According to the postulated mechanism underlying equation 10, the measured initial rate depends only on the flux of the reagent, but the subsequent shape of the curve is dependent on the stability constant s. This is illustrated generally in Fig. 7, which also shows in particular that the experimental curves at 26.7°C and 69.9°C can best be fitted with the values s = 0.465 and s = 0.548 respectively. This slight but definite change in the value of s with temperature is analysed below in terms of the activation energies of the two reaction rates whose balance determines the value of s, viz. the speeds of diffusion and deactivation.

The deactivation step must clearly be the neutralisation which reverses the formation (equations 1 or 20) of the reagent, and which reforms inactive covalent HCl. This step would not be expected to require any activation energy: ΔH (deactivation) = 0. The diffusion rate of the species of the size of an ion pair reagent through rubber generally has a very low activation energy ΔH (diffusion). The difference:

$$\Delta H \text{ (diffusion)} - \Delta H \text{ (deactivation)} = d(\Delta H)$$

is thus qualitatively predicted to be a very small positive quantity. The value

$$d(\Delta H) = +0.8 \text{ Kcal./mole},$$

found from the measured s values in Table 13, is in qualitative agreement with this prediction.

The balance between the diffusion and the deactivation rates is struck in the Table on the basis that s measures, by definition, the chance of the reagent surviving one diffusion jump without deactivation. The average number $\bar{N}$ of jumps before deactivation (in fully hydrochlorinated rubber) is given by:

$$\bar{N} = 1/(1 - s)$$

and this is proportional to the ratio of the two rates:

$$1/(1 - s) = k_d/k_j$$
$$= (\text{diffusion rate})/(\text{deactivation rate}) \quad \ldots\ 22$$

Accordingly:

$$d(\Delta H) = -2.303R\ d \log\ 1/(1 - s)/d(1/T) \quad \ldots\ 23$$

Table 13.

Temp.	s measured	$\bar{N} = 1/1 - s$	$d(\Delta H)$ from 23
26.7°C	0.465	1.87	0.8 Kcal.
69.9	0.548	2.21	

Concentration and Mean Life-time of the Transient Reactive Species. - The average perpendicular distance $\bar{h}$ of diffusion of the ion-pair reagent into hydrochlorinated rubber, before suffering deactivation, is $\bar{N}$ times the jump length of 5Å, i.e. about 10Å (cf. Table 13). The time taken by the reagent to traverse this distance, i.e. its mean life-time $\bar{t}$, is estimated to be only about 3×10^{-9} sec. from the Einstein equation:

$$\bar{t} = \bar{h}^2/2D_r \qquad \ldots\ 24$$

To arrive at this estimate, the diffusion coefficient D_r of the reagent species through the polymer is taken to be 1.5×10^{-6} cm.^{2}/sec. from Grun's measurements (23) on substances of various molecular weights diffusing through rubber.

In analogy to the low stability of the reagent in the polymer, its concentration in the aqueous phase is found to be only of the order 6×10^{-13} to 6×10^{-12} mole/l., as shown below. For comparison, various estimates ranging from 5.9×10^{-12} to 4×10^{-8} mole/l. for undissociated HCl (as distinct from ion pairs) in 0.01N to 1.00N hydrochloric acid (24) may be quoted. The concentration range for the ion-pair reagent stated is

derived from equation 19, using the following parameters:

(a) The scaling factor $\phi/m = 2.5 \times 10^{-3}$ to 2.5×10^{-2}/sec. is found experimentally (cf. Table 8) for the time scale.

(b) The number m_1 of unsaturated units per cm.^{2} of rubber surface is estimated, from Bunn's data (10), to be approximately 6×10^{-10} mole.

(c) The diffusion coefficient D of the reagent through water is taken as that valid for HCl itself, viz. 2.5×10^{-5} cm.^{2}/sec. (23).

(d) The length of the diffusion jump (l) of the reagent in water is taken as 1 Å.

(e) The accomodation coefficient $\alpha = 1$.

The calculations in this section illustrate the dependence of the surface hydrochlorination on the thermal bombardment of the rubber surface by an exceedingly rare reagent of short life.

Effect of Particle Size. - A diffusion-controlled reaction affecting only the thin outer skin of a curved body, say a few percent of the radial dimension of a cylinder or sphere, is always represented to a first approximation by the rate law appropriate to a planar body with an

equivalent surface area. In generalised Hill-Hermans diffusion, the plane body treatment will be shown below to hold even as a second approximation. Spherical curvature affects the plane body rate law (equation 10) in two ways which counteract each other. Firstly, the movement of the diffusion wave front is accelerated because the flow lines, starting at m_1 points on the interface, converge (cf. Fig. 15) upon m_a points in the a^{th} layer where

$$m_1 > m_a.$$

This may be taken to increase the rate constant $k_{i,s}$ of the i^{th} layer by the factor m_i/m_1. Simple geometry shows that for a sphere, comprising L concentric layers, the moles (m_1) of sites of reactive lattice points in the i^{th} layer are given by:

$$m_i/m_1 = \left[(L - i + 1)/L\right]^2 \qquad \ldots. 25$$

Secondly, an allowance is due for the fact that the accelerated diffusion wave meets fewer reactive positions on successive layers, which causes a progressive mass law reduction in the observed rate. According to the derivation of equation 10, the ratio m_a/m_1 of reactive sites in the a^{th} layer to those in the first layer must

be applied as a correcting factor to $C_{a,i,s}$.

The two corrections just proposed lead from equation 10 to the second approximation rate law for a spherical particle:

$$H = \sum_{i=1}^{\infty}\left[\sum_{a=1}^{\infty} C_{a,i,s}(L - a + 1)^2/L^2\right] \quad x \left[1 - \exp.(-k_{i,s}t'.L^2/L + i + 1)^2\right] \quad .... \ 26$$

The spacing between molecular layers in rubber is $5\mathring{A}$, so that the particle radius r is given by:

$$r = 5L \ (\mathring{A}) \quad .... \ 27$$

When equation 26 is compared with equation 10, using the experimental value s = 0.465 at 26.7°C, they are found not to differ measurably for spheres of $L > 40$ layers, i.e. $r > 200\mathring{A}$. Although latices covering a 20-fold range in average particle radius $\bar{r}$ have been studied (Hevea = $4500\mathring{A}$ and Latex VI = $180\mathring{A}$) only the finest latex prepared (Latex VI) fell below this size limit. Rate measurements on this latex are seen in Fig. 9 to be in good agreement with equation 26. The effect of curvature is in the predicted sense and of the correct

order of magnitude. The sense is that of a progressive deceleration of the reaction rate, as the decrease in available unsaturation from one spherical layer to the next, according to equation 26, outweighs somewhat the effect of the acceleration of the diffusion wave front. The correct representation by the curve of the magnitude of the effect depends on the parameter L = 18, or, by equation 27, $\bar{r} = 90\text{Å}$ for the particles of Latex VI.

The direct normal evaluation of $\bar{r}$ via equation 3 (cf. page 6), from the measured intercept P = 48 ± 2 in Fig. 4 and using $\tau = 15\text{Å}$, actually leads to $\bar{r} = 76\text{Å}$. However, because of the high curvature of the particles concerned, it is estimated that the depth τ of penetration of the surface reaction is raised to about 18Å, and hence the radius $\bar{r}$ to 90Å. Again, only approximate verification of $\bar{r}$ was possible by means of electron microscopy (cf. page 25). The small particles were not sufficiently resolved without metal shadowing. Shadowing gave excellent resolution, but the results obtained by this method are known to be high. The correction applicable for larger particles (cf. equation 4, page 6) consists in subtracting 115Å from the measured radius. Owing to the broader distribution curve than those for Latices I, II,

and V, a statistical evaluation of the 791 particles of Latex VI on the shadowed micrograph was deemed necessary. The uncorrected value of $\bar{r}$ was 222Å.

Application of the correction mentioned above leads to $\bar{r}$ = 107Å, in quite good agreement with the value 90Å deduced above from the intercept P. However, it must be admitted that the correction of -115Å here exceeds the radius of the smallest shadowed particles visible (cf. Appendix 8), which detracts from the value of the measurement. Clearly, equation 4 cannot hold at very low values of $\bar{r}$, and the shadowing effect, although constant after a specific particle size is reached, must progressively decrease below this value.

Effect of Sulphuric Acid on the Bulk Rate. - It was found earlier (cf. page 45) that the presence of 17.4% H_2SO_4 in the serum affected the surface locus rate curve only in a negligible way. The presence of a similar percentage (20%) in Latex 8 (cf. page 11) exerts only a small deceleration on the bulk rate measured at 2 atm. and 26.7°C. However, as shown in Fig. 5, this effect takes an interesting form when natural Hevea latex is used, which confirms the interpretation given (7) of the

early linear slow portion of the rate curve observable only with natural latex. It was suggested that this latex contains a retarder which deactivates a fixed number of ion-pairs before the full linear rate curve takes over suddenly at the kink. It is seen in the figure that the retarded portion preceding the kink is not measurably affected by the presence of H_2SO_4, while the subsequent unretarded portion is definitely reduced in slope (i.e. reaction rate).

In concordance with the theory of retardation given by Gordon and Taylor (7), the two unretarded rate lines extrapolate back to the point -27% on the composition axis, as did six curves obtained by these workers under a variety of HCl pressures and temperatures. The constant negative intercept is interpreted as the total of the retardation effect, just as the (variable) positive intercept P of the retarded rate plot (preceding the kink) is interpreted as the measure of the fast surface reaction.

The conclusions of Gordon and Taylor have been further confirmed in the present work. In deriving data for the dependence of bulk locus rate on HCl

pressure, two further runs on natural Latices 4 and 9 were carried out at $1\frac{1}{2}$ and $2\frac{1}{2}$ atm. and 26.7°C (Fig. 6). Extrapolation of the fast bulk rate curves to the composition axis confirms the value -27 mole% (cf. Table 7).

---------oOo---------

SECTION 2.

AN ESTIMATION OF THE PROPORTION OF ISOLATED ISOPRENE UNITS IN CYCLISED NATURAL RUBBER BY HYDROCHLORINATION.

2a. INTRODUCTION.

Ring Closure in Polyisoprene Compounds. - A process of ring closure occurs widely among polyisoprene compounds of low molecular weight (25, 26, 27). The reaction is characterised by the elimination of unsaturation content while the original empirical formula is retained.

Natural rubber is known to undergo a similar reaction under the influence of a number of acidic catalysts (28); several polycyclic (29, 30) and cross-linked (31) formulae were proposed for the cyclised polymer, e.g.:

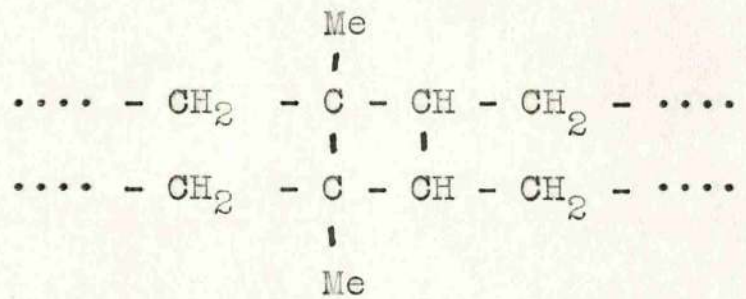

.... 28

The formation of such <u>intermolecular</u> rings was later discounted on physical and chemical evidence (30, 32), notably by Fischer and McColm (33, 34) who accurately measured the residual unsaturation at 57%, using three distinct methods (iodine, sulphur, oxygen) on the bulk cyclised polymer. The constancy of this value contrasts markedly with the theoretically expected 50% unsaturation.

Gordon (32) has shown that <u>intramolecular</u> 5- and 7-membered rings are unlikely, since A-sense* protonation (35) and carbonium-ion transfer (36) would be required in the one case, and attack on a saturated center in the other. Of six possible 6-membered rings four have been considered (30). Only one, originally due to D'Ianni (37), is supported by independent evidence (infra-red absorption):

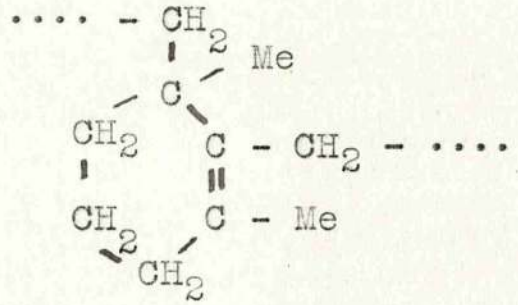

.... 29

---

* i.e. in the anti-Markownikoff sense:

.... - CH_2 - CHMe - CHCl - CH_2 - ....

Gordon's Cyclisation Mechanism. - It was not appreciated that the residual unsaturation indicates that the cyclisation reaction is subject to statistical control until Gordon (32) proposed a mechanism for cyclisation which combines true Markownikoff (M-sense) protonation and carbonium-ion transfer with structure 29:

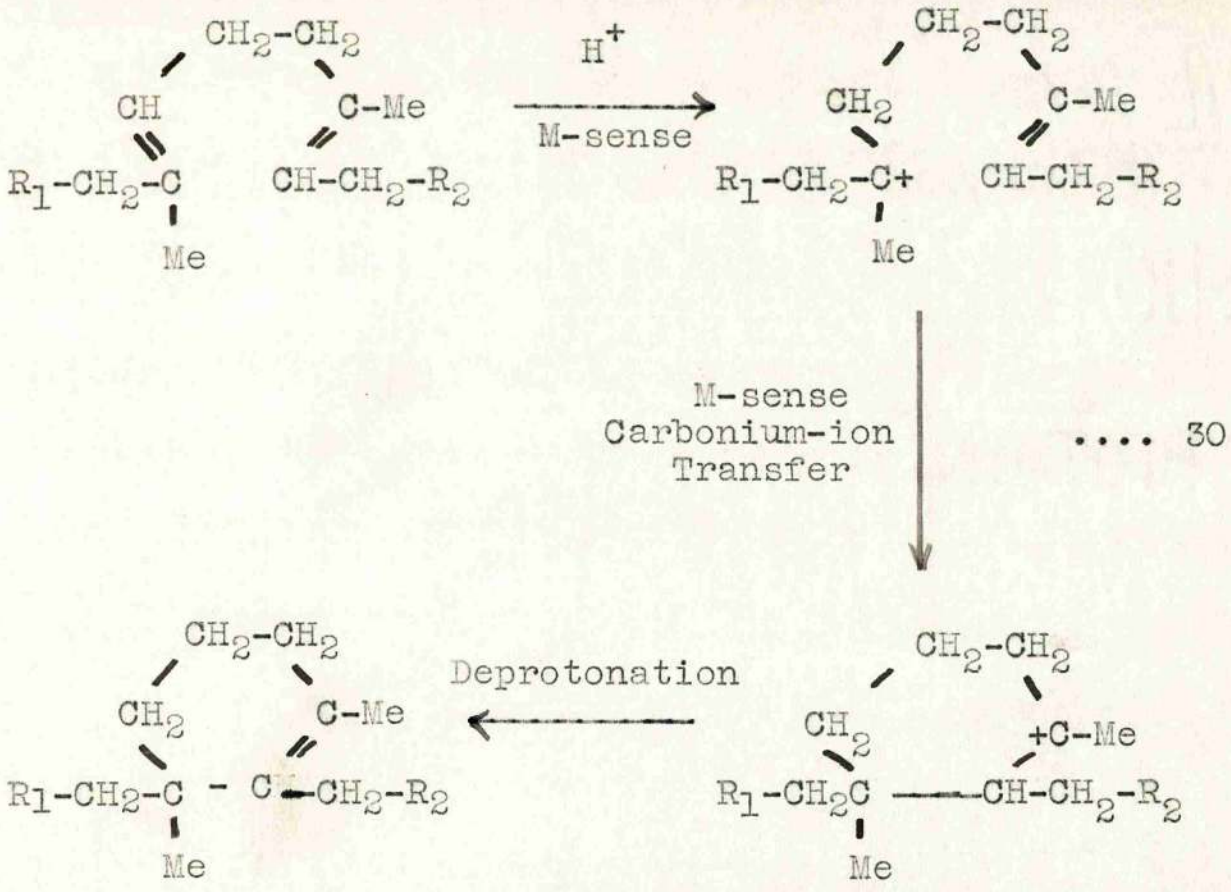

The Statistical Effect of Interaction of Neighbouring Units in Chain Polymers. - The mechanism underlying equation 30 places the cyclisation reaction in a group

which has been treated generally, on a statistical basis, by Flory (38). In a polymer having the regular head-to-tail structure:

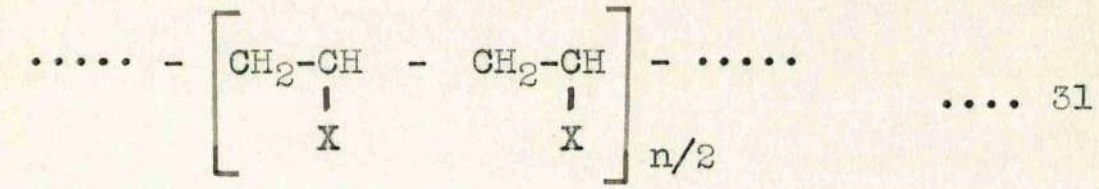

.... 31

where X is a functional group such that neighbouring pairs of monomer units can jointly condense, random coupling will occasionally leave isolated ('widowed') units between two pairs of reacted neighbours:

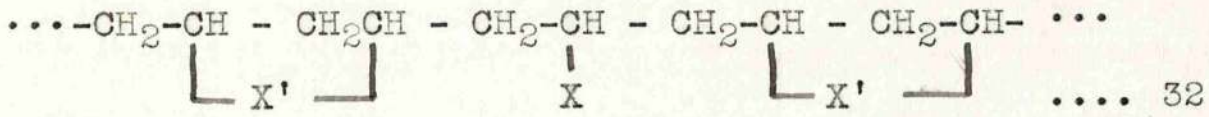

.... 32

If the probability of reaction of any pair of unreacted monomer units is constant, then the fraction of 'widows' may be calculated as follows:

In a group of polymer molecules containing n structural units of type 31, let the average number of 'widows' be S_n. Then $S_0 = 0$, $S_1 = 1$, $S_2 = 0$, and $S_3 = 1$. When $n = 4$, initial coupling may take place in the 1:2-, 2:3-, or 3:4-position:

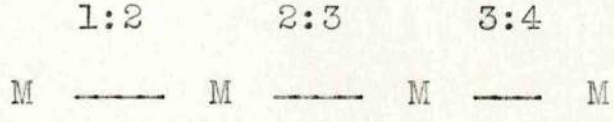

This is equivalent to leaving an n = 2 molecule (in the case of 1:2- and 3:4-linkage) or two n = 1 molecules (in the case of 2:3-linkage). Hence:

$$S_4 = (2S_2 + 2S_1)/3,$$

and $$S_5 = (2S_3 + 2S_2 + 2S_1)/4.$$

In general, therefore, it may written that

$$S = (2/n-1)(S_1 + S_2 + S_3 + \cdots\cdots + S_{n-2}) \quad \ldots\ 33$$

Thus, $$S_n(n-1) - S_{n-1}(n-2) = 2S_{n-2}.$$

By subtracting S_{n-1} from each side of this equation, and letting $S_n - S_{n-1} = D_n$, we have:

$$(n-1)D_n = S_{n-2} - D_{n-1}, \quad \ldots\ 34$$

and $$(n-2)D_{n-1} = S_{n-3} - D_{n-2}. \quad \ldots\ 35$$

The difference (equation 34 - equation 35) leads to the relationship:

$$D_n - D_{n-1} = (-2)^{n-1}/(n-1)! \cdot (D_1 - D_0),$$

and since, from this equation,

$$D_2 - D_1 = -2(D_1 - D_0) = S_2 - S_1 - (S_1 - S_0) = -2,$$

then $$D_1 - D_0 = 1,$$

and $$D_n = 1 - 2/1! + 4/2! + 8/3! + \cdots + (-2)^{n-1}/(n-1)! \quad \ldots\ 36$$

When $n \rightarrow \infty$, equation 36 becomes the series expansion for $1/e^2 = 0.1353$. Thus, for a high molecular weight ($n \geq 20$), the proportion U of isolated monomer units

is very nearly 13.53%.

Application to the Cyclisation of Rubber. - In the cyclisation of rubber the final unsaturation content is therefore:

$$\left[0.5(1 - 1/e^2) + 1/e^2\right] 100 = 56.8\%,$$

in striking agreement with Fischer and McColm's experimental value (cf. page 60).

Preliminary investigations by Gordon (32) showed that the kinetics of the cyclisation reaction approximates closely to a first order law (cf. Section 2c). Later, using an improved experimental technique, this worker (19) revealed that slight variations from this law are excellently accommodated by the above statistical theory, which confirms the molecular mechanism in equation 30.

-----oOo-----

2b. SUMMARY.

A technique is described for freeing fully cyclised rubber latices from high concentrations of H_2SO_4 catalyst in the serum. The method is applicable to other problems involving the removal of ionised solutes from aqueous solutions in general; the final concentration of solute is not greater than 0.05M.

Four cyclised natural (Hevea) rubber latices, independently prepared from two batches of Dunlop 60% latex, have been treated in this way, and subsequently hydrochlorinated using a micro-technique. Reaction progress was followed by density measurements on the purified polymer, calibrated against chlorine content. The initial hydrochlorination rates were independent of the concentration of unreacted double bonds in the

cyclised polymer. However, reaction rates varied from latex to latex over a 100-fold range. In three cases reaction progress came to a halt at a chlorine content of 12.3 $\pm$ 0.2 mole% hydrochlorination.

This value approximates closely to one due to Flory (38), which predicts theoretically the proportion of 'widowed' monomer units in intramolecular chain-polymer mechanisms involving co-operation between two adjacent monomer units. It is concluded that double bonds in the ring structure of cyclised rubber, unlike those in the isolated isoprene units, are unreactive to HCl. The latter can therefore be estimated quantitatively.

A mechanism of rubber cyclisation involving intramolecular ring closure, to give a structure first proposed by D'Ianni (37) and subsequently supported on kinetic and statistical grounds by Gordon (19, 32), is confirmed.

--------ooOoo--------

2c. EXPERIMENTAL.

Density-Gradient Method for Following Reaction Progress. - The progress of cyclisation, and subsequent hydrochlorination, of four natural rubber latices to be described was followed by density measurements on samples of the purified polymer. The principles and accuracy of the method were discussed earlier (cf. Section 1c). The density ranges in question:

(a) Cyclisation of natural rubber: 0.9040 - 0.9880 g./cm^3., and

(b) Hydrochlorination of cyclised rubber: 0.9020 - 1.0200 g./cm^3.

were covered by three density-gradient tubes (cyclisation: Tubes 1 and 2, Appendix 1; hydrochlorination: Tube S, Appendix 10). Owing to the narrower density

range in (b), the number of calibrated floats was high (0.0037 g./cm^3/float) in comparison with (a) (0.0116 g./cm^3/float). It is doubtful whether this represents an appreciable increase in accuracy of density determination, which depends primarily on the linearity of the gradient solution.

Latex samples (20-40 mg.) were flocculated, purified, dried, and pressed, prior to density measurement, in the manner described in Section 1c. Extra care was taken to free solid cyclised rubber from H_2SO_4, which is less volatile than HCl, by prolonged washing. The high concentration of Vulcastab LW in Latex C (cf. Table 14) made flocculation unnecessarily difficult, and increased the required amount of acetone in the flocculating medium to about 75%. In addition, the resulting flocculate was finely divided and difficult to filter.

Preparation of Cyclised Rubber Latices. - The preparation of four cyclised rubber latices (A, B, C, and D) was based on kinetic measurements by Gordon (32), using 70-80% H_2SO_4 in the serum. A linear relationship exists

between log k_s (the cyclisation rate constant) and C (the percentage concentration of H_2SO_4 on the water plus acid content):

$$\log k_s = 6 + 0.17C - 7105/T \quad \ldots\ 37$$

where T is the temperature on the absolute scale. A trial run, at the composition listed in Table 14 (reaction time t = 10 hr., k_s = 0.0115 min.$^{-1}$, C = 74.8%), overshot the target density (32) (cf. page 67) after 7 hr. at 68°C. The onset of serious oxidation, to which cyclised rubber is readily susceptible (32), was evidenced by the evolution of much SO_2.

Table 14.

Composition of Cyclising Media.

Latex	Hevea (64%)	Vulcastab LW	H_2SO_4 (98%)	C
Trial	75 g.	3.0 ml.	96.5 g.	74.8%
A	50	2.5	68.0	75.3
A*	50	2.5	82.5	77.0
B	50	2.5	73.5	76.6
C	50	5.0	82.5	76.6
D	50	2.5	73.5	76.6

* Latex A fortified with further H_2SO_4 since initial k_s too low.

Subsequent latices were prepared at reaction temperatures below 65°C (Table 14), and were blanketted throughout against atmospheric oxidation with CO_2 ('Drikold') or nitrogen (cylinder), a small percentage of oxygen in both of these gases being ignored.

Table 15.

Cyclised Hevea Latices - Reaction Conditions.

Latex A	19 hr. 45°C d=0.91	3 hr. 60°C 0.91	1 hr. 64°C 0.93 g./cm.^{3}		
Latex A*	17 hr. 40°C 0.97	4 hr. 64°C 0.9869	1¼ hr. 64°C 0.9873	64°C 0.9874	
Latex B	11¾ hr. 60°C 0.98	½ hr. 64°C 0.98	1 hr. 64°C 0.9838	2 hr. 64°C 0.9845	2½ hr. 64°C 0.9844
Latex C	3 hr. 60°C 0.9856				
Latex D	16 hr. 45°C 0.96	2 hr. 50°C 0.97	3 hr. 55°C 0.9842	1 hr. 55°C 0.9841	1 hr. 56°C 0.9845

* Latex A increased from C = 75.3% to C = 77.0%.

Relatively low reaction temperatures (40-45°C) were used initially (Table 15), but these were increased as the current value of k_s, from density measurement, became available. Cyclisation was taken as complete when the polymer density reached a steady value within the range $0.9820 \leqslant d \leqslant 0.9870$ g./cm.^{3}, over three consecutive determinations. The value C = 75.3 for Latex A gave an impracticably low value to k_s and was subsequently increased to C = 77.0.

Quantitative estimations of k_s and C were unnecessary, but cyclisation rates were of the order of magnitude predicted by equation 37. No apparent relationship exists between the concentration of H_2SO_4 and the final density of cyclised rubber.(cf. Table 15).

Removal of H_2SO_4 from Cyclised Rubber Latex. - It was shown in Section 1 that bulk and surface hydrochlorination rates in rubber latices are scarcely affected by concentrations of H_2SO_4 in the serum as high as 20%. However, since higher concentrations of catalyst were used in Latices A-D (viz. C = 75-80%), this was removed prior to hydrochlorination as a precaution against abnormal kinetics.

A new and successful method for the removal of H_2SO_4 from cyclised rubber latex by electrolysis, using suitable semi-permeable membranes (cf. Table 16) Suggested by Permaplex Ltd.

Table 16.

Semi-permeable Membranes for Electrolysis.

Membrane.	Functional group.	Impermeable to:
Permaplex A10 ('Zeo-carb 225')	SO_3H	Cations (H^+)
Permaplex C10 ('DE-acidite FF')	Quaternary NH_4	Anions ($SO_4^=$)

Both membranes are essentially impermeable to ions of the same charge as the functional group up to concentrations of 1N. Above this, the Donnan effect may cause leakage and therefore decreased selectivity. The process is illustrated diagramatically on page 73.

Under the influence of a potential difference between a and c, H^+ and $SO_4^=$ ions from the acid-latex compartment b pass into c and a respectively through the semi-permeable membranes, which act as barriers to the ion of opposite charge in each case. The electrical

circuit through the cell is completed by the discharge of H^+ ions as gaseous hydrogen in compartment c:

$$2H^+ + 2e = H_2$$

and of $SO_4^=$ ions as H_2SO_4 in compartment a, with the evolution of oxygen:

$$2SO_4^= + 2H_2O = 2H_2SO_4 + O_2 + 4e$$

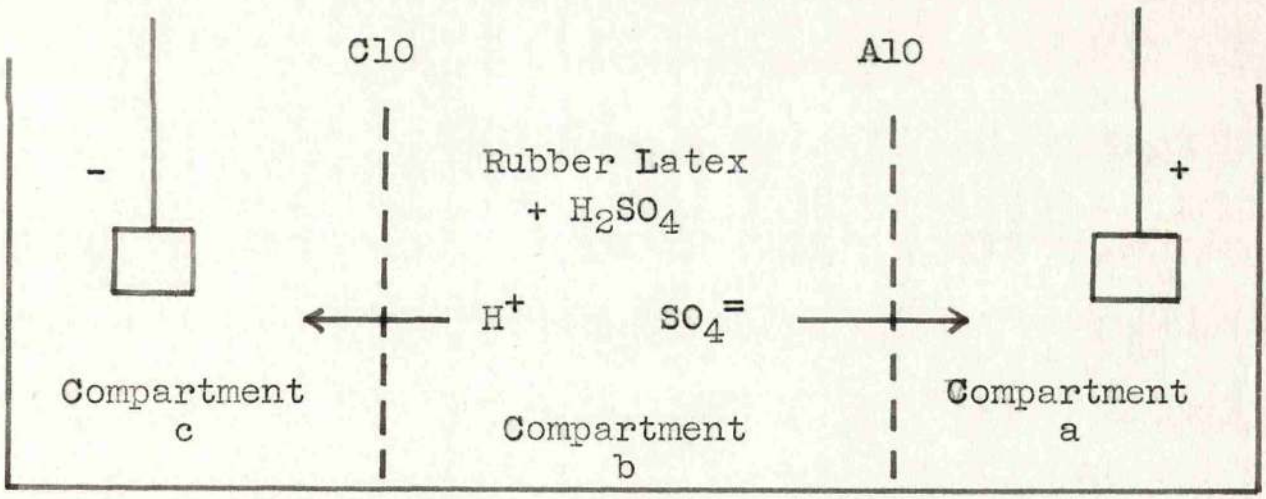

In effect, the process is a transfer of H_2SO_4 from b to a. 10% aqueous Na_2SO_4 was found to be a suitable electrolyte for compartments a and c.

Design and Operation of the Electrolytic Cell. - The three separate compartments (a, b, and c, Fig. 15) were built up individually using acid-resisting rubber sections, held together with rubber solution. Square

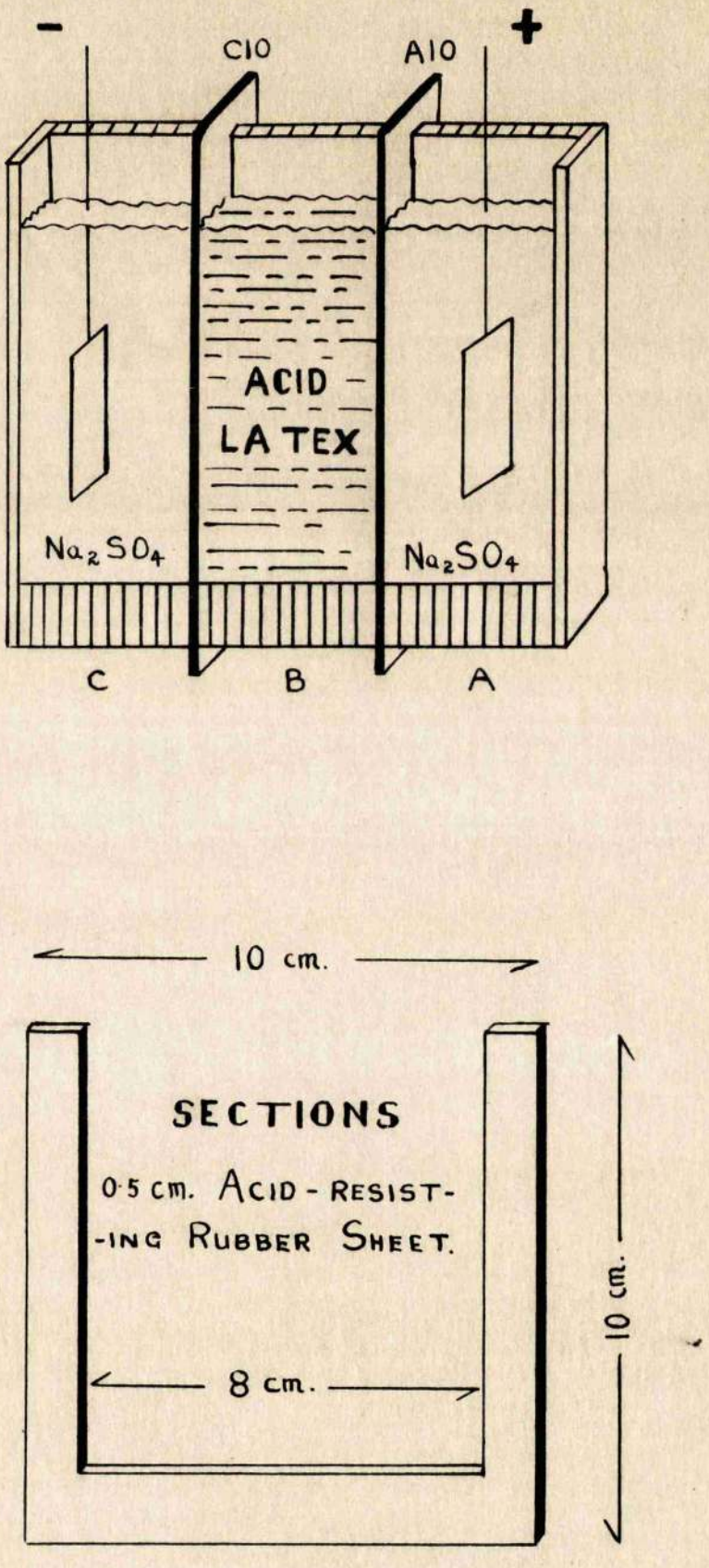

Fig. 15 - Construction of the Electrolytic Cell.

end-pieces were fitted to compartments a and c. The semi-permeable membranes were cut to overlap the rubber sections by 0.5 cm. all round, and the cell was joined together, as a whole, using rubber solution at the rubber/membrane surfaces. No leaks developed after an extended period provided the cell was clamped horizontally. Final capacities in the three compartments were:

Compartments a and c (section 2 cm.) - 120 ml.

Compartment b (section 1 cm.) - 60 ml.

Compartments a and c were filled with electrolyte (75 ml.) and the cyclised rubber latex was placed in b. A potential of 312 volts, across two platinum electrodes in a and c, fell to 17 volts at a steady current of 450 mA. This value was a maximum set by the acceptable temperature rise within the cell. An upper limit of 35°C was adopted (critical temperature of membranes = 60°C).

To ensure correct working, the total amount of gas evolution at the two electrodes was roughly checked against the theoretical. The anode compartment became rapidly acid, and a slight simultaneous alkalinity (to indicator paper) which developed at the cathode was attributed to a slow penetration of $SO_4^=$ ions through membrane C10. The anode solution was renewed at 30 min.

intervals to prevent back diffusion of accumulating H_2SO_4

A rough calculation on Latex B (C = 76.6) shows that the latex compartment contained about 21 g. of H_2SO_4. At a current i = 450 mA, the required electrolysis time is given by:

$$t = F/i = 26.5 \text{ hr.}$$

which is in good agreement with the experimental figure of 25.5 hr.

The removal of H_2SO_4 from compartment b caused a 50% volume decrease, and consequently a thickening of the latex. To avoid undue coagulation, 15 ml. of distilled water were added to the latex during electrolysis, over a period of 12 hr. The characteristic red colour of freshly cyclised rubber latex progressively turned to cream as the acid was removed. Completion of the electrolysis process was heralded by a gradual rise in cell temperature, resulting from an increase in internal resistance due to the removal of conducting ions from compartment b, and to coagulation of solid polymer on the membrane surfaces. The latter effect was caused either by local overheating in the cell or to discharge effects on the

colloidal polymer.

The process was forced to completion in the case of Latex C by steadily increasing the voltage across the cell. In this way, a large percentage of polymer was lost through coagulation. The resulting acid-free latex was re-concentrated by evaporation *in vacuo* (60°C) in a stream of CO_2. Processing of Latices A, B, and D was stopped on reaching a current of 300 mA, so that no concentration was necessary. The final acid contents were surprisingly low and constant at pH 3.9 (Latex A), pH 4.1 (Latex B), and pH 3.6 (Latex D), measured against a standard potassium phthalate buffer (0.05M = pH 3.99) on a Marconi meter. Based on an estimation of the composition of acid-free latex (cf. part 4 of Table 19), the H_2SO_4 concentration in the aqueous phase is calculated to be not greater than 0.001% (0.05M).

The above method is equally applicable to other problems involving the removal of ionised solutes from aqueous media, while avoiding the addition of further contaminants.

Typical operating conditions are recorded in the following table:

Table 17.

Working Conditions in the Electrolytic Cell (Latex A).

Location.	Top temp.	Bottom temp.	Current. i	Voltage. Loaded.	Unloaded.
Anode a	36°C	22.0°C			
Latex b	34	20.5	450 mA	17 v	312 v
Cathode c	34	20.5			

The sodium content of acid-free Latex C, estimated as Na_2SO_4 (39), was only 0.27% - a quantity not in excess of that to be expected in natural rubber. This showed that the cell was working efficiently without undue back-diffusion or electro-osmotic effect. The densities of the cyclised latices, after electrolysis, were re-determined as initial densities (d_o) for subsequent hydrochlorination. Small reductions on the previous values of d_o for Latices A, C, and D (cf. Table 15) were evident. Latex B was unaffected in this way.

Table 18.

Initial Densities (d_o).

Latex	A	B	C	D
d_o g./cm.^{3}	0.9868	0.9845	0.9850	0.9824

Hydrochlorination of Cyclised Acid-free Rubber Latices. - Hydrochlorinated derivatives have been prepared from acid-free cyclised Latices A, B, C, and D. The experimental technique and micro-reactor used were described in Section 1c (cf. Fig. 1).

(a) Technique. - Several minor changes in procedure were necessary when using cyclised rubber latices:

1. Slow reaction rates (in Latices A, B, and D) necessitated an increase in HCl pressure to $2\frac{1}{2}$ atm. (190 cm. Hg). This is an upper limit for this design of glass/polythene apparatus.
2. At $2\frac{1}{2}$ atm. and $-70^{\circ}C$, HCl gas liquefies in the reaction flask (B, Fig. 1), and collects as a layer on the frozen latex. Care is required to evaporate the reactant slowly, to avoid violent disturbance of the mercury column A. The procedure is as follows: When the mercury level in the narrow limb of A reaches 25 cm. from the base, the reaction flask is removed from the freezing mixture. If the total pressure so generated falls short of 190 cm., it is brought up rapidly by heating the generator C.
3. A sharp rise in softening temperature is evident in the cyclised/hydrochlorinated polymer, even at

low (2 mole% or less) hydrochlorination. Superheated steam is required for pressing.

4. Stored latices require to be stringently guarded atmospheric oxidation by a blanket of inert gas. Even with this precaution, Latex C was found to oxidise after only two weeks storage.

(b) Results of Hydrochlorination. - Under similar conditions of temperature (26.7°C) and pressure (2 atm. HCl) the four latices were found to hydrochlorinate at widely differing rates. Only Latex C was comparable with natural rubber in this respect. Comparatively severe conditions ($2\frac{1}{2}$ atm., 0°C) were required to raise the reaction rates of Latices A, B, and D to a practicable value (0.5-1.0 mole% hydrochlorination per hr.)

As a calibration of hydrochlorination against polymer density, six micro-samples, drawn at different stages of reaction, were submitted for chlorine analysis (Appendix 11a) to Drs. Weiler and Strauss, Oxford. Fig. 16 shows that the plot of specific volume (V) against hydrochlorination (wt.%) is linear. For this plot, the small variations in initial density d_o (cf. page 77) were corrected to the average value $d_o = 0.9847$ g./cm.^{3}. Thus in Appendix 11a, reported

specific volumes are corrected by a small constant factor for each latex , according to equation 38:

$$V = 1/\left[d - (d_o - 0.9847)\right] \quad \text{cm.}^3/\text{g.} \qquad \ldots\ 38$$

The kinetic curves (mole% hydrochlorination versus time of reaction) for Latices A (Fig. 17), B (Fig. 18), C (Fig. 19), and D (Fig. 20) are based on density determinations on the hydrochlorinated/cyclised polymer, adjusted according to equation 38 (Appendices 11b-11c) and interpolated directly in Fig. 16.

Composition of Latex Media. - Estimations of the compositions of latex media involved, are useful in summarising the experimental procedure described in this Section. Table 19 (page 81) lists appropriate data for a rubber latex cyclised and hydrochlorinated under standard conditions (C = 75%, d_o = 0.9847 g./cm.^{3}, mole% hydrochlorination = 12.2%). The calculations are based on 100 g. of cyclised rubber latex (before removal of H_2SO_4).

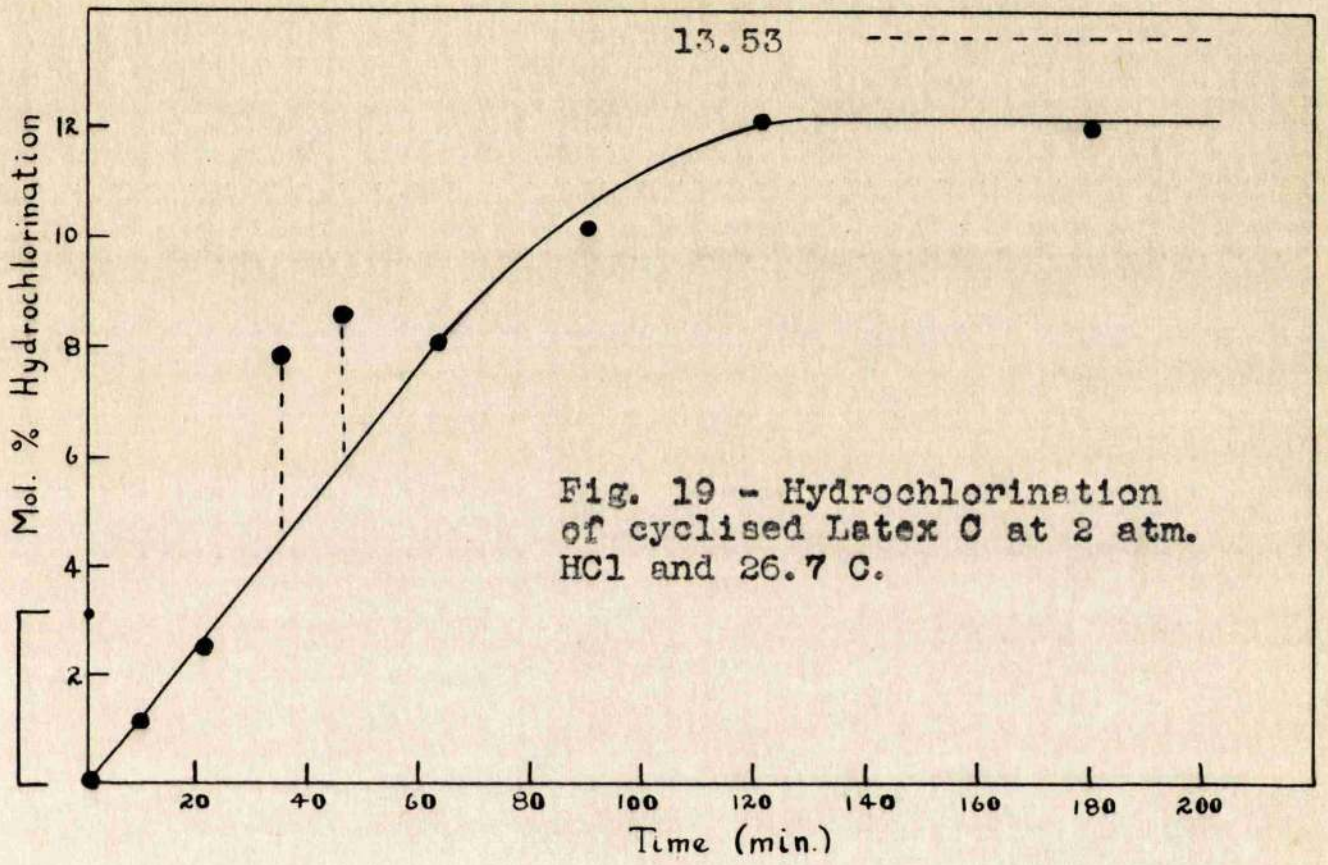

Fig. 19 - Hydrochlorination of cyclised Latex C at 2 atm. HCl and 26.7 C.

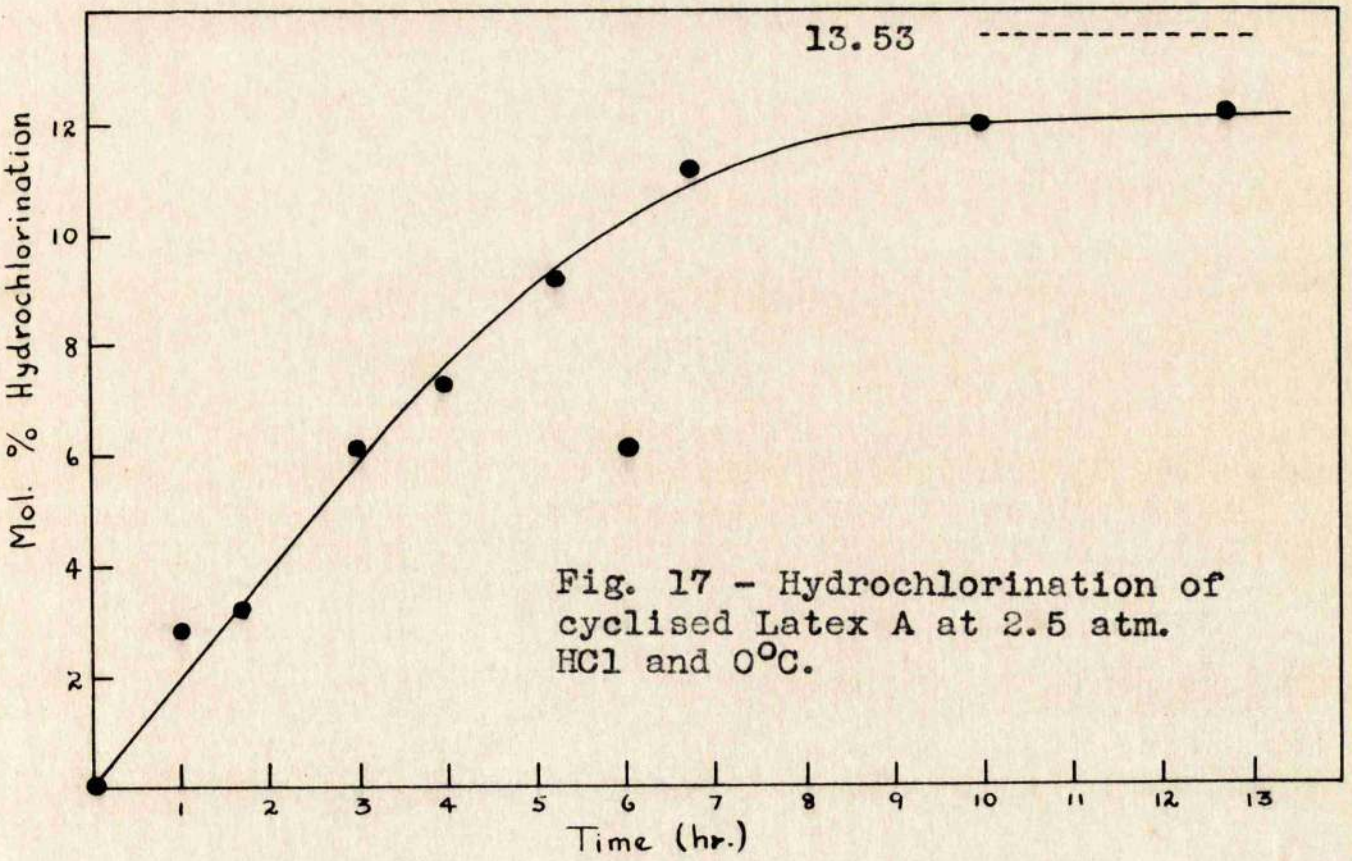

Fig. 17 - Hydrochlorination of cyclised Latex A at 2.5 atm. HCl and 0°C.

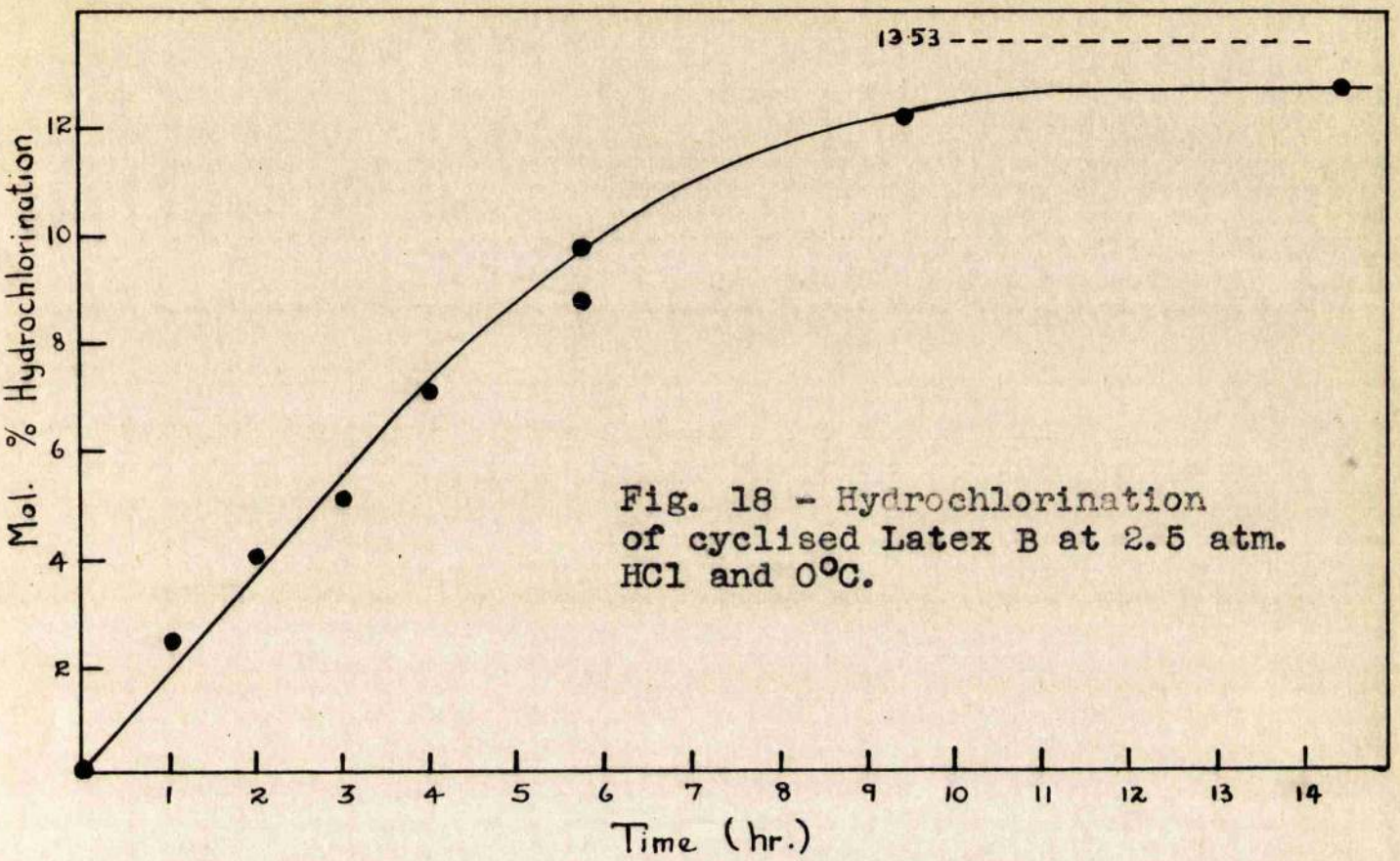

Fig. 18 - Hydrochlorination of cyclised Latex B at 2.5 atm. HCl and 0°C.

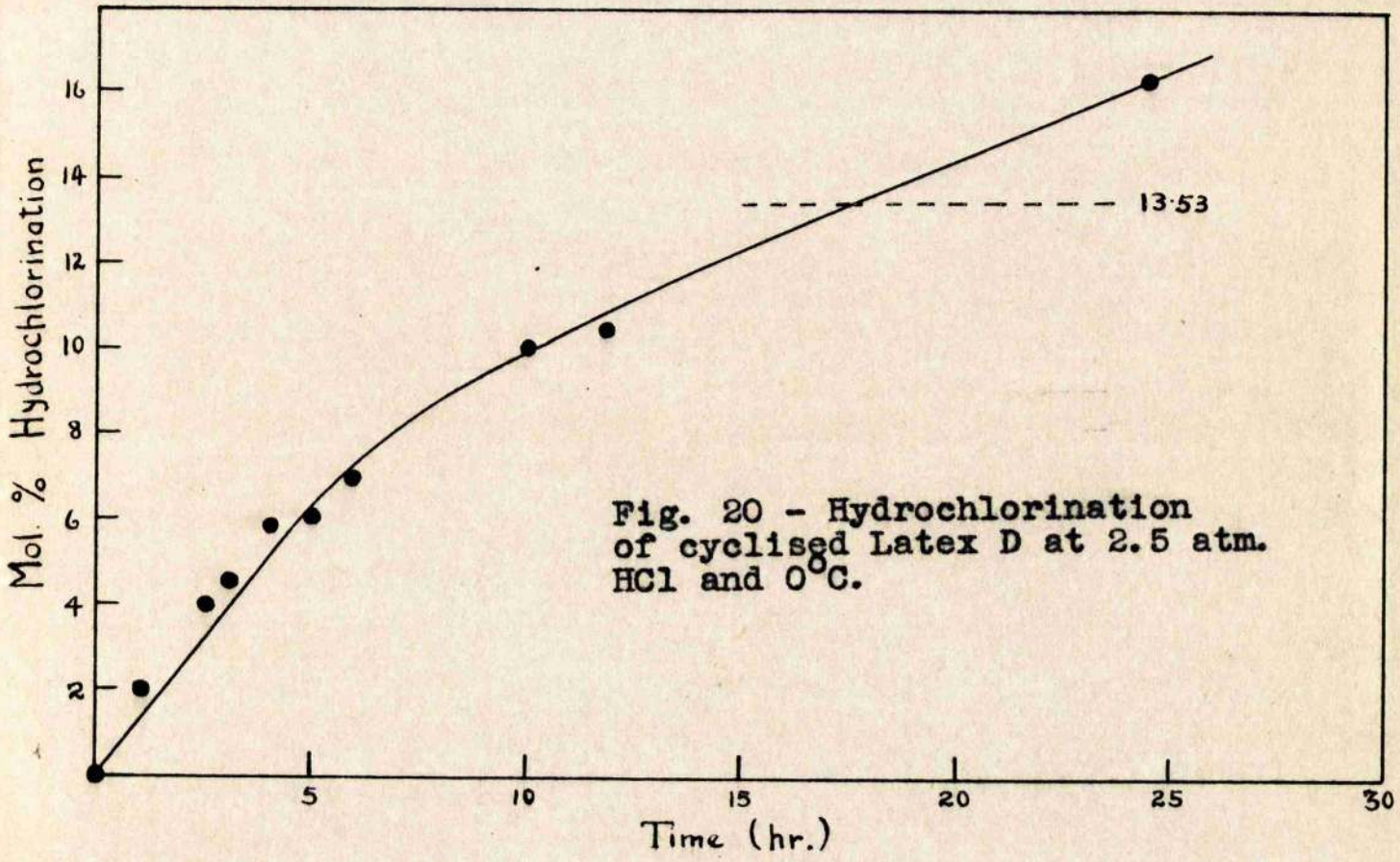

Fig. 20 - Hydrochlorination of cyclised Latex D at 2.5 atm. HCl and 0°C.

Table 19.

Compositions of Latex Media at 26.7°C.

	Medium.	Constituents.	Individual compositions.			Total composition.		
			wt.	vol.	dens.	wt.	vol.	dens.
1	Natural rubber latex.	water	18.2	18.3	0.997	45.5	48.5	0.983
		rubber	27.3	30.2	0.904			
2	Prepared cyclising emulsion.	water	18.2	18.3	0.997	100.0	78.4	1.275
		rubber	27.3	30.2	0.904			
		H_2SO_4	54.5	29.9	1.824			
3	Cyclised rubber latex	water	18.2	18.3	0.997	100.0	75.9	1.318
		polymer	27.3	27.7	0.985			
		H_2SO_4	54.5	29.9	1.824			
4	Acid-free latex.	water	48.0	48.2	0.997	75.3	75.9	0.992
		polymer	27.3	27.7	0.985			
5	Cyclised hydrochlortd. latex	water	48.0	48.2	0.997	77.0	76.9	1.001
		polymer	29.0	28.7	1.009			

------oOo------

2d. DISCUSSION.

Hydrochlorination of Cyclised Rubber Latices. - The hydrochlorination of four cyclised Hevea rubber latices, independently prepared from two separate batches of natural latex, has been shown to follow a similar kinetic pattern in three cases. Within the experimental accuracy, the initial portion of the plot of M (mole% hydrochlorination) against t (reaction time) in Figs. 17-20 is linear; and, on this basis, the following experimental zero-order rate constants (k_e) have been calculated:

Table 20.

Experimental Zero-order Rate Constants (k_e).

Latex.	C	D	A	B
Pressure.	2 atm.	$2\frac{1}{2}$	$2\frac{1}{2}$	$2\frac{1}{2}$
Temperature.	26.7°C	0.0	0.0	0.0
Reaction rate.	6.00 mole%/hr.	0.89	0.99	1.26
Rate constant.*	0.0222 $min.^{-1}$	0.0033	0.0036	0.0047
Maximum conversion.	12.16 mole%	-	12.24	12.51

* Based on 13.53 mole% hydrochlorination = 100% reaction.

Only in the case of Latex D did the hydrochlorination proceed beyond M = 13.53 (near which there is a sudden arrest in the reaction rates of Latices A, B, and C), although 75% of the original unsaturation remained unaffected.

Varying Reactivity to HCl of Double Bonds in Cyclised Rubber. - According to Gordon's cyclisation mechanism in equation 30, the structure of the 'starting' cyclised polymer (cf. part 4 of Table 19) is governed by the relation:

$$U/I = 0.568$$

where I = total number of isoprene units in an average cyclised rubber chain, and U = the total number of double bonds in a similar chain. The present work has established basically that the quantity U is composed of double bonds of two different types in the polymer chain, since a percentage may be isolated chemically by enhanced reactivity towards HCl.

Mechanism of Hydrochlorination. - The unsaturation content (12.1-12.5 mole%) reactive to HCl is close to Flory's theoretical value (13.53 mole%) determining the

number of isolated units which would result from the statistical effect envisaged by Gordon in equation 30. It is concluded that the kinetic curves in Figs. 17-20 represent (almost) stoichiometric completion of the reaction:

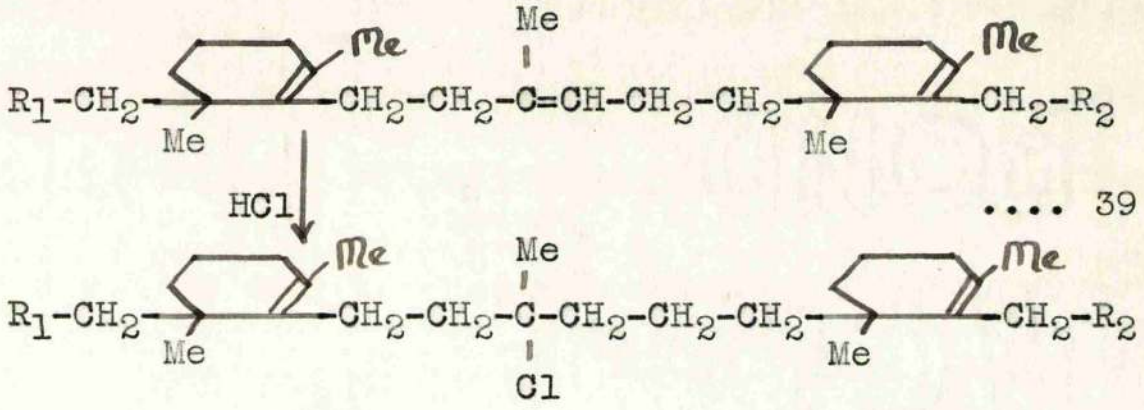

where HCl attack is exclusively on the <u>chain</u> double bond (and is, of course, expected to result in normal Markownikoff addition). Although Gordon's kinetic evidence (19) is already conclusive regarding the accuracy of the cyclisation mechanism underlying equation 30, the present work is a fundamentally new approach to the problem, in t that it differentiates between the two different types of unsaturation present, and thereby permits separate quantitative estimation. The evidence is now overwhelmingly in support of Gordon's proposed mechanism (equation 30).

The reactivity of structure I, constituting di-isoprene rings, is restricted towards saturation with HCl in comparison with structure II, which occurs in polyisoprene chains:

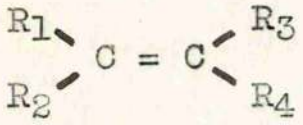

I

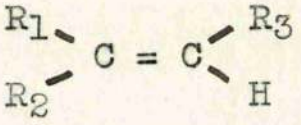

II

This is due either to the presence of four substituents or, more likely, to the increased stability of six-membered rings.

The Enhanced Reactivity of Latex D. - At best, the difference in reactivity between the two types of unsaturation must be small, since in the case of Latex D hydrochlorination was carried beyond the theoretical value (13.53 mole%), although k_e was comparable with Latices A, and B. This result confirms the work of Fischer and McColm (33, 34) who, in preparing hydrochlorinated derivatives from cyclised rubber, found an inconsistency in the chlorine content of several samples. Using solid rubber under various conditions, conversion was carried as far as M = 34.5 mole% in one case. The irregularities

were attributed to changes in unsaturation content during the reaction. Assuming that initial hydrochlorination involves only chain double bonds, then conversion beyond M = 13.53 has two possible routes:

(1) Direct addition of HCl across a ring double bond to give:

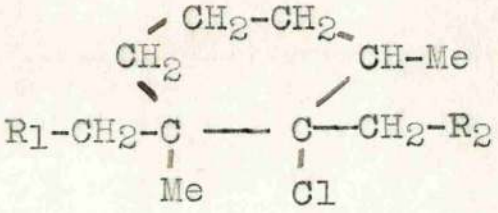

(2) Splitting of the ring structure, and subsequent hydrochlorination in the normal manner associated with polyisoprene chains:

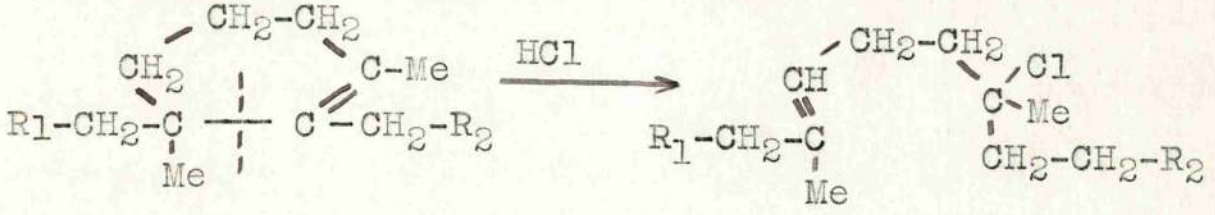

The nature of the calibration curve (Fig. 16) favours the latter mechanism since:

$$d(\text{wt.\% hydrochlorination})/dV = 763 \qquad \ldots\ 40$$

This value enables the plot to be extrapolated linearly to W = 100 wt.% hydrochlorination, using $V_o = 1.015$

for polyisoprene (12):

$$1.015 - (100/763) = 0.882 \text{ cm.}^3/\text{g.}$$

Since the completion of the second route results finally in fully hydrochlorinated rubber, the above extrapolation can be compared with the value $V_o = 0.906$ cm.^{3}/g. for rubber hydrochloride found by Crampsey, Gordon, and Taylor (12). Considering the long extrapolation involved, and the inaccuracies in micro-analysis inherent in Fig. 16, the agreement is excellent.

Maximum Hydrochlorination of Latices A, B, and C. - The maximum conversion of Latices A, B, and C (M = 12.1-12.5) is, on the average, 1.2 mole% short of Flory's theoretical value (i.e. little more than the experimental error of 1%, see below). The closeness of the three values, however, (cf. Table 20) suggests that they represent a real deficiency in chlorine content compared with the theoretical, in the ratio 12.3/13.5 = 9/10. This is not unexpected, since it is paralleled in bulk hydrochlorination of natural rubber (5, 6), where the maximum conversion is about M = 93% . This has been attributed in the past (12) to a gradual reduction in the diffusion rate, through the increasingly crystalline substrate (rubber hydrochloride), of the reactant. The molecule represented

in equation 39 is too irregular for any chance of crystallisation, and the evidence suggests, rather, that, for some unknown reason, 8-10% of isoprene units in natural rubber are unavailable for hydrochlorination.

In view of the zero-order kinetics and the similarities in substrate, it seems likely that hydrochlorination of cyclised rubber is governed by a mechanism akin to that described by Gordon and Taylor (cf. Section 1a, page 4) for bulk hydrochlorination of natural rubber. An alteration of the equilibrium:

$$2HCl \rightleftharpoons (H_2Cl^+.Cl^-)$$

in favour of the covalent form, by a slight change of substrate from rubber to cyclised rubber, would result in a lower reaction rate, in agreement with the experimental.

Relative Hydrochlorination Rates in Latices A, B, C, and D. - The variation in hydrochlorination rates among the four cyclised latices studied remains unexplained. The experimental rate constants (k_e, Table 20), although spread over a seven-fold range (0.0222-0.0033), cannot be satisfactorily compared in this form owing to the inconformity of reaction conditions. However, a method is available for adjusting values of k_e to a standard set of

reaction conditions (here: 2 atm. HCl, 26.7°C) which, in effect, changes the time-axes of Figs. 17, 18, and 20 by a factor. In Section 1 (cf. Table 7) it was shown that a pressure increase from 2 to 2½ atm. raises the bulk hydrochlorination rate of natural rubber by a factor of 3.9. In addition, by lowering the reaction temperature from 26.7°C to 0°C, a further factor of 4 is incurred (7). On the assumption that comparable conditions prevail in the cyclised latices under discussion (a fact which is bourne out, at least qualitatively, by the trial runs on Latices A, B, and D at lower pressures and higher temperatures, cf. Appendices 11b, 11c, and 11e), values of k_e listed in Table 20 represent a true variation in reaction rate constant (k_r) of more than 100-fold (Table 21).

Table 21.

Relative Reaction Rate Constants (k_r).

Latex	A	B	C	D
k_r*	0.00023	0.00030	0.02220	0.00021

* At 2 atm. HCl and 26.7°C.

Effect of Starting Material on k_r. - The small spread in the values of k_r among the latices A, B, and D is

significant since they are taken from the same batch of natural latex, in contrast to Latex C. Although the range k_r = 0.00021-0.00030 $min.^{-1}$ (cf. Table 7) is just outwith the experimental accuracy, it cannot be claimed that k_r = 0.02220 $min.^{-1}$ for Latex C is a property only of the starting material without further experimental confirmation. In this connection the effect of a basic retarding substance in the natural latices used may be considered. The reaction rate of Latex C (6 mole%/hr.) is comparable with that of the retarded hydrochlorination rate k_1 (cf. page 4) in natural rubber (15 mole%/hr.) under the same reaction conditions. It is unlikely that greater or smaller concentrations of such a substance could affect changes in k_r after cyclisation, since all retarder would be removed (7) by the high concentrations of H_2SO_4 used as cyclisation catalyst.

Effect of Particle Size of Cyclised Latices on k_r. - Electron microscope photographs (for experimental details cf. Section 1c, page 25) at 6000X of particles of Latex B revealed a high degree of coagulation (about 10μ), which was of the order of hundreds of particles. It is uncertain whether such coagulation is due to colloidal discharge during electrolysis or to overheating on the electron

microscope staging. The latter alternative was supported by a projection microscope test at 2000X, in which the average particle size was less than 1μ. A hydrochlorination rate, varying in value with a change in particle size after cyclisation, due to the retarded rate of penetration of HCl into giant particles (1 particle $> 10^4$ molecules) would be characterised by high reaction order (cf. Section 1d) in contrast to the present results.

Accuracy of Kinetic Measurements. - The accuracy of the plots in Figs. 17-20 rests on three factors:

(a) Chlorine Analyses in the Calibration Curve (Fig. 16). - The line is well defined by six points, although a seventh is wide. Scatter is almost certainly due to chlorine analysis, which was on the micro-scale. At the outside the accuracy is to 1 wt.% hydrochlorination, although a considerably better figure can be claimed since the plot is confirmed, on extrapolation to W = 100% by outside evidence (cf. page 86 et seq.).

(b) Density Measurements. - The overall scatter of polymer films is only about 0.5% reaction (cf. page 18), and this resolves to a better (about 0.3% reaction) when 10-15 films are used for averaging.

(c) Determination of Reaction Time. - Uncertainties in

in reaction time (t), when starting and stopping the micro-reactor (Fig. 1), may be considered as a source of error. Hydrochlorination begins as soon as the frozen latex melts, but is negligible until complete saturation with HCl is achieved. This point in procedure was taken as zero-time. On completion of the reaction, the pressure is returned to atmospheric and the latex immediately flocculated, giving the end-point. Using a standard technique, the uncertainty in t, combining both causes, does not exceed 10 sec. - a value equivalent to only 0.3% reaction at the minimum t used (5 min.).

Acknowledgment.

Acknowledgment is due to Dr. M. Gordon and Mr. A. Papadopoulos, late of the Technical Chemistry Department, Royal Technical College, Glasgow, for the preparation of Latex C and for preliminary work in the design of (perspex) electrolytic cell which led to the version described here.

------oOo------

SECTION 3.

GLASSY AND RUBBERY COEFFICIENTS OF EXPANSION AND SECOND ORDER TRANSITION TEMPERATURES OF RUBBER-RUBBER HYDROCHLORIDE COPOLYMERS - A TEST OF THE IDEAL COPOLYMER THEORY.

3a. INTRODUCTION.

In contrast to the melting point (T_m) (40), the second order transition point (θ) of a polymer is a property of the amorphous region only (41). In particular, θ in natural rubber, which contains up to 20% of crystalline material below $T_m = 10^{\circ}C$, is barely influenced by changes in crystallinity. Table 22 summarises reported thermal data for natural rubber in the region of the second order transition temperature:

Table 22.

θ	β_g	β_r	Method.
-	0.00021	-	Thermal expansion (42).
-	-	0.00061	" (43).
$-73^{\circ}C$	0.0002	0.0007	" (44, 45).
-67 to $-71^{\circ}C$	-	-	Interferometer (46).
$-70^{\circ}C$	-	-	Heat capacity (47).
-73 to $-76^{\circ}C$	-	-	" (48).
$-75^{\circ}C$	-	-	Thermal conductivity (49).

The Position of θ in Copolymers. - The second order transition temperature (θ) of a copolymer lies between θ_1 and θ_2, the second order transition temperatures of the individual component polymers. The work of Ueberreiter (50) and Jenkel (51), on the systems butadiene-styrene ($\theta_1 = -85^{\circ}C$, $\theta_2 = +81^{\circ}C$) and methylacrylate-styrene ($\theta_1 = +3^{\circ}C$, $\theta_2 = +81^{\circ}C$), showed that a plot of θ against M_2 (mole% styrene) curves towards the composition axis. Later workers (52, 53) interpreted from this that $\theta \propto m_2^2$, where m_2 = mole fraction of styrene. Further work, however, on the systems dimethylbutadiene-acrylonitrile (54) and butadiene-acrylonitrile (55) suggested that this parabolic law is only of limited validity.

Since then, several methods have been adopted to arrive at a linear relationship between functions of θ and composition, notably by Gerke (56), Edgar (57), Coleman (58), and Catsiff and Tobolsky (59).

The Ideal Copolymer Theory. - As a general theory, Gordon and Taylor (60) have derived equations for predicting the value of θ in binary copolymers from thermal expansion data alone, provided that ideal volume additivity of individual repeat units can be assumed.

The specific volume of a rubbery copolymer (V_r) is given by:

$$V_r = (1 - w_2)_1V_r + w_2({}_2V_r) \quad \ldots\ 41$$

where the prescripts 1 and 2 represent the individual component polymers. Equation 41 is valid only when both pure polymers are in the rubbery state (i.e. above Θ_2). Similarly, the glassy specific volume of the copolymer (V_g) below Θ_1, where both pure polymers are glassy, is:

$$V_g = (1 - w_2)_1V_g + w_2({}_2V_g) \quad \ldots\ 42$$

Between Θ_1 and Θ_2 there is a specific temperature (Θ) at which the copolymer (w_2) has a second order transition point. Thus, a plot of specific volume (V) against w_2 will change in slope where temperature $T = \Theta$. The exact position of this kink at T can be determined by joining the points ${}_1V_r$ and ${}_2V_r$, and the points ${}_1V_g$ and ${}_2V_g$, which move with temperature according to their appropriate coefficients of expansion ${}_1\beta_r$, ${}_2\beta_r$, ${}_1\beta_g$, ${}_2\beta_g$, respectively. Thus Θ is related to temperature by the equation:

$$w_2 = (\Theta - \Theta_1)/\ k(\Theta_2 - \Theta) + \Theta + \Theta_1 \quad \ldots\ 43$$

where $k = ({}_2\beta_r - {}_2\beta_g)/({}_1\beta_r - {}_1\beta_g) = \Delta({}_2\beta)/\Delta({}_1\beta)$ 44

Equation 43 predicts θ without recourse to a mechanistic theory, requiring only the following measurements:

(a) Rubbery (V_r) and glassy (V_g) coefficients of expansion of the two individual pure polymers.

(b) Second order transition points (θ_1 and θ_2) of the individual pure polymers.

A plot of equation 43 for the system butadiene-styrene, using the published values:

$$\left.\begin{aligned}\Delta({}_1\beta) &= 660 \times 10^{-3}\\ \Delta({}_2\beta) &= 185 \times 10^{-3}\end{aligned}\right\} \quad k = 0.28 \qquad \begin{aligned}\theta_1 &= -85^{\circ}C\\ \theta_2 &= +84^{\circ}C\end{aligned}$$

was shown by Gordon and Taylor (60) to be in agreement with experimental values, and Loshaek (61) has since verified this for a new system.

------oOo------

3b. SUMMARY.

Copolymers of the rubber-rubber hydrochloride system have been prepared by hydrochlorination of acid-stabilised natural (Hevea) rubber latex.

The thermal expansion of micro-samples (1 mg.) has been followed by a density gradient technique, based on a method described by Gordon and MacNab (16). The method has been extended down to -70°C by a suitable choice of gradient solution, and rubbery coefficients of expansion (β_r), and in some cases the corresponding glassy coefficient (β_g) and the second order transition temperature (θ), have been measured over the composition range $0 \leqslant w_2 \leqslant 0.935$.

A second series of β_r determinations between 0°C and 50°C has been carried out on 4-5 g. samples by a dilatometer method, using mercury as the confining liquid.

The merits of the two methods are discussed. The micro-method is shown to be adaptable at high values of w_2, while the macro-method is suitable only below

w_2 = about 0.30. A linear relationship exists between β_r and θ (combining data from both methods), and the plot has been extrapolated to the value $_2\beta_r$ = 0.00048 (at w_2 = 1), which is otherwise unobtainable. The plot of θ versus w_2 is shown to curve towards the composition axis in a manner described by earlier workers (60). Extrapolation gives θ_2 = +36°C (at w_2 = 1). Values of β_g, although less accurate, do not vary appreciably from an average value (0.00024).

Comprehensive thermal data around the second order transition temperatures are now available for both pure component polymers (rubber and rubber hydrochloride). Substitution of the values found in equation 43 supports Gordon and Taylor's ideal copolymer theory (60).

-------oOo-------

3c. EXPERIMENTAL.

Preparation of Rubber-Rubber Hydrochloride Copolymers. - Two methods of preparation of rubber hydrochloride were employed, values of w_2 being determined by the density gradient method described in Section 1 (page 17).

(a) For Gradient Tube Method (Micro-samples). - 10-20 mg. samples were prepared, flocculated, purified, dried, and pressed using the micro-method described in Section 1 (cf. page 12 et seq.) at 2 atm. HCl and 26.7°C. Each sample gave 10-15 pressed films.

(b) For the Dilatometer Method (Macro-samples). - 5-10 g. samples were prepared by passing gaseous HCl (1 atm., 0°C) into acid-stabilised Dunlop 60% latex (40 g.) (cf. page 11) until the required w_2 was obtained. The hydrochlorinated latex was flocculated in 25/75 boiling acetone/water (20 vols.), filtered (Whatman No.1), washed (distilled water, 20 vols.), dried in vacuum (16 hr., 40°C), and purified by evacuation 48 hr., mercury diffusion pump). Sheets of gas-free polymer film (thickness 2-3 mm.) were produced by hot pressing (80-120°C, depending on w_2) between smooth aluminium plates

(12 x 12 x 0.2 cm.). Unpressed edges and sections were removed with a clean blade, and the remainder sliced to 2-3 mm. cubes.

Density-gradient Method for Determining β_r, β_g, and θ. - A modified density-gradient tube was used to follow 1-2 mg. samples of pressed rubber-rubber hydrochloride copolymer for thermal expansion. The obtainable composition range (6) was $0 \leq w_2 \leq 0.935$. The method is a development of that used by Gordon and MacNab (16) for similar measurements on polystyrene.

A Pyrex density-gradient tube (Fig. 21) was constructed with a side-arm (b) carrying a thermistor imbedded in Beck-Koller R1343 resin, and a detachable stopper (c). The tube was immersed in a thermostat (a wide-necked vacuum flask containing water or water/EtOH) and supported by the stopper and side-arm. Heat (via a nichrome coil d) was provided by a mains transformer (6 v.), and thermostatic control (0.05C°) ensured by efficient stirring (e) and by a Tektor proximity on-off switch (g) operated by the mercury column of an accurate thermometer (f). A further refinement (Fig. 22) was included for smooth operation. The tube (a), carrying the Tektor arm, moves along the thread (b) and stabilising slide (c) by rotation of the handle (d). By a

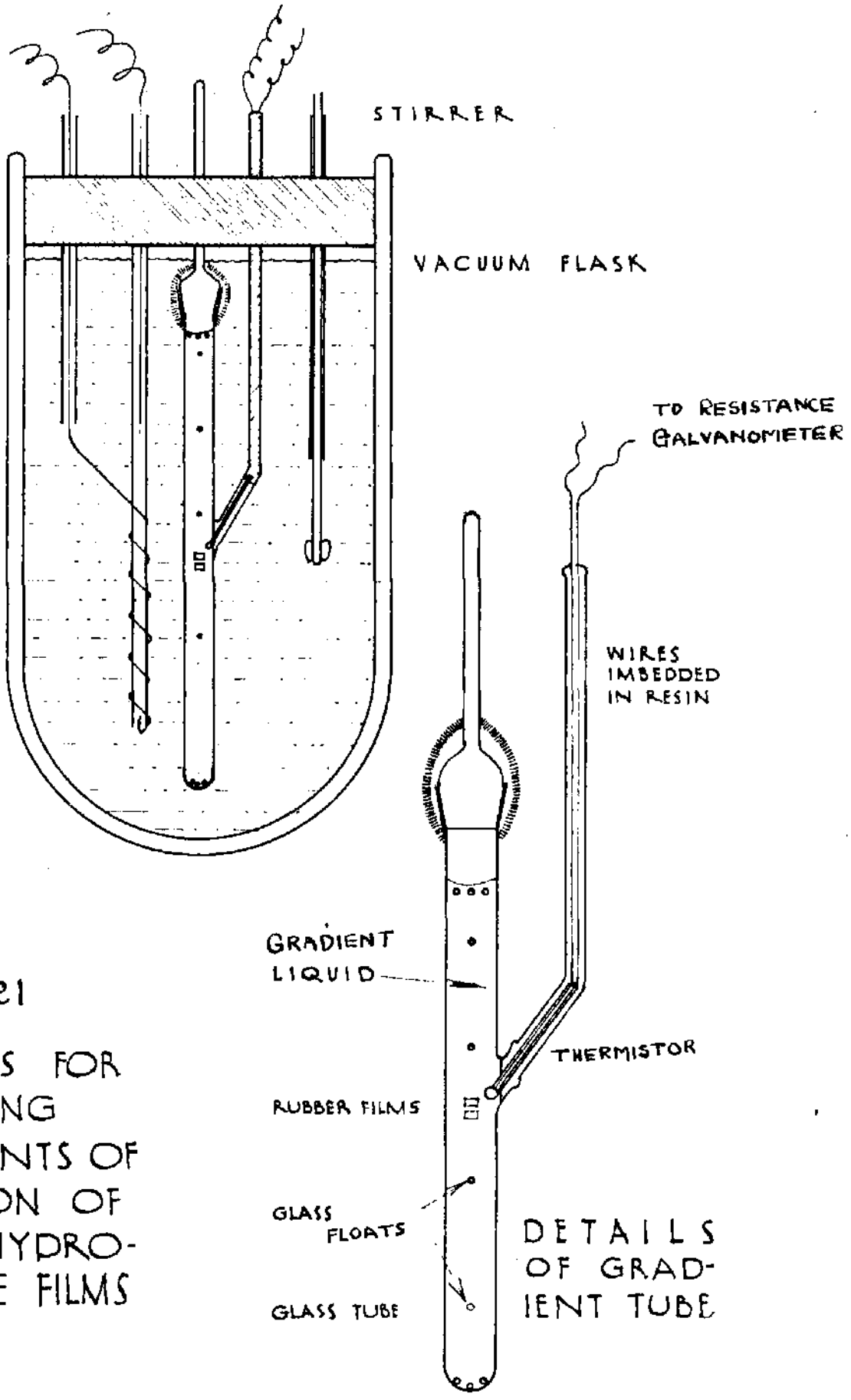

FIG. 21

APPARATUS FOR MEASURING COEFFICIENTS OF EXPANSION OF RUBBER HYDROCHLORIDE FILMS

suitable choice of screw-pitch, each revolution equalled 0.1C°. In this way fine control of temperature within the thermostat was possible by external operation. The thermistor provided accurate temperature measurement inside the gradient tube. Its electrical leads passed along the side-arm, in the resin bed, to a Wheatstone bridge. The thermistor resistance (R) at temperature (T) was balanced using a ballistic galvanometer. The vacuum flask was provided with an unsilvered strip (1 cm. wide) on two sides for illumination and viewing.

When using the apparatus at temperatures below the mercury range, the heating current was operated by hand.

Operation. - The gradient tube is filled with the appropriate gradient solution (see below) and about 12 density floats are introduced together with a micro-sample of polymer. The thermostat is lowered to the minimum temperature and held for 30 min. to allow for settling. The floats rise to the surface while while the polymer film remains suspended, owing to the difference in expansion coefficients. The position of the film is adjusted to about 1 cm. above the thermistor, by addition or removal of denser solution through a capillary reaching to the base. During heating all parts of the apparatus expand under their own coefficients of expansion, so that the density at any height in the tube varies with

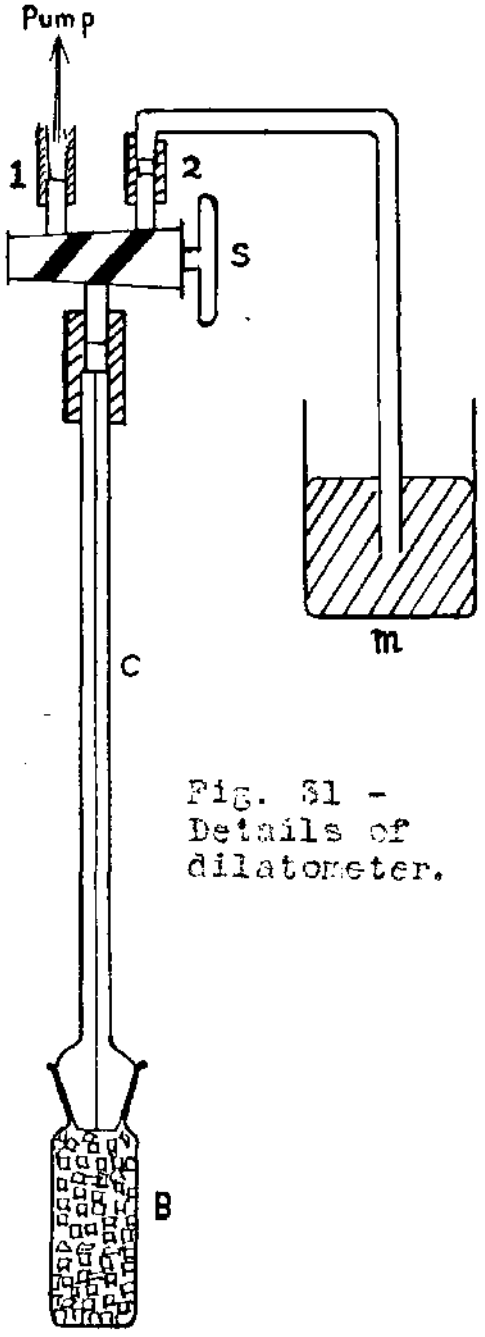

Fig. 21 - Details of dilatometer.

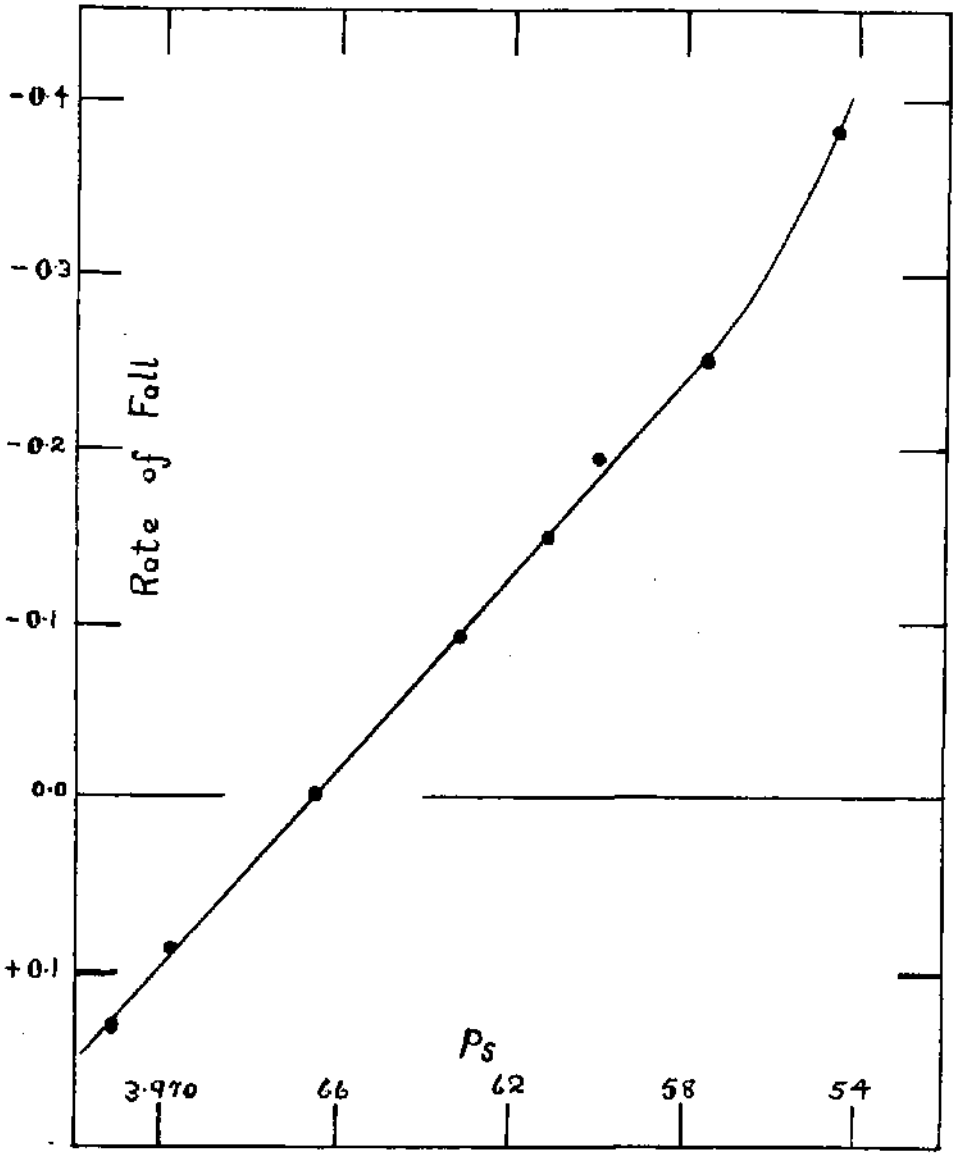

Fig. 24 - Determination of float density.

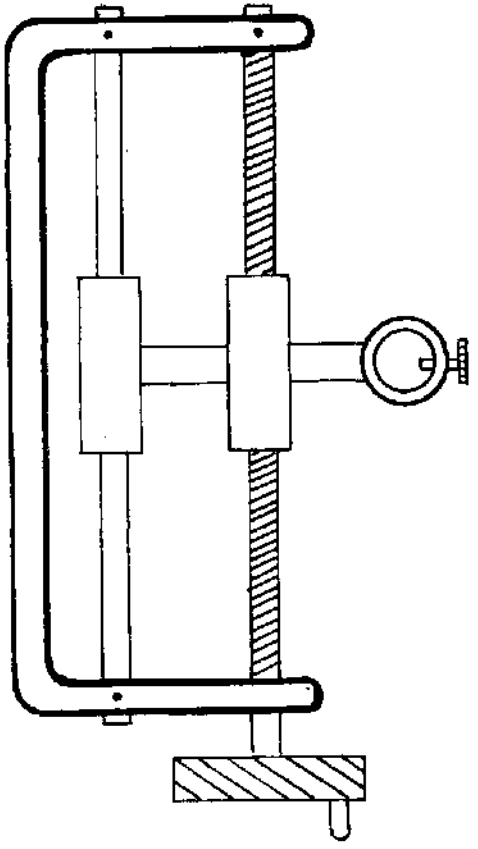

FIG. 22

the temperature. Since the aqueous solutions used have approximately the same coefficient of expansion as the (rubbery) polymer (0.0005-0.0006), there is little change in the position of the latter relative to the thermistor. The (Pyrex) floats, however, expand with the much smaller coefficient (0.00001), and sink past the films on heating. At temperature T, where dens.(film) = dens.(float) = dens. (solution), the centres of gravity of the film and float are coincident horizontally, and this is determined with a cathetometer. A series of such determinations, over the temperature range dT, defines the coefficient of expansion dV/dT of the sample. In some cases a temperature range extending above and below Θ was used, and the second order transition temperature located at the intersection of the two linear thermal expansion plots β_g and β_r.

A slow heating rate is required, especially in the region of coincidence, since (a) temperature determination is affected by a time lag while thermal equilibrium is established and (b) density measurement depends on the settling times of the moving float and film; and this is influenced by the viscosity of the gradient solution. Suitable heating rates are:

Below -10°C - 0.1C°/min. Above +10°C - 0.2C°/min.

Near coincidence - 0.05C°/min. or less.

Preparation and Use of Gradient Solutions. - The choice of gradient solution depends on (a) the temperature range dT, and on (b) the overall change in specific volume dV of the sample over this range. Bekkedahl's values of β_r and β_g (cf. Table 22) served as preliminary estimates for copolymers at low w_2.

Table 23.

Density range,	$T_{min.}$	Solvent.	Solute.
0.90-1.00 g./cm.^{3}	-70°C	MeOH/water	LiBr
0.95-1.05	-50		Lactic acid
1.00-1.15	-20	"	"
0.90-1.15	0.0	water	KI/$Na_2S_2O_3$

The preparation of low-temperature gradient solutions is restricted by freezing points, viscosity, and precipitation of solute. An estimate of the sample density at the minimum temperature is first required, and a solution (cf. Table 23) of that density is made up. After testing at the minimum temperature, the solution is divided into two equal portions (A and B). The gradient tube is half-filled with A, while solvent is added to B to lower the density by 0.02. A and B are interdiffused to produce a gradient of density in the tube. It is important that all solutions be evacuated (water pump) before use to prevent bubble formation by dissolved gases.

Thermistor Calibration. - A thermistor (type F2311/300, marketed by Standard Telefone Ltd.) covered the range -70°C to +70°C. The makers' data shows that the resistance (R) varies with absolute temperature (T) as follows:

$$R = ae^{b/T} \qquad \ldots\ 45$$

where a and b are constants; but the plot of log R against 1/T deviated appreciably from linearity. Prior to assembly in the gradient tube, the thermistor was calibrated against standard temperatures (cf. Table 24).

Table 24.

Standard.	Temp.	R	Log R	1/T
Steam	100.24°C	214.0 ohms	2.3304	0.002679
$Na_2SO_4 10H_2O$	32.38	1321.0	3.1210	0.003278
Ice	0.00	4140.0	3.6170	0.003661

A more detailed calibration was also carried out at 2C° intervals over the full range (cf. Appendix 12), against a spirit (-70°C to -10°C) and an N.P.L. mercury (-10°C to +70°C) thermometer corrected to the standards in Table 24. The calibration, interpreted as a plot of log R versus 1/T , deviated from equation 45 to the extent shown by the following parabolic equation:

$$1/T = 0.000754 \log R + 0.000929 + 0.000016(\log R - 3.5927) \times (\log R - 2.0132) \qquad \ldots\ 46$$

Even with this correction, an inaccuracy was evident below -20°C to the extent of 1.5C° at -70°C. Direct interpolation in Appendix 12 was adopted.

Float Calibration. - The density range (0.89-1.15) was covered by 72 Pyrex floats (Tubes A, B, and C, Appendix 13), which were evenly spaced by differential etching with 40% HF.

Float densities were measured by the method shown in Fig. 23. The rim of a Pyrex beaker (b) was smoothly ground to carry a Perspex lid (l), supporting an inlet tube (t) (1.5 cm.). The density of a Pyrex plunger (p) was adjusted to about 1.25 g./cm.^{3} with lead shot imbedded in wax. To determine the density of float f, aqueous $KI/Na_2S_2O_3$, EtOH, or lactic acid is placed in the beaker and allowed to settle (to eliminate convection currents); the smooth lid and narrow tube prevent excess evaporation. The plunger is suspended from a (semi-micro) balance arm through the tube. The float is centralised using a fine glass probe, and its rate of fall or rise recorded against the weight of plunger in solution (P_s) using a cathetometer. The density is then adjusted (nearer the balance point) by addition of solvent (or denser solution) and the procedure repeated several times on both sides of the balance point.

A plot of P_s against rate of fall (cf. sample, Fig 24) is interpolated to the balance with an accuracy of 0.0005

FIG. 23

FLOAT CALIBRATION APPARATUS

FLOTATION METHOD

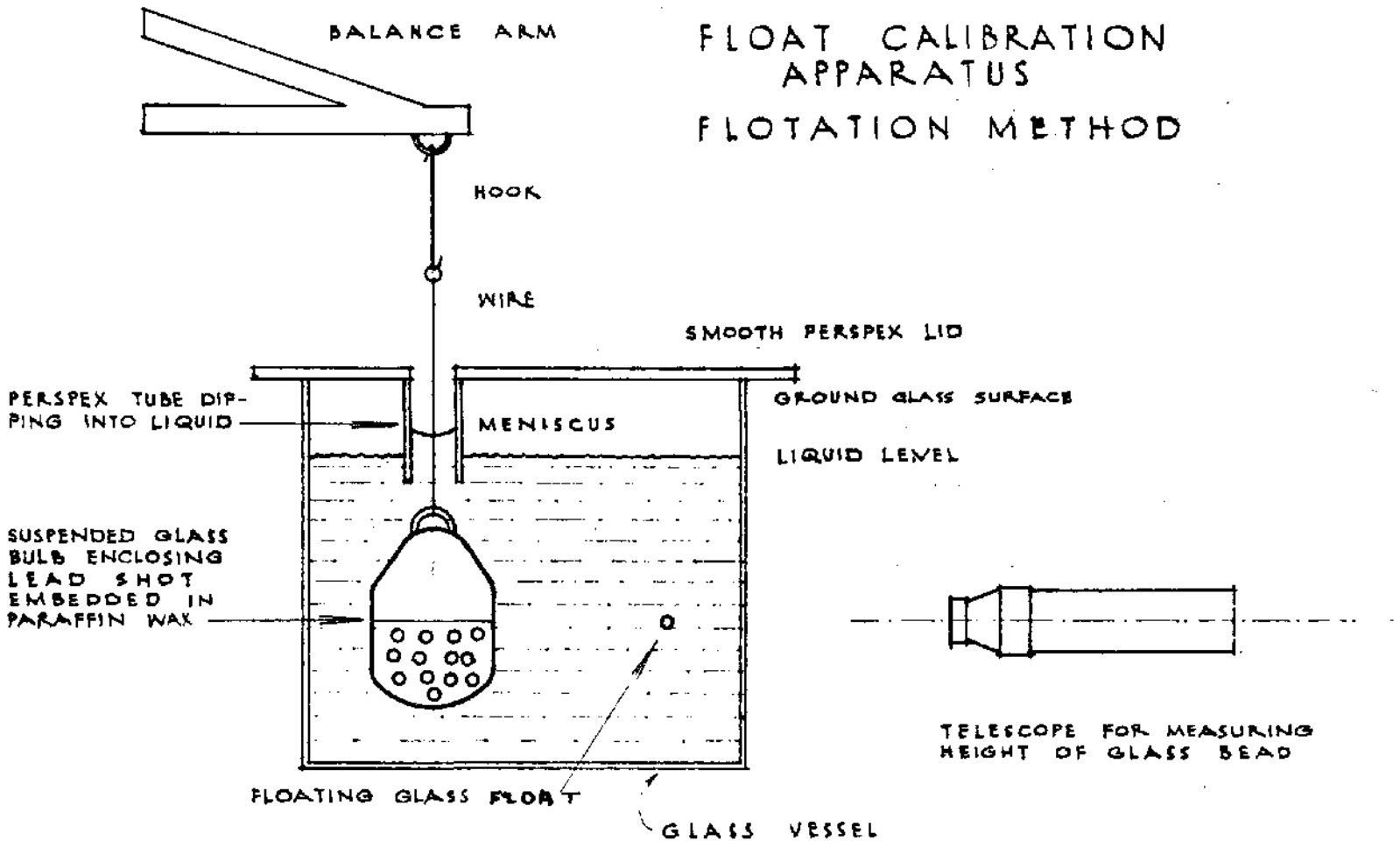

g./cm.^{3} The method benefits from the fact that a true balance point cannot be determined accurately by a single observation, since drift is readily produced by small convection currents. The addition of one drop of a dilute solution of a wetting agent (e.g. Teepol) improves the smoothness of weighing (P_s) by lowering the surface tension of the meniscus (m).

A preliminary calibration of the plunger was carried out by weighing in air and distilled water. The float density was estimated using the following corrections:

Wt. of plunger (air) = P_a ; air temp. = ${}_1T_a$, dens. = ${}_1d_a$

Wt. of plunger (water) = P_w; temp. = T_w, dens. = d_w

Wt. of plunger (solution) = P_s ; air temp. = ${}_2T_a$, dens. = ${}_2d_a$

solution temp. = T_s

Dens. of balance weights = d_b; Barometric pressure = B.

1. Approximate volume of plunger = $(P_a - P_w)/d_w$

2. Wt. of plunger in vacuum = $P_{av} = P_a + {}_1d_a(P_a - P_w)/d_w - P_a \cdot {}_1d_a/d_b$

3. Corrected wt. of plunger (water) = $P_{wv} = P_w(1 - {}_2d_a/d_b)$

4. Corrected wt. of plunger (solution) = $P_{sv} = P_s(1 - {}_2d_a/d_b)$

5. Volume of plunger at T_w = $(P_{av} - P_{wv})/d_w = V_{Tw}$

6. Volume of plunger at 20°C = $V_{20} = V_{Tw} - (T_w - 20)10^{-5}$

7. Density of float at 20°C = $(P_{av} - P_{sv})/V_{20}$

As an example, the following data are recorded for float B22:

P_a = 30.84551; $_1T_a$ = 21.1°C; B = 75.71 cm.; $_1d_a$ = 0.001201.

P_w = 6.30307; T_w = 23.3°C; d_w = 0.99747.

P_s = 3.96655; T_s = 22.7°C; $_2T_a$ = 23.4°C; $_2d_a$ = 0.001193.

d_b = 7.7. V_{20} = 0.91548; Float density = 1.09232 g./cm.^{3}

Thermal Expansion Plots (Gradient Tube Method). - The experimental results of 24 thermal expansion determinations are reported in Appendix 14. Of these, a selection of five (runs 3, 11, 12, 15, 19, and 24) are chosen to illustrate the accuracy of the plot of specific volume (V) against temperature (cf. Figs. 25-29). Fig. 25 is included as an example of crystallisation in natural rubber (w_2 = 0) below 10°C. This is reflected as an anomalous decrease in V (dotted portion) below 15°C due to belated melting of crystallites. Determinations of β_g must be considered less accurate than β_r owing to the scarcity of experimental points below θ in most cases. Since β_g = only 0.0002, films fall rapidly in the gradient solution below θ, so that the vertical dimension of the apparatus become the limiting factor. The reproducibility of the method is illustrated in Fig. 26 (runs 11 and 12) in which the same measurements were repeated after 24 hr. (w_2 = 0.308). Fig. 29 shows a straightforward determination of β_r at w_2 = 0.935 (maximum hydrochlorination).

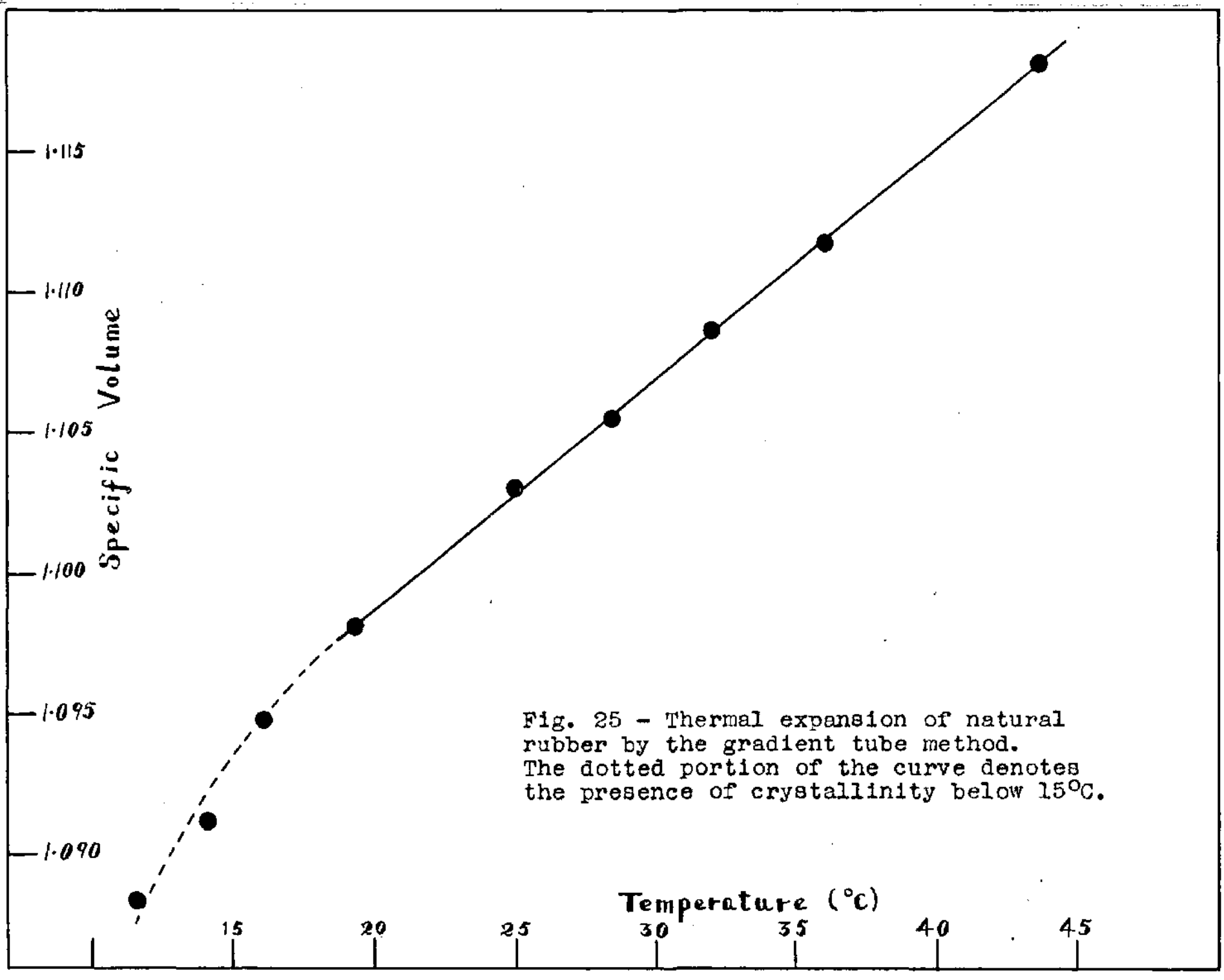

Fig. 25 - Thermal expansion of natural rubber by the gradient tube method. The dotted portion of the curve denotes the presence of crystallinity below 15°C.

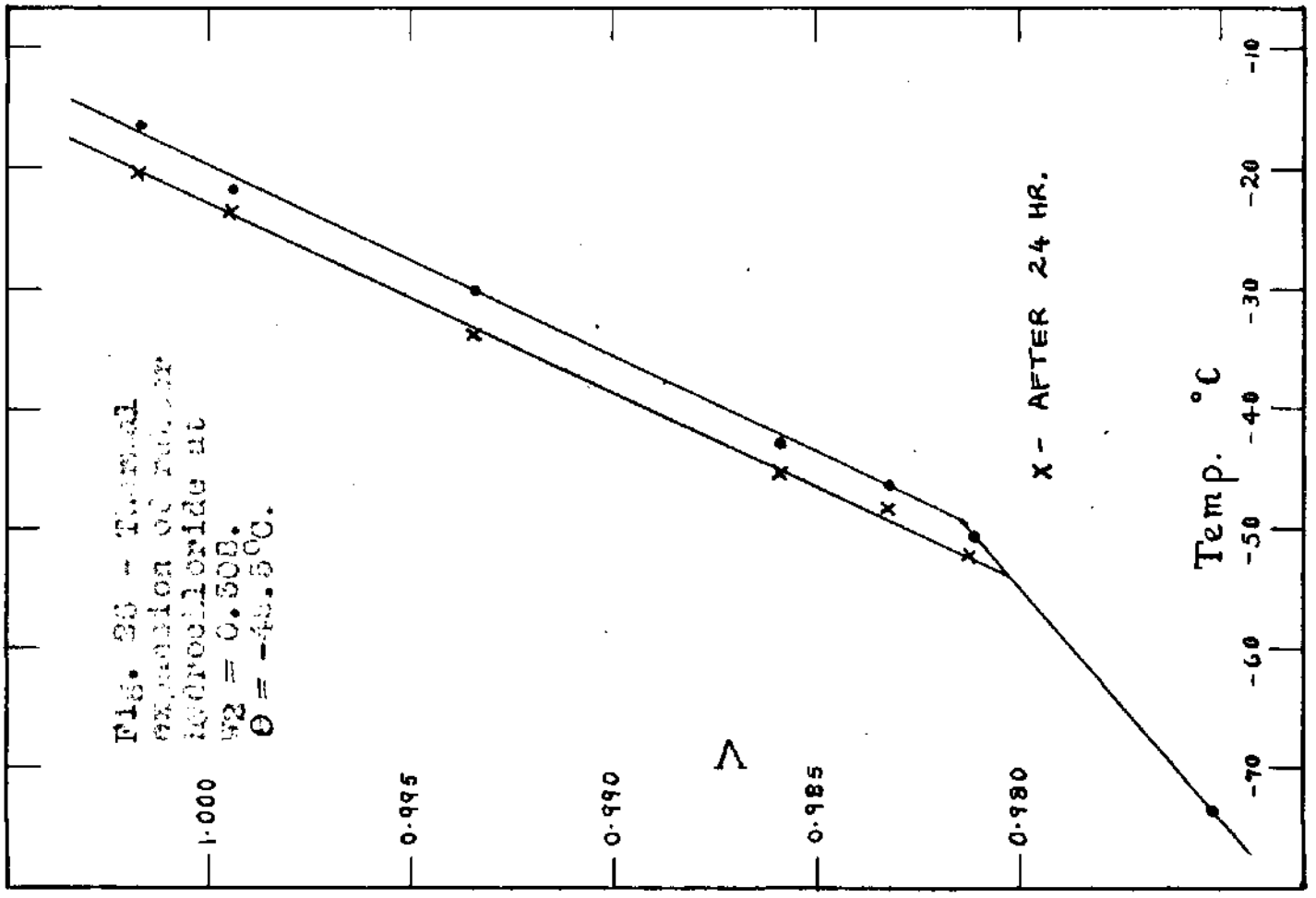

Fig. 26 - Thermal expansion of rubber hydrochloride at $w_2 = 0.508$. $\theta = -45.5°C$.

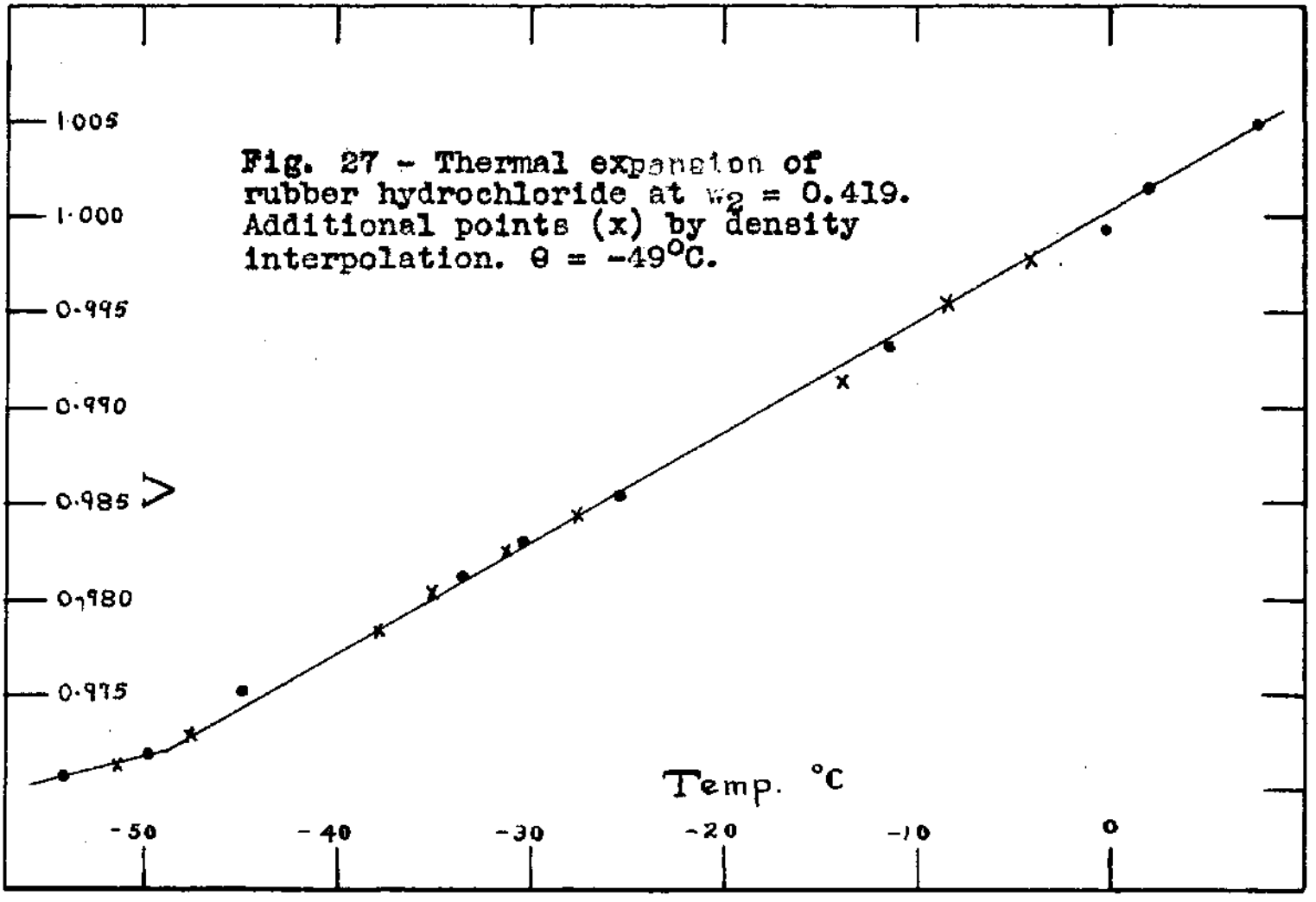

Fig. 27 - Thermal expansion of rubber hydrochloride at $w_2 = 0.419$. Additional points (x) by density interpolation. $\theta = -49°C$.

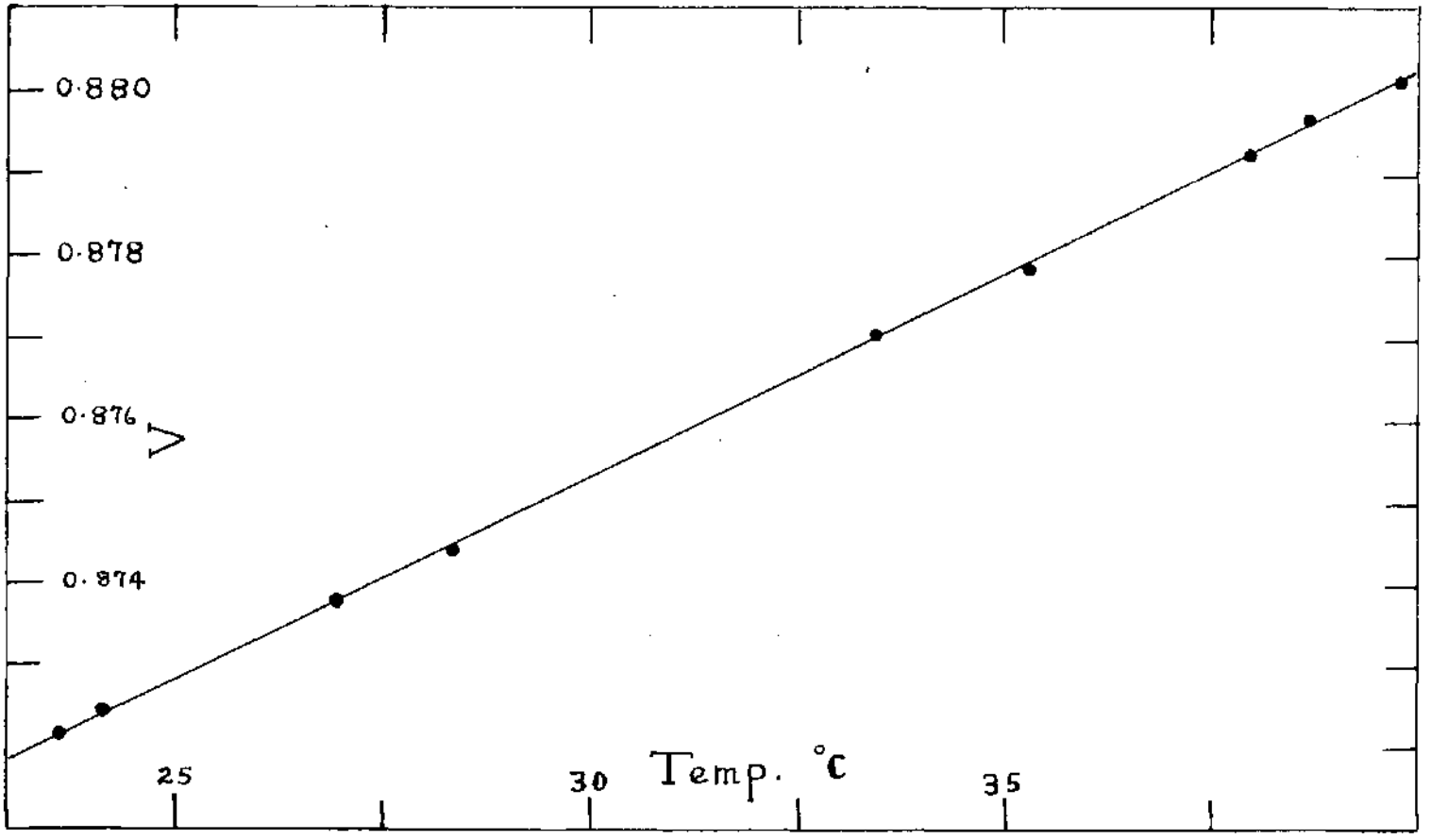

Fig. 29 - Thermal expansion of rubber hydrochloride at $w_2 = 0.935$.

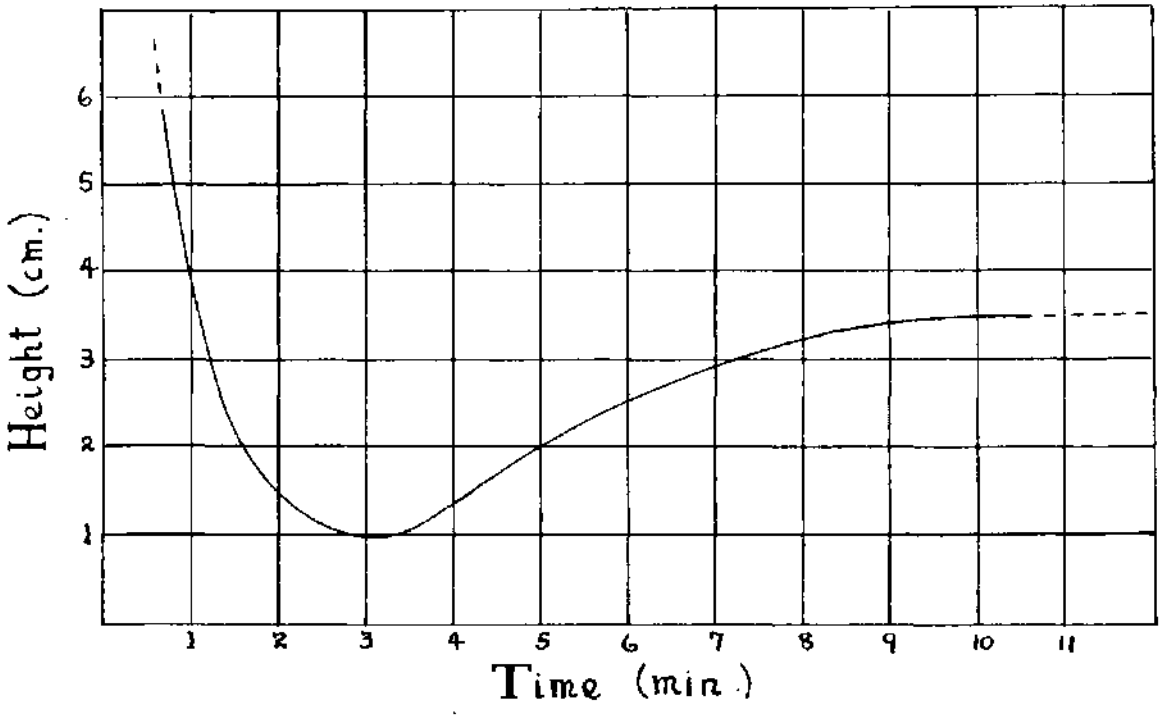

Fig. 36 - Behavior of rubber hydrochloride sample in acetone gradient solution.

Height Variation Method for Determining Θ. - A new sensitive method for determining second order transition points, independently of expansion coefficients, has arisen from these investigations (cf. Appendix 15). A plot of sample height versus temperature (as $\beta_g \rightarrow \beta_r$) changes in slope around Θ. The intersection of the two linear plots fixes the transition point to within narrow limits. Three such determinations were carried out at $w_2 = 0.882$ and 0.935. Fig. 30 shows the method is reproducible to less than 2C°.

Determination of β_r (Dilatometer Method). - Volume changes in six samples of rubber-rubber hydrochloride copolymer were measured in a dilatometer of the design shown in Fig. 31 - a modification of that described by Bekkedahl and Wood (43, 44) for similar measurements on pure rubber. The construction was of Pyrex glass, incorporating a B14 cone and socket sealed to Veridia precision bore (0.5 mm.) capillary (20 cm.). The total enclosed volume was 8.4798 cm.^{3} at 25.8°C. The joint was lightly smeared with silicone (high vacuum) grease, and retained by phosphor-bronze springs.

Operation. - Polymer samples were prepared and cut into 2-3 mm. cubes, as outlined on page 99, and tightly packed into the dilatometer bulb (b). The stem was connected (pressure tubing) to a two-way stopper (s), and from there to the pump (position 1), and a mercury pool (m) (position 2).

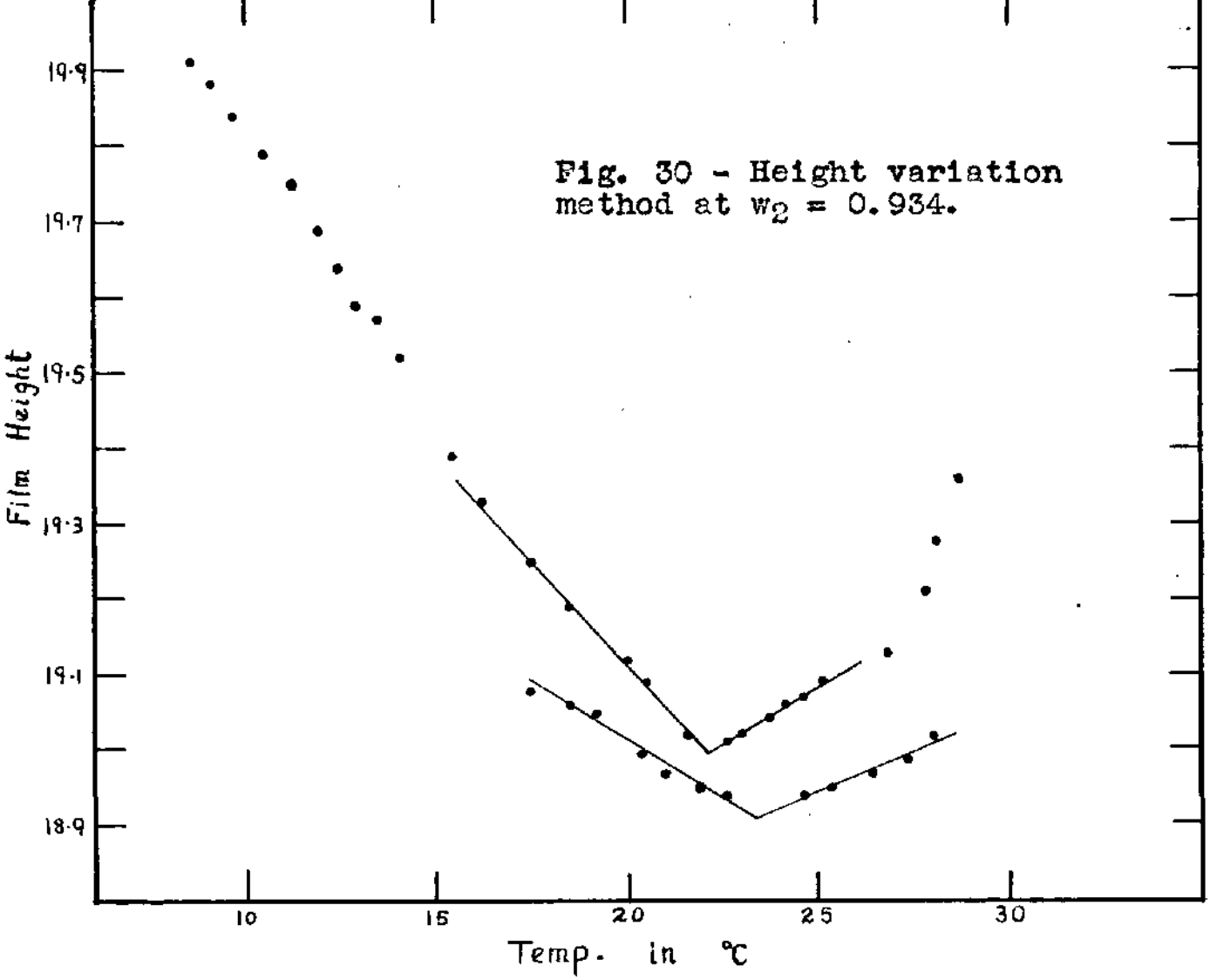

Fig. 30 - Height variation method at $w_2 = 0.934$.

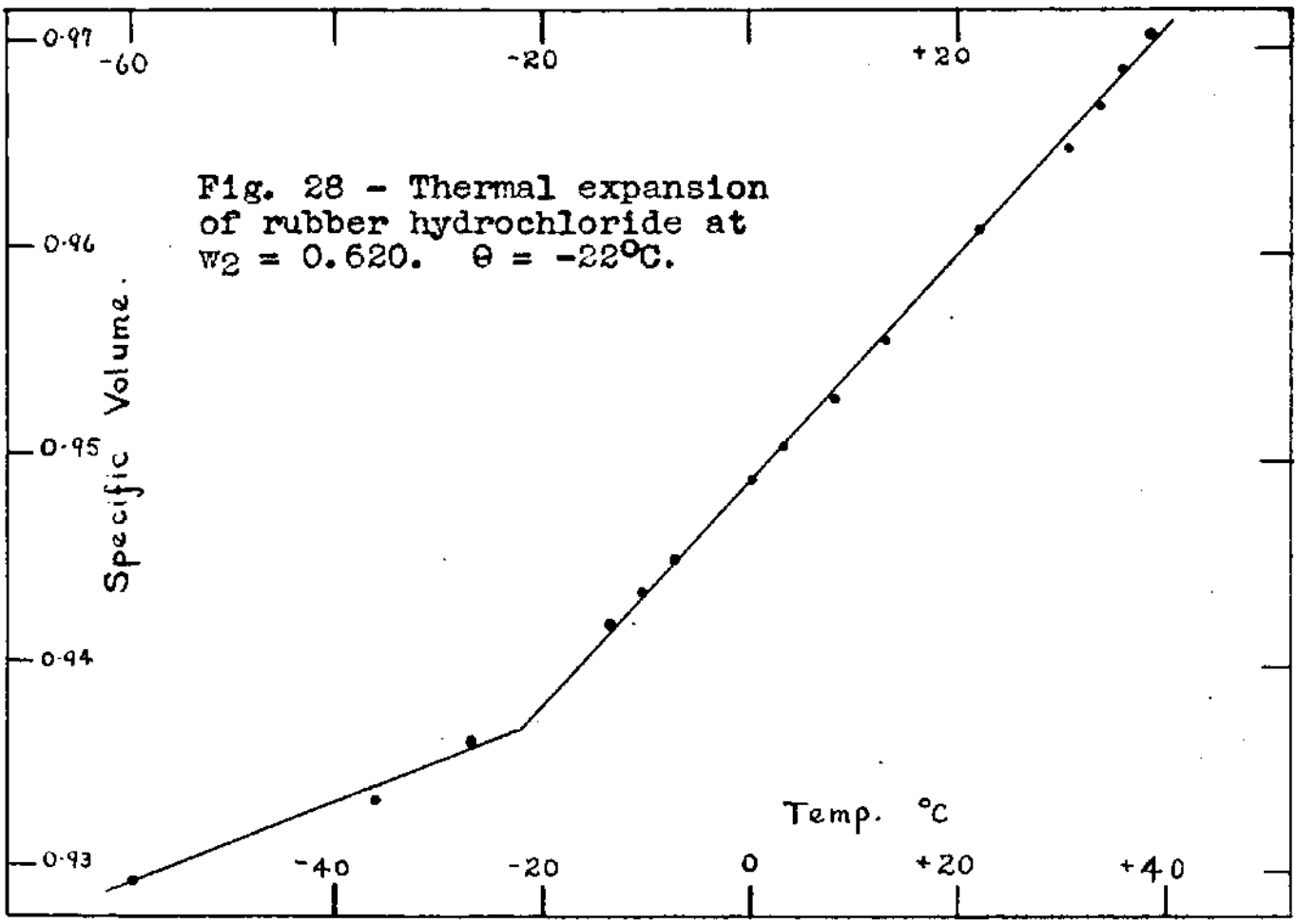

Fig. 28 - Thermal expansion of rubber hydrochloride at $w_2 = 0.620$. $\theta = -22^{\circ}C$.

After evacuation (5 min., mercury diffusion pump), mercury was drawn in to fill the connections as far as the stopper (position 2). The dilatometer was again evacuated (60 min.) and the mercury introduced to surround the polymer sample. The mercury height in the stem was adjusted to suit the starting temperature by heating or cooling the bulb before disconnection. The thermostating apparatus was that described on page 100. The dilatometer was immersed to within 0.50 cm. of the stem tip, and the mercury height recorded every 0.5C°, allowing 6 min. settling time at each measurement (rate of heating - 0.25C°/min.)

Thermal Expansion Plots (Dilatometer Method). - Two plots (cf. Figs. 32 and 33), at w_2 = 0.0 and 0.144, are included here as illustrations of the thermal expansion of five samples of copolymer and one of pure rubber investigated by the dilatometer method (cf. Appendix 16). The precision of the technique rests on the coincidence of the plot of capillary height versus temperature during upward and downward runs (cf. samples A and B). The experimental data are listed in Table 25 for all six samples. β_r was calculated as follows:

Overall volume increase = dV

$$dT\left[(V_m.\beta_m) + (V_r.\beta_r) - (V_m + V_r).\beta_g\right] \quad .... \quad 47$$

where coeff. of cubical expansion of mercury = β_m = 0.0001963

Table 25.

Experimental Data - Dilatometer Method.

Sample	Density	w_2	Wt. polymer	Wt. Hg	Vol. polymer
A	1.0497	0.665	4.2490	57.841	4.0490
B	1.1198	0.875	3.9736	66.071	3.5485
C	1.0687	0.728	3.8849	65.766	3.6352
D	0.9040	0.000	3.5746	60.239	3.9546
E	0.9500	0.233	3.7014	61.407	3.8962
F	0.9324	0.144	3.8810	57.711	4.1624

Sample	Vol Hg	Ht. range	Temp. range	$V_r + V_m$	β_r
A	4.2560	22.659	20.31	8.3050	0.000372
B	4.8776	22.947	20.14	8.4261	0.000407
C	4.8550	23.132	16.78	8.5902	0.000528
D	4.4526	19.812	11.71	8.4072	0.000658
E	4.5389	20.090	12.69	8.4351	0.000610
F	4.2662	20.161	12.38	8.4286	0.000641

and coeff. of cubical expansion of Pyrex = $g = 0.00001$, calculated on a capillary diameter of exactly 0.5 mm., which was tested along its whole length by measuring the dimensions of a mercury pocket in various positions. The accuracy of the method is evident from the linearity of Figs. 32 and 33.

-------oOo-------

Fig. 32 - Thermal expansion of natural rubber by the dilatometer method.

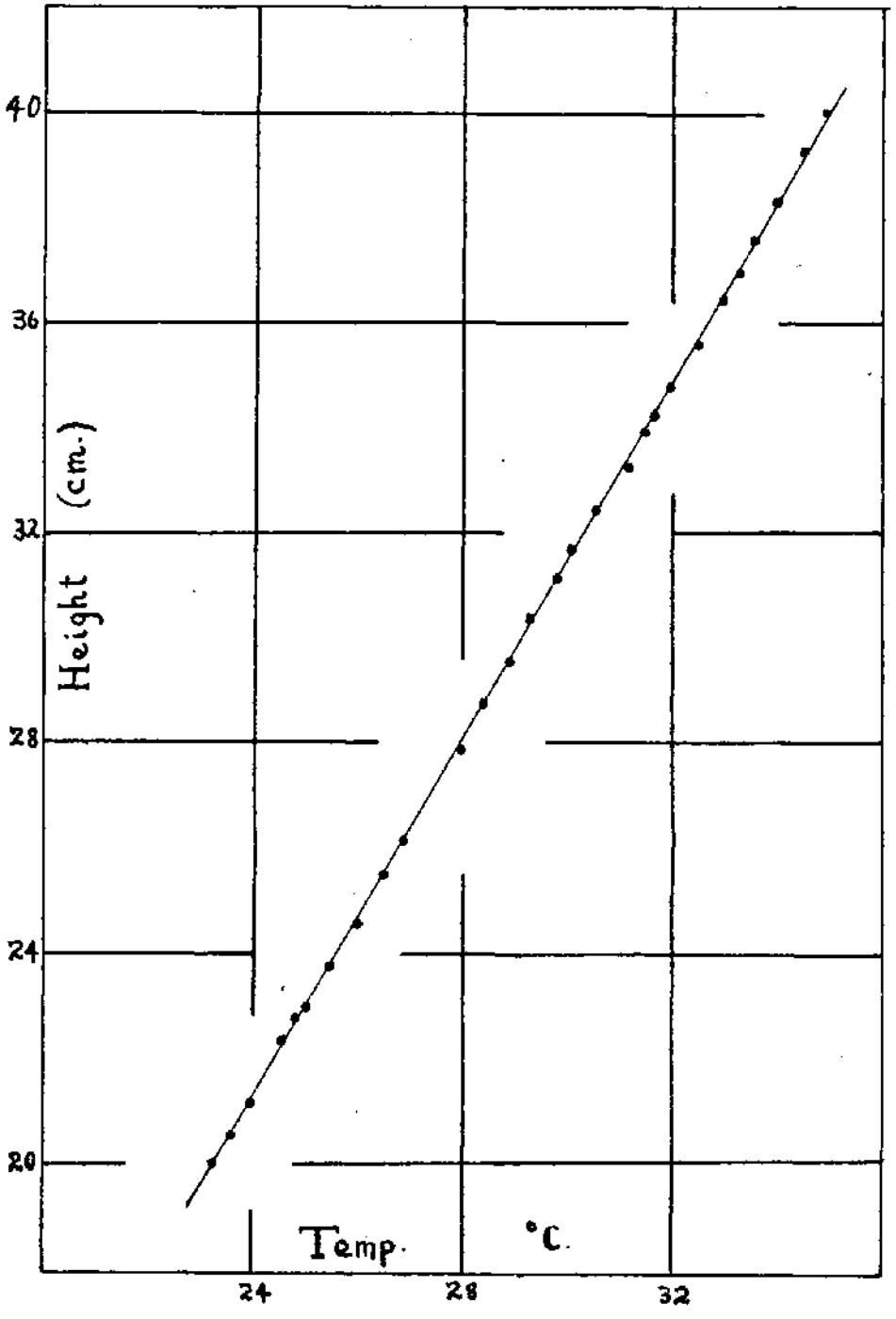

Fig. 33 - Thermal expansion of rubber hydrochloride ($w_2 = 0.144$) by dilatometer.

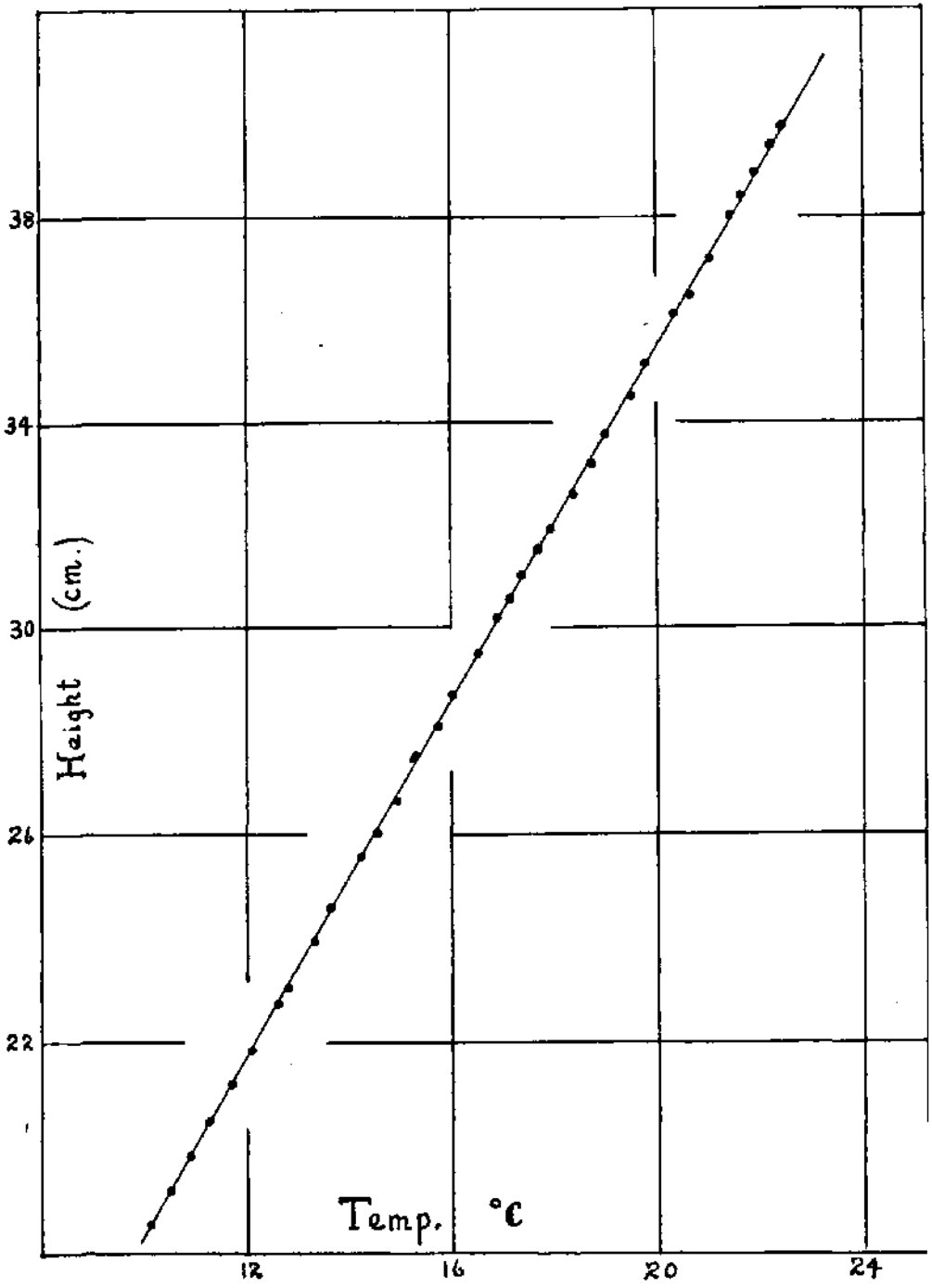

3d. DISCUSSION.

The Copolymer System Rubber-Rubber Hydrochloride. - The hydrochlorination of isoprene units in natural rubber (cf. page 1) provides a readily available copolymer system in which the hydrochlorinated unit is equivalent to that of styrene in the butadiene-styrene system (cf. page 96).

Although values of β_r, β_g, and θ for pure rubber are obtainable from the literature (Table 22), the ideal copolymer theory is not immediately applicable to the system in the absence of corresponding data for the pure hydrochloride, which cannot be prepared from natural rubber (12). In consequence, thermal expansion properties were measured over the available composition range $0 \leqslant w_2 \leqslant 0.935$, to provide extrapolated values for θ_2, ${}_2\beta_r$, and ${}_2\beta_g$ at $w_2 = 1$.

Experimental Values of θ, β_r, and β_g. - The calibration plot, for synthetic polyisoprene, of specific volume (V) against w_2 (Fig. 2) is free from the effects of crystallisation of the hydrochlorinated portion (cf. page 14); it is therefore analagous to that described on page 95 for the butadiene-styrene system. According to Gordon and Taylor's

ideal copolymer theory, the kink at $w_2 = 0.82$ predicts a second order transition point at that composition when $T = 26.7^{\circ}C$ (the calibration temperature). This value agrees with Fig. 34 in which Θ is plotted against w_2 from the present measurements. This data is not available from the corresponding calibration plot for natural rubber (Fig. 2) which is non-linear above $w_2 = 0.65$ owing to crystallisation.

A linear relationship between β_r and w_2 can be predicted on the basis of the ideal copolymer theory, thus: Above Θ, the monomer unit of each species in the copolymer occupies a volume proportional to ${}_1V_r$ or ${}_2V_r$ respectively, and each expands according to its appropriate coefficient of expansion (${}_1\beta_r$ or ${}_2\beta_r$). The overall increase in volume $d(V_r)$ throughout the copolymer, over the temperature range dT, is:

$$d(V_r) = (1 - w_2)({}_1V_r \cdot {}_1\beta_r \cdot dT) + w_2({}_2V_r \cdot {}_2\beta_r \cdot dT)$$

whence $d(V_r)/dT = w_2({}_2V_r \cdot {}_2\beta_r - {}_1V_r \cdot {}_1\beta_r) + {}_1V_r \cdot {}_1\beta_r$

Similarly, below Θ:

$$d(V_g)/dT = w_2({}_2V_g \cdot {}_2\beta_g - {}_1V_g \cdot {}_1\beta_g) + {}_1V_g \cdot {}_1\beta_g$$

Present measurements of β_r from both experimental methods are listed in Table 26; and, in addition, six runs due to Dunlop (62), using a dilatometer method are included. The combined data are plotted in Fig. 35.

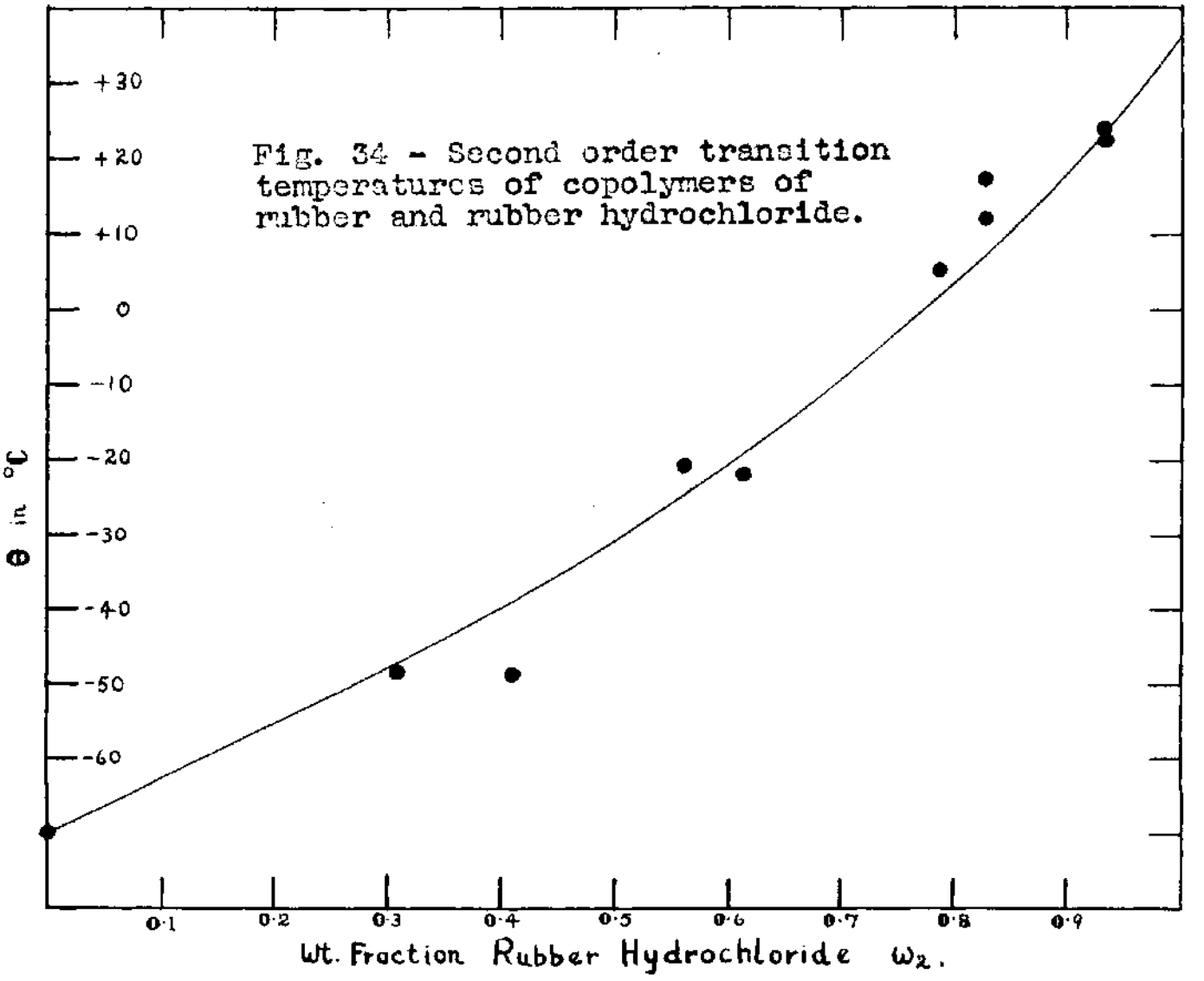

Fig. 34 - Second order transition temperatures of copolymers of rubber and rubber hydrochloride.

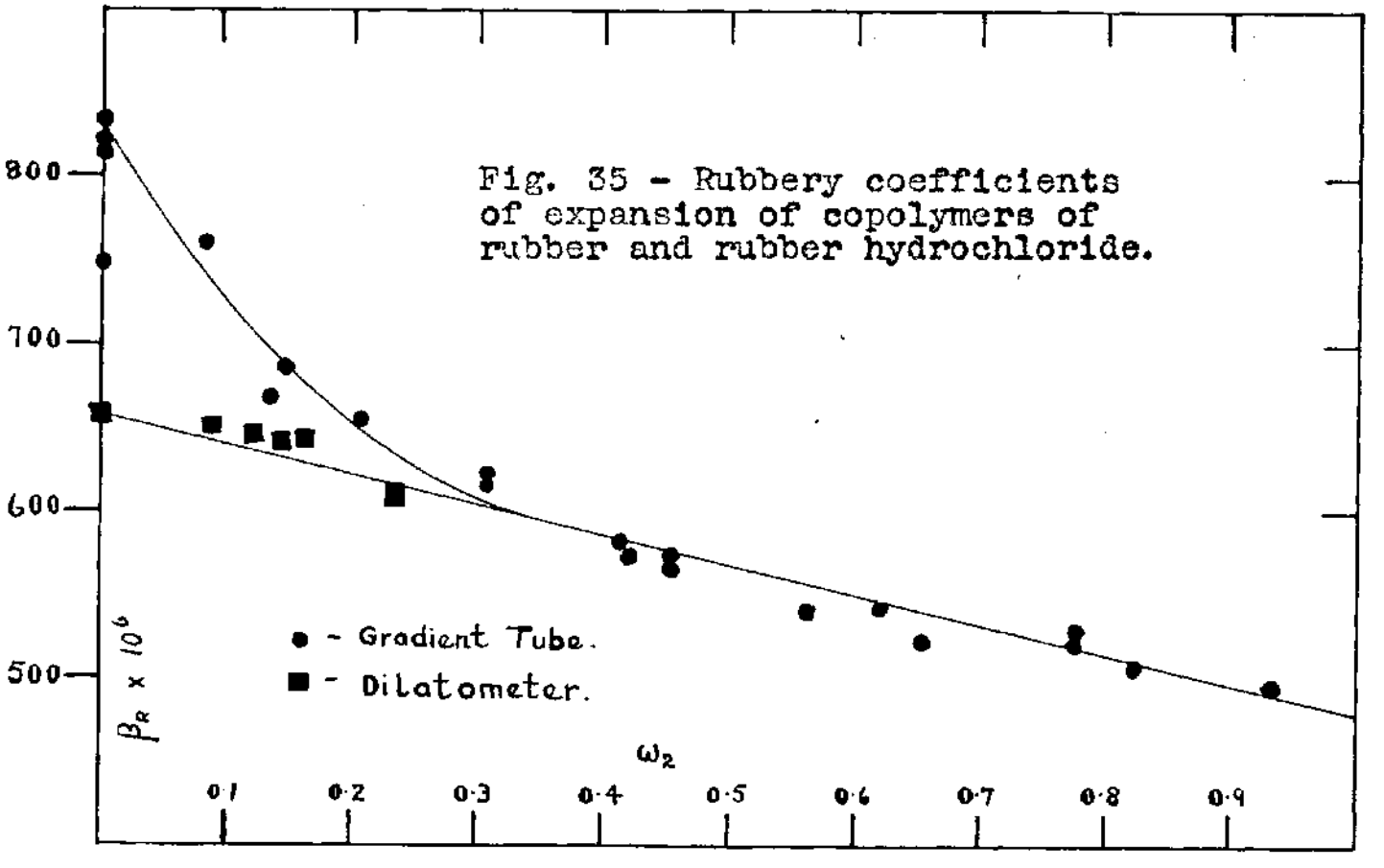

Fig. 35 - Rubbery coefficients of expansion of copolymers of rubber and rubber hydrochloride.

Table 26.

β_r in Rubber-Rubber Hydrochloride Copolymers.

w_2	β_r	Method.
0.0	0.000748	Gradient Tube.
0.0	817	"
0.0	821	"
0.0	982	"
0.0	833	"
7.5	0.000759	"
13.2	659	"
14.6	0.001038	"
14.6	0.000682	"
20.6	654	"
30.8	0.000621	"
30.8	617	"
30.8	663	"
41.4	581	"
41.9	574	"
45.3	0.000567	"
45.3	574	"
56.0	541	"
62.0	542	"
65.2	523	"
77.4	0.000526	"
77.4	520	"
82.2	507	"
93.5	495	"
66.5	0.000372	Dilatometer.
87.5	407	"
72.8	573	"
0.0	658	"
14.4	641	"
23.3	610	"
8.5	0.000650 *	"
10.5	512 *	"
12.0	646 *	"
16.0	644 *	"
39.0	638 *	"
65.0	582 *	"

* Dunlop's values (62).

The linear portion AB agrees well with Bekkedahl's values $_1\beta_r$ = 0.00061-0.00070 (Table 22) when extrapolated to $w_2 = 0$. This is also supported by the dilatometer measurement on pure rubber (Table 26, 0.000658).

$_2\beta_r$ is determined by the short extrapolation to $w_2 = 1$ at the value 0.00048. Values of β_g were less accurate, using the gradient technique, for reasons discussed earlier.

Table 27.

β_g in Rubber-Rubber Hydrochloride Copolymers.

w_2	0.308	0.419	0.620	0.774
β_g	0.000261	0.000213	0.000218	0.000280

Considering the experimental difficulties involved, the scatter in measured values of β_g (Table 27) is not unduly large. The average value $_2\beta_g$ = 0.00024 can be adopted with safety since β_g has been shown to be relatively constant in a number of polymers (53, 60). In particular, Gordon and Taylor adopted 0.00020 for polybutadiene (60), and the validity of this assumption is further supported by the present work.

Measurements of Θ by the gradient tube method are recorded in Table 28. At w_2 = 0.560 and 0.822, the location of Θ was based on the assumed value β_g = 0.00024 in combination with a single value for V_g below Θ (Appendix 14).

Table 28.

θ in Rubber-Rubber Hydrochloride Copolymers.

(Gradient Tube and Height Variation Methods - Appendix 15).

w_2	0.308	0.419	0.560	0.620	0.774	0.822	0.822	0.935	0.935
θ°C	-48.5	-49.0	-21.0	-22.0	+5.0	+12.0	+17.8	+22.2	+23.6

A plot of θ versus w_2 (Fig. 34) has been extrapolated to the value θ = +36°C at w_2 = 1 . The accuracy of determination of θ by the gradient tube method bears good comparison with that of previous work. w_2 is defined to 0.005 or less. A number of practical difficulties, associated with thermal expansion measurements (53), have largely been overcome by adopting a standard equilibrium settling time of 6 min.

Application of these Results to the Ideal Copolymer Theory. - The conformity of the present results with Gordon and Taylor's ideal copolymer theory is evident from the application of the following data to equation 43:

$\theta_1 = -69°C$ $\quad {}_1\beta_r = 0.000658$ $\quad {}_1\beta_g = 0.000210$ (53)

$\theta_2 = +36°C$ $\quad {}_2\beta_r = 0.000480$ $\quad {}_2\beta_g = 0.000240$

$\Delta({}_1\beta) = 0.000448$ $\quad \Delta({}_2\beta) = 0.000240$

k (from equation 44) = 240/448 = 0.536

therefore $\quad w_2 = \theta + 69/0.464\theta + 88$ 48

Table 29.

Evaluation of Equation 48.

w_2	0.1	0.2	0.3	0.4	0.5	0.6	0.7	0.8	0.9
$\theta^{\circ}C$	-63.1	-56.7	-49.5	-41.5	-32.6	-22.4	-12.5	+2.2	+17.5

Equation 48 is coincident with the experimental data in Table 28 (cf. Fig. 34), confirming the ideal volume mixing of monomer units (isoprene and isoprene hydrochloride), over the temperature range $-70^{\circ}C$ to $+36^{\circ}C$. A weakness in the ideal copolymer theory envisaged by Gerke (63) lies in the fact that the plot of equation 43 is oversensitive to alterations in $k = \Delta({}_2\beta)/\Delta({}_1\beta)$, in which case relatively small adjustments to k can effect movement of the plot into better coincidence with experimental data. The strength of this argument is lessened by the present work, since any alteration in the found value of k would be detrimental to the fit in Fig. 34. Therefore, in addition to the systems discussed by Gordon and Taylor (60) and Loshaek (61), copolymers of rubber and rubber hydrochloride firmly support the ideal copolymer theory.

Bunn (10) and Gordon and Taylor (cf. Fig. 2) have shown, from X-ray and density measurements respectively, that a considerable amounts of crystallinity are present in the copolymer at high values of w_2 and normal temperatures. There is no evidence in Fig. 35 that this affects the linearity of

the plot of β_r against w_2 above $w_2 = 0.8$, which means that the coefficients of expansion of rubbery and crystalline rubber hydrochloride are the same.

Relative Merits of the Two Experimental Techniques. - Copolymer preparation by hydrochlorination of rubber latex reduces the risk of the following adverse factors which normally impair the measurement of thermal expansion in polymers:

(a) Effect of Impurities. - The occurance of foreign matter in natural latex (proteins, etc.) is less than 5%, and much less than this figure in the purified latices used here. The accuracy of $_r$ and $_g$ measurements are therefore not likely to be effected by such impurities. The plasticising action (on θ) of residual monomer from a polymerisation process is excluded.

(b) Effect of Molecular Weight and Structure. - Since polymerisation and chain fission processes, which influence the position of θ (7), are absent from the hydrochlorination reaction, the molecular weight of the end product is independent of reaction conditions and equal to that of the starting material (rubber).

The above factors apply equally to both experimental techniques employed. However, additional advantages acrue in the density gradient method, arising fundamentally from the 10,000-fold reduction in the quantity of polymer required

for thermal expansion measurement:

(a) Preparation of Samples. - During the hydrochlorination of 40 g. samples of acid-stable rubber latex for the dilatometer method, the quantity of HCl gas evolved is large (60:1) in comparison with stoichiometric requirement, since the majority is wastage due to bubbling off. This source of loss is readily controlled by the micro-technique where the exact pressure can be measured. Furthermore, continuous stirring of large volumes of latex induces frothing and consequently the possibility of uneven hydrochlorination.

(b) Purification of Samples. - Purification of the samples used for both experimental methods (cf. page 99) is dependent on the speed of diffusion of gases (HCl, air, etc.) and vapourised liquids (water, acetone) out through the body of the polymer under the influence of high vacuum. This varies roughly with the square of the linear dimensions of the sample, so that the advantage of the micro-technique is substantial.

(c) Pressing of Samples. - As little as 10 mg. of flocculated polymer spread to an area of about 1 $cm.^2$ when pressed in steam between microscope slides to expel the air. In practise, 100 $cm.^2$ is an upper limit for such an area using normal laboratory presses (a hand-press was used in this work). Of this, 50% is unavailable owing to poor pressing. The

laboriousness of pressing and cutting a 4 g. sample is appreciable.

The irregularity of β_r above $w_2 = 0.30$ using the dilatometer (cf. the present results and those of Dunlop in Table 26) is attributable to the thermal decomposition of the copolymer at the high temperatures (up to 120°C) required for pressing.

(d) Technique. - No difficulty was experienced in operating the high-vacuum technique (Fig. 31) for dilatometry. Although the the sample is in the form of an uneven mass of 3 mm. cubes, there is no evidence that air or vacuum bubbles remained after filling with the confining liquid. Even with the most efficient packing, however, the polymer:mercury volume ratio cannot be improved beyond 1:1, which requires a weight ratio of less than 1:10, thereby reducing the accuracy of weighing.

(e) Effect of Low Temperatures. - Although experimental temperatures were often below -60°C, the accuracy of β_r by the density-gradient method was equal, for the most part, to that claimed by Gordon and MacNab (16) for polystyrene. By including a pair of sample films for each run, their movement in the gradient tube can be checked one against the other, thus avoiding sticking or slow settling at low temperatures.

(f) Solvent Absorption. - Absorption of the confining liquid

(viz. MeOH from gradient solution) is a serious disadvantage of the gradient tube method when applied to the rubber-rubber hydrochloride system at low hydrochlorination. It is reflected as a wide deviation from linear (i.e. high β_r) of the plot of β_r against w_2 below w_2 = about 0.20 (cf. Fig. 35). The result confirms that of Bekkedahl (44) who used acetone and EtOH as confining liquids for natural rubber in a dilatometer technique. The amount of absorbed solvent appears to vary inversely with the hydrochlorinated content, and becomes negligible above w_2 = about 0.20. A sample of pure rubber introduced into a gradient solution, prepared from acetone/water mixtures, behaved in the manner illustrated in Fig. 36. (A) The film fell rapidly in the tube under gravity, gradually slowing as normal density equilibrium was approached. As the solvent was absorbed, the film rose again (B) to a steady level (c), which represented saturation. High values of β_r can be attributed to thermal expansion of the solvent.

Method.	Composition Limits.	Temp. range.
Gradient Tube	w_2 = 0.2-1.0	above -75°C
Dilatometer.	w_2 = 0.0-0.3	above -10°C

------oOo------

APPENDICES

APPENDIX 1.

Calibration Floats in Tubes I - IV.

and Tube S.

(a) Tube I.

Float.	Density.*
I(1)	0.8755
I(2)	0.9068
I(3)	0.9298
I(4)	0.9456
I(5)	0.9589
I(6)	0.9719

(b) Tube II.

Float.	Density.
II(1)	0.9791
II(2)	0.9882
II(3)	1.0006
II(4)	1.0232

(c) Tube III.

Float.	Density.
III(1)	1.0416
III(2)	1.0663
III(3)	1.0853
III(4)	1.1092

(d) Tube IV.

Float.	Density.
IV(1)	1.1167
IV(2)	1.1359
IV(3)	1.1529
IV(4)	1.1670

(e) Tube S.

Float.	Density.
S1	0.9791
S2	0.9795
S3	0.9838
S4	0.9882
S5	0.9892
S6	0.9952
S7	1.0006
S8	1.0068
S9	1.0148
S10	1.0172
S11	1.0193

* $g./cm.^3$

APPENDIX 2.

Hydrochlorination of Synthetic Latex VI.

($P = 48.5$, $\bar{r} = 90\text{Å}$, $L = 18$).

(a) At 249 mm. partial pressure of HCl at 26.7°C. (Figs. 8, 9, and 10).

(Continued on page ii)

Reaction Time (t) min.	Polymer Density. g./cm.^{3}	Mole% Reaction (M)	t' = 0.6667t	H = 0.06945M	Specific Volume (V)
0.0	0.9018	0.0	0.0	0.00	1.1089
5.5	0.9516	18.4	3.7	1.28	1.0509
15.0	0.9708	25.9	10.0	1.80	1.0301
20.3	0.9823	30.4	13.5	2.11	1.0182
45.0	1.0057	40.1	30.0	2.79	0.9943
75.0	1.0210	45.8	50.0	3.15	0.9813
160.0	1.0242	48.0	106.5	3.33	0.9764
171.5	1.0243	48.1	114.4	3.34	0.9763
238.0	1.0343	52.4	158.6	3.64	0.9669
299.0	1.0282	49.8	199.0	3.46	0.9726

(b) 57 mm. at 26.7°C. (Fig. 8).

Reaction Time (t) min.	Polymer Density. g./cm.^{3}	Mole% Reaction (M)	t' = 0.1105t	Specific Volume (V).
0.0	0.9018	0.0	0.00	1.1089
5.0	0.9135	4.2	0.55	1.0947
7.5	0.9187	6.1	0.83	1.0885
15.0	0.9319	10.9	1.66	1.0731
20.5	0.9290	9.9	2.27	1.0764
25.0	0.9387	13.3	2.76	1.0653
30.0	0.9296	10.1	3.32	1.0757
60.0	0.9533	19.1	6.63	1.0490
85.5	0.9585	21.0	9.45	1.0433
145.0	0.9743	27.3	16.02	1.0264
180.5	0.9822	30.4	19.94	1.0181
600.0	1.0204	46.4	66.30	0.9799

(c) 229 mm. at 44.2°C. (Fig. 11).

Reaction Time (t) min.	Polymer Density. g./cm.^{3}	Mole% Reaction (M)	t' = 0.75t	Specific Volume (V).
0.0	0.9018	0.0	0.0	1.1089
5.0	0.9485	16.7	3.8	1.0543
15.5	0.9412	23.9	10.6	1.0625
45.0	0.9787	38.4	33.7	1.0219
60.0	1.0080	40.0	45.0	0.9920
150.5	1.0176	44.2	112.9	0.9827
601.0	1.0337	51.5	450.8	0.9674

(d) 249 mm. at 26.7°C (containing 17.4% H_2SO_4). (Fig. 10).

Reaction Time (t) min.	Polymer Density g./cm.^{3}	Mole% Reaction (M).	Specific Volume (V).
0.0	0.9018	0.00	1.1089
5.0	0.9509	17.54	1.0516
10.5	0.9599	21.18	1.0418
20.0	0.9775	28.13	1.0230
45.0	0.9943	35.33	1.0057
75.0	1.0087	40.90	0.9914
120.0	1.0214	46.34	0.9790
297.0	1.0343	51.95	0.9668
160.0	1.0255	48.12	0.9751

(e) 1517 mm. at 26.7°C (bulk hydrochlorination). (Fig. 4).

Reaction Time (t) min.	Polymer Density g./cm.^{3}	Mole% Reaction (M).	Specific Volume (V).
0.0	0.9018	0.0	1.1089
2.0	0.9948	35.6	1.0052
5.3	1.0318	51.4	0.9692
9.0	1.0482	58.7	0.9540
10.0	1.0800	73.5	0.9259
12.0	1.0470	57.7	0.9551
12.8	1.0500	59.5	0.9524
14.0	1.0586	63.4	0.9447
22.5	1.0775	72.3	0.9281
25.0	1.0764	71.8	0.9290
31.5	1.0877	77.2	0.9194
40.0	1.0873	85.2	0.9197
45.0	1.0993	89.7	0.9097
75.0	1.1123	101.5	0.8990

APPENDIX 3.

Bulk Hydrochlorination of Natural Latex 8. (Fig. 5).

1517 mm. at 26.7°C (i.e. 2 atm. HCl)

Latex 8 contains 20% H_2SO_4 on the acid + water content.

(continued on page iv).

Reaction Time (t) min.	Polymer Density g./cm.^{3}	Mole% Reaction (M).	Specific Volume (V).
0.0	0.9039	0.0	1.1063
18.0	0.9236	7.0	1.0827
34.0	0.9308	9.5	1.0743
47.5	0.9452	14.3	1.0580
61.5	0.9508	16.2	1.0517
80.0	0.9694	21.7	1.0316
90.0	1.0120	40.5	0.9881
90.0	0.9856	28.7	1.0146
105.0	0.9977	34.9	1.0023
120.0	1.0352	50.0	0.9660
139.0	1.0622	60.4	0.9415
150.0	1.0836	68.5	0.9228
190.0	1.1185	81.0	0.8941
270.0	1.1292	84.5	0.8856

APPENDIX 4.

Bulk Hydrochlorination of Natural Latex 4.

1138 mm. at 26.7°C (i.e. 1.5 atm. HCl). (Fig. 6).

Reaction Time (t) min.	Polymer Density g./cm.^{3}	Specific Volume (V).	Wt.% Reaction (W).	Mole% Reaction (M).
0.0	0.9040	1.1062	0.0	0.0
30.0	0.9214	1.0853	9.7	6.6
90.0	0.9482	1.0546	22.2	15.5
140.0	0.9628	1.0386	29.3	20.9
195.0	0.9986	1.0014	45.5	35.6
210.0	1.0164	0.9837	53.2	42.5
240.0	1.0338	0.9673	60.2	49.2
300.0	1.0913	0.9163	79.9	71.5

APPENDIX 5.

Hydrochlorination of Natural Latices 5 and 9. (Fig. 6).

1900 mm. at 26.7°C (i.e. 2.5 atm. HCl).

(a) Latex 5 (from Batch I of Dunlop 60% latex).

Reaction Time (t) min.	Polymer Density g./cm.^{3}	Specific Volume (V).	Wt.% Reaction (W).	Mole% Reaction (M).
0.0	0.9047	1.1057	0.00	0.00
15.0	0.9407	1.0630	18.20	12.70
20.0	0.9450	1.0582	20.70	14.80
30.0	0.9689	1.0323	30.24	23.70
35.0	0.9729	1.0279	33.90	24.90
41.0	1.0062	0.9938	40.88	31.20
45.0	1.0128	0.9874	51.70	38.00
50.0	1.0568	0.9463	69.10	58.90
55.0	1.0820	0.9242	76.90	68.20
63.0	1.0997	0.9093	82.00	74.90

(b) Latex 9 (from Batch II of Dunlop 60% latex).

0.0	0.9040	1.1062	0.00	0.00
7.5	0.9182	1.0891	7.70	5.20
20.0	0.9350	1.0695	16.10	11.20
30.0	0.9523	1.0501	24.20	17.00
45.0	0.9840	1.0163	39.00	29.30
50.0	1.0279	0.9729	57.70	46.80
52.0	1.0357	0.9655	60.80	50.30
56.0	1.0595	0.9438	70.10	60.60
63.0	1.0847	0.9219	77.70	67.90

APPENDIX 6.

Hydrochlorination of Synthetic Latex V.

($P = 22$, $\bar{r} = 260\text{Å}$, $L = 46$).

(continued on page vi).

(a) 163 mm. at 26.7°C. (b) 249 mm. at 26.7°C.

Both runs taken from Gordon and Taylor (9). (Figs. 7 and 9).

t' = 0.448t	t' = 0.285t	H = 0.1516M	t' = 0.6667t	H = 0.06945M
2.25	1.43	0.72	2.66	1.32
2.69	1.71	1.34	5.33	1.86
5.38	3.42	1.34	6.67	2.27
9.00	5.70	1.68	8.00	2.02
14.40	9.11	2.02	13.38	2.27
20.20	12.83	2.21	15.38	2.32
27.80	17.70	2.52	18.02	2.37
35.90	22.80	2.72	23.30	2.68
47.20*	29.80	2.83	31.30	2.89
107.80	68.30	3.42	60.00	3.37
			81.20	3.65
			160.00	3.99

(c) 167 mm. at 69.9°C (total pressure = 255 mm.). (Fig. 7).

Reaction Time (t) min.	Polymer Density g./cm.^{3}	Mole% Reaction (M).	t' = 0.285t	H = 0.1516M	Specific Volume (V).
0.0	0.9060	0.00	0.00	0.00	1.1038
5.5	0.9236	6.60	1.57	1.00	1.0820
10.5	0.9290	8.40	2.99	1.27	1.0760
15.5	0.9310	9.06	4.42	1.37	1.0740
16.0	0.9328	9.70	4.56	1.47	1.0720
21.0	0.9391	11.95	5.99	1.81	1.0650
31.0	0.9438	13.95	8.83	2.12	1.0590
45.0	0.9490	15.60	12.82	2.37	1.0540
61.5	0.9544	17.70	17.53	2.68	1.0480
90.5	0.9608	20.10	25.78	3.05	1.0410
121.0	0.9646	21.90	34.48	3.32	1.0360
151.5	0.9694	23.30	43.17	3.53	1.0320
180.0	0.9672	22.62	51.30	3.43	1.0340
209.5	0.9698	23.68	59.70	3.59	1.0311
241.0	0.9810	28.40	68.68	4.32	1.0190
389.5	0.9794	27.45	111.00	4.16	1.0210

APPENDIX 7.

Partial Pressure of HCl in Aqueous Solution.

Total pressure (P) = p_1 (HCl) + p_2 (water vapour).

Sample determination of p_1 at 44.2°C when P = 255 mm.

For published data, cf. Reference 17.

% HCl	P		Log P		p_1		Log p_1	
	40°C	50°C	40°C	50°C	40°C	50°C	40°C	50°C
6	50.6	86.0	1.7042	1.935	0.01	0.02	$\bar{2}$.000	$\bar{2}$.301
10	47.0	80,1	1.6721	1.904	0.03	0.07	$\bar{2}$.477	$\bar{2}$.845
14	44.2	72.3	1.6454	1.859	0.12	0.28	$\bar{1}$.079	$\bar{1}$.447
18	36.9	63.6	1.5670	1.804	0.52	1.11	$\bar{1}$.716	0.045
20	34.4	59.2	1.5366	1.772	1.06	2.21	0.025	0.344
22	32.4	56.4	1.511	1.751	2.18	4.42	0.339	0.645
24	31.6	55.6	1.501	1.745	4.5	8.9	0.653	0.949
26	33.2	59.0	1.521	1.771	9.2	17.5	0.964	1.243
28	40.2	72.5	1.604	1.860	19.1	35.7	1.281	1.553
30	57.8	103.0	1.762	2.013	39.4	71.0	1.596	1.851
32	96.7	168.7	1.985	2.228	81.0	141	1.909	2.149
34	174.5	297.0	2.242	2.473	161	273	2.207	2.436
36	333.4	558.4	2.523	2.747	322	535	2.508	2.728
38	607.5	972.4	2.784	2.988	598	955	2.777	2.980

At Log P = Log 225 = 2.407 the interpolated value of p_1 in the plot of Log P against Log p_1 is 229 mm.

APPENDIX 8.

Particle Size Distribution in Synthetic Latex VI. (Fig. 12).

Electron microscope magnification = 12,400 x

Enlarger magnification = 5.74 x

Overall magnification = 71,176 x

Uncorrected R.M.S.D. = 452Å (continued on page viii).

Measured Particle Diameter mm.	Diameter in Å.	Number of Particles N.	N/20
0.8	112.4	9	0.45
1.2	168.6	29	1.45
1.6	224.8	105	5.25
2.0	280.9	83	4.15
2.4	337.2	106	5.30
2.8	393.4	162	8.10
3.2	449.5	89	4.45
3.6	505.8	90	4.50
4.0	562.0	32	1.60
4.4	618.3	39	1.95
4.8	674.4	31	1.55
5.2	730.7	11	0.55
5.6	786.8	4	0.20
6.0	843.1	0	0.00
6.4	899.3	1	0.05

APPENDIX 9.

Evaluation of Rate Equation 10 from Equations 9 and 12.

(a) $S = 0$, $L > 40$, $\bar{r} > 200$Å. (Approximated by $H = 1 - e^{-t'}$).

t'	0.1	0.3	0.5	1.0
H	0.0952	0.2592	0.3935	0.6321

(b) $S = 0.465$, $L > 40$, $\bar{r} > 200$Å.

t'	1	10	25	50	75	100	150	200
H	0.7176	2.1315	2.7620	3.2540	3.5426	3.7420	4.0369	4.2240

(c) $S = 0.465$, $L = 22$, $\bar{r} = 110$Å.

t'	1	10	25	50	75	100	150	200
H	0.7121	2.0682	2.6107	2.9995	3.2162	3.3647	3.5690	3.7086

(d) $S = 0.465$, $L = 18$, $\bar{r} = 90\text{Å}$.

t'	1	10	25	50	75	100	150	200
H	0.7110	2.0773	2.6364	3.0289	3.2709	3.4284	3.6182	3.8000

(e) $S = 0.548$, $L > 40$, $\bar{r} \geq 200\text{Å}$.

t'	1	10	25	50	75	100	150	200
H	0.7262	2.2941	3.0139	3.5814	3.9597	4.1402	4.4829	4.7195

(f) $S = 0.600$, $L > 40$, $\bar{r} \geq 200\text{Å}$.

t'	1	10	25	50	75	100	150	200
H	0.7352	2.3986	3.1865	3.8075	4.2155	4.4225	4.8021	5.0571

(g) $S = 1$, $L > 40$, $\bar{r} > 200\text{Å}$.

t'	$\frac{1}{4}$	$\frac{1}{2}$	1	2	3	4	5	7.5
H	0.191	0.369	0.687	1.220	1.658	2.032	2.364	3.107
t'	10	12.5	15	17.5	20	22.5	25	
H	3.670	4.224	4.707	5.114	5.521	5.896	6.251	

APPENDIX 10.

Calibration Floats in Tube S.

Float.	Original.	Density.	Specific Volume.
S1	II(1)	0.9791	1.0213
S2	A13	0.9795	1.0209
S3	A14	0.9838	1.0164
S4	II(2)	0.9882	1.0119
S5	A15	0.9892	1.0109
S6	A16	0.9952	1.0048
S7	II(3)	1.0006	0.9994
S8	A19	1.0068	0.9932
S9	A20	1.0148	0.9854
S10	A21	1.0172	0.9831
S11	A22	1.0193	0.9811

APPENDIX 11.

Hydrochlorination of Cyclised Rubber.

(a) Experimental Data for Calibration Curve. (Fig. 16).

Latex.	Specific Volume.	Wt% Chlorine	Wt.% Reaction	Mole% Reaction	Polymer Density.
C	1.0156	0.00	0.00	0.00	0.9846
B	1.0115	0.77	2.27	1.49	0.9886
B	1.0084	1.55	4.57	3.02	0.9916
D	1.0035	2.91	8.57	5.77	0.9965
B	1.0078	3.24	9.56	6.44	0.9923
C	0.9920	5.73	16.86	11.69	1.0081
D	0.9823	7.98	23.34	17.46	1.0180

(b) Hydrochlorination of Cyclised Latex A. (Fig. 17).

HCl Pressure	Reaction Temp.	Reaction Time	Specific Volume	Wt.% Reaction	Mole% Reaction
2.0 atm.	26.7°C	180 min.	1.0095	4.15	2.90
2.5	"	103	1.0088	4.70	3.15
2.5	"	360	1.0030	9.05	6.30
2.5	0.0	0	1.0134	0.00	0.00
2.5	"	59	1.0093	4.33	2.87
2.5	"	103	1.0088	4.70	3.15
2.5	"	180	1.0031	8.99	6.06
2.5	"	235	1.0011	10.51	7.15
2.5	"	315	0.9973	13.38	9.14
2.5	"	360	1.0030	9.05	6.10
2.5	"	405	0.9938	16.05	11.08
2.5	"	607	0.9926	17.02	11.93
2.5	"	768	0.9919	17.59	12.24

(c) Hydrochlorination of Cyclised Latex B. (Fig. 18).

2.0 atm.	26.7°C	293	1.0034	8.75	5.90
"	"	701	0.9989	12.12	8.24
2.5	0.0	60	1.0102	3.80	2.51
2.5	"	120	1.0068	6.18	4.12
2.5	"	181	1.0051	7.59	5.08
2.5	"	243	1.0011	10.58	7.16
2.5	"	346	0.9979	12.90	8.79
2.5	"	345	0.9968	13.73	9.38
2.5	"	577	0.9920	17.48	12.12
2.5	"	872	0.9913	18.00	12.51
2.5	"	0	1.0158	0.00	0.00

(d) Hydrochlorination of Cyclised Latex C. (Fig. 19).

HCl Pressure.	Reaction Temp.	Reaction Time.	Specific Volume	Wt.% Reaction	Mole% Reaction
2.0 atm.	26.7°C	0.0 min.	1.0152	0.00	0.00
"	"	10.0	1.0126	1.81	1.19
"	"	20.3	1.0100	3.80	2.51
"	"	63.0	0.9990	12.09	8.16
"	"	35.0	0.9997	11.53	7.91
"	"	45.5	0.9982	12.68	8.66
"	"	90.0	0.9954	14.82	10.16
"	"	180.0	0.9924	17.19	11.91
"	"	121.0	0.9919	17.51	12.16

(e) Hydrochlorination of Cyclised Latex D. (Fig. 20).

2.0 atm.	26.7°C	0.0	1.0181	0.00	0.00
"	"	0.0	1.0179	0.00	0.00
"	"	40.5	1.0161		
"	"	60.0	1.0145		
"	"	90.0	1.0122		
"	"	120.0	1.0142		
2.5 atm.	0.0	60.5	1.0105	3.42	2.25
"	"	150.0	1.0065	6.41	4.27
"	"	183.0	1.0057	7.05	4.70
"	"	240.0	1.0036	8.60	5.77
"	"	297.0	1.0031	8.99	6.06
"	"	352.0	1.0012	10.45	7.07
"	"	598.0	0.9957	14.60	10.02
"	"	705.0	0.9948	15,30	10.53
"	"	1068.0	0.9546	}	-
"	"	1463.0	0.9845	23.25	16.48

APPENDIX 12. Thermistor Calibration.

Temp. T °Abs.	Thermistor Resistance R	1/T	Log R.
199.0	180,000	0.0050256	5.2553
200.6	162,000	49855	5.2095
203.8	130,000	49073	5.1139
206.1	115,000	48525	5.0607
209.4	91,500	47760	4.9614
209.7	88,500	47687	4.9469
212.6	73,900	47037	4.8686

Temp. T °Abs.	Thermistor Resistance R.	1/T	Log R.
214.5	66,250 ohms	0.0046624	4.8212
214.1	65,800	46577	4.8182
217.1	57,420	46066	4.7591
217.3	57,000	46019	4.7559
220.5	47,300	45351	4.6749
221.1	45,280	45232	4.6559
224.2	38,380	44607	4.5841
224.3	38,100	44583	4.5809
227.3	31,900	43995	4.5038
228.6	29,860	43748	4.4751
230.4	26,900	43403	4.4298
232.7	24,080	42977	4.3817
235.8	20,600	42409	4.3139
238.2	17,740	41985	4.2491
240.4	16,600	41597	4.2201
244.1	13,500	40967	4.1303
245.1	13,270	40786	4.1230
249.6	10,900	40064	4.0374
254.1	8,930	39358	3.9508
256.4	8,750	39002	3.9420
259.4	7,221	38553	3.8586
263.6	6,050	37940	3.7818
264.7	5,748	37781	3.7595
268.0	5,060	37313	3.7595
272.6	4,140	36684	3.6208
273.2	4,177	36606	3.6170
275.08	3,915	36353	3.5927
276.26	3,746	36198	3.5736
277.34	3,593	36057	3.5555
279.58	3,299	35766	3.5184
281.72	3,045	35496	3.4836
285.08	2,691	35078	3.4300
286.78	2,528	34870	3.4028
288.30	2,393	34686	3.3798
291.43	2,145	34314	3.3314
291.68	2,118	34284	3.3259
293.50	1,992	34072	3.2993
296.40	1,824	33779	3.2610
299.69	1,616	33368	3.2086
301.90	1,503	33124	3.1769
304.13	1,393	32881	3.1440
305.33	1,340	32751	3.1270
308.14	1,224	32453	3.0878

Temp. T °Abs.	Thermistor Resistance R.	1/T	Log R.
309.43	0.001,174 ohms	0.0032317	3.0697
311.47	1,101	32106	3.0418
314.24	1,010	31823	3.0043
315.92	959.8	31654	2.9822
317.67	908.5	31479	2.9583
319.49	860.4	31299	2.9347
321.35	814.0	31099	2.9106
322.87	778.2	30972	2.8911
325.49	726.8	30723	2.8614
328.55	683.5	30437	2.8347
329.44	647.3	30355	2.8111
332.54	593.4	30072	2.7734
333.96	569.0	29944	2.7551
336.35	534.4	29731	2.7278
338.37	506.5	29553	2.7046
344.65	429.9	29015	2.6334

APPENDIX 13.

Calibration Floats in Tubes A, B, and C.

(a) Floats in Tube A.

Float	Specific Volume	Float	Specific Volume	Float	Specific Volume
A1	1.1181	A2	1.1148	A3	1.1117
A4	1.1086	A5	1.1055	A6	1.1030
A1	1.0982	A2	1.0949	A7	1.0913
A3	1.0884	A4	1.0825	A5	1.0710
A6	1.0655	A7	1.0596	A8	1.0563
A9	1.0483	A10	1.0430	A11	1.0328
A12	1.0289	A13	1.0209	A14	1.0164
A15	1.0109	A16	1.0048	A17	1.0014
A18	0.9992	A19	0.9932	A20	0.9854
A21	0.9831	A22	0.9811	A23	0.9751
A24	0.9720				

(b) Floats in Tube B.

Float	Specific Volume	Float	Specific Volume	Float	Specific Volume
B1	0.9709	B2	0.9691	B3	0.9674
B4	0.9669	B5	0.9655	B6	0.9613
B7	0.9560	B8	0.9536	B9	0.9510
B10	0.9492	B11	0.9451	B12	0.9440
B13	0.9422	B14	0.9364	B15	0.9339
B16	0.9298	B17	0.9293	B18	0.9246
B19	0.9228	B20	0.9216	B21	0.9199
B22	0.9155	B23	0.9063	B24	0.9028
B25	0.9012	B26	0.8958	B27	0.8931
B28	0.8913	B29	0.8860		

(c) Floats in Tube C.

C1	0.8846	C2	0.8824	C3	0.8817
C4	0.8802	C5	0.8796	C6	0.8793
C7	0.8779	C8	0.8771	C9	0.8744
C10	0.8738	C11	0.8724	C12	0.8722

APPENDIX 14.

Rubbery and Glassy Coefficients of Expansion and Second Order Transition Temperatures of Rubber/Rubber Hydrochloride Copolymers - Gradient Tube Method.

Run 1. - w = 0 (natural rubber).

Float	R	Log R	1/T	Temp.	dV/dT	θ
A2	2499 ohms	3.3978	0.0034831	13.92°C		
A1	2171	3.3367	34355	17.89		
A6	1766	3.2472	33671	23.81		
A5	1548	3.1897	33222	27.83		
A4	1380	3.1399	32849	31.24	0.000748	-
A3	1172	3.0690	32444	35.04		
A2	1066	3.0278	32000	39.32		
A1	947.1	2.9763	31611	43.17		

Run 2 - Natural Rubber $w_2 = 0$.

Float	R	Log R	1/T	Temp.	dV/dT	θ
A3	2833 ohms	3.4523	0.0035254	10.48°C		
A7	2600	3.4150	34985	12,66		
A2	2199	3.3422	34398	17.53		
A1	1935	3.2867	33975	21.15		
A6	1616	3.2086	33368	26.51	0.000817	-
A5	1443	3.1593	32994	29.91		
A4	1286	3.1093	32570	33.85		
A3	1118	3.0483	32155	37.81		
A2	1018	3.0076	31848	40.81		
A1	847.0	2.9415	31351	45.79		

Run 3 - Natural Rubber w2 = 0.

A3	2730	3.4362	35126	11.51		
A7	2487	3.3957	34815	14.05		
A2	2316	3.3647	34573	16.06		
A1	2056	3.3131	34180	19.33		
A6	1702	3.2309	33543	24.94	0.000821	
A5	1519	3.1815	33160	28.39		
A4	1349	3.1300	32773	31.95		
A3	1184	3.0734	32345	35.99		
A2	1070	3.0294	32-13	39.19		
A1	932.3	3.9695	31561	43.67		

Run 4 - Natural Rubber w2 = 0.

A8	8140	3.9106	38833	-15.67		
A7	6280	3.7980	38069	-10.50		
A6	5700	3.7559	37750	-8.28		
A5	4300	3.6335	36779	-1.29	0.000982	-
A4	3325	3.5217	35794	6.20		
A3	2638	3.4213	35024	12.34		
A2	2000	3.3010	34085	20.20		
A1	1797	3.2546	33729	23.30		

Run 5 - Natural Rubber w2 = 0.

A8	8060	3.9063	38810	-15.51		
A7	6100	3.7853	37968	-9.80		
A6	5010	3.6998	37280	-4.94		
A5	3990	3.6010	36492	0.85		
A4	3150	3.4983	35611	7.63	0.000833	
A3	2420	3.3838	34723	14.81		
A2	1819	3.2598	33770	22.94		
A1	1625	3.2108	33385	26136		

Run 6 - Rubber Hydrochloride $w_2 = 0.075$.

Float	R	Log R	1/T	Temp.	dV/dT	θ
A4	1885 ohms	3.2754	0.0033889	21.90°C		
A3	1426	3.1541	32956	30.25		
A7	1263	3.1014	32489	34.62		
A2	1066	3.0278	32000	39.32		
A1	938.1	2.9722	31573	43.55		
A6	787.4	2.8962	31005	49.35	0.000759	-
A5	713.0	2.8531	30527	54.40		
A4	640.7	2.8067	30322	56.61		
A3	568.0	2.7548	29942	60.80		
A2	517.3	2.7138	29626	64.36		
A1	454.7	2.6578	29199	69.30		

Run 7 - Rubber Hydrochloride $w_2 = 0.132$.

A10	10880	4.0367	0.0040058	-23.5		
A9	7172	3.8556	38529	-13.6		
A8	4379	3.6414	36940	-2.47		
A7	3571	3.5528	36034	4.34		
A6	2611	3.4168	34997	12.56	0.000659	-
A5	2004	3.3018	34092	20.14		
A4	1210	3.0828	32415	35.32		

Run 8 - Rubber Hydrochlroide $w_2 = 0.146$.

A12	22940	4.3606	42800	-39.5		
A11	17380	4.2400	41863	-34.3		
A10	8782	3.9436	39010	-16.8		
A9	5929	3.7730	37877	-9.17		
A8	3702	3.5684	36158	3.38	0.001038	-
A7	2930	3.4669	35366	9.58		
A6	2159	3.3342	34336	18.06		
A5	1756	3.2445	33670	23.82		
A4	1130	3.0531	32191	37.47		

Run 9 - Rubber Hydrochloride $w_2 = 0.146$.

A12	23510	4.3713	42890	-40.03		
A11	17460	4.2420	41890	-34.50		
A10	8990	3.9538	39386	-19.30		
A9	6076	3.7836	37953	-9.70		
A8	3854	3.5860	36217	-3.93		
A7	3114	3.4934	35573	7.93		
A6	2346	3.3703	34618	15.69	0.000682	-
A5	1827	3.2617	33785	22.81		
A4	1169	3.0679	32304	36.38		

Run 10 - Rubber Hydrochloride $w_2 = 0.206$.

Float	R	Log R	1/T	Temp.	dV/dT	θ
A14	17450 ohms	4.2417	0.0041866	-34.4°C		
A13	12130	4.0838	40455	-25.0		
A12	7333	4.8653	38589	-14.0		
A11	5660	3.7528	37724	-6.7		
A10	3245	3.5112	35712	6.84		
A9	2306	3.3628	34100	19.99	0.000654	-
A8	1553	3.1911	33233	27.73		
A7	1274	3.1052	32528	34.25		
A6	988.0	2.9948	31750	41.78		

Run 11 - Rubber Hydrochloride $w_2 = 0.308$.

A23	175000	5.2430	50148	-73.77		
A22	45000	4.6532	45217	-51.02		
A21	33400	4.5237	44147	-46.46	0.000621	-48.5°C
A20	27100	4.4330	43428	-42.91	0.000261	
A19	14400	4.1584	41164	-30.25		
A18	10100	4.0043	39794	-21.89		
A17	8520	3.9304	38939	-16.37		

Run 12 - Rubber Hydrochloride $w_2 = 0.308$.

A22	45700	4.6599	45257	-52.22		
A21	36500	4.5623	44441	-48.16		
A20	31100	4.4928	43901	-45.40		
A19	17100	4.2330	41769	-33.77	0.000625	-
A18	10900	4.0374	40064	-23.60		
A17	9400	3.9731	39540	-20.27		

Run 13 - Rubber Hydrochloride $w_2 = 0.308$. (repeat of Run 12 after 24 hr.).

A14	1624	3.2106	33382	26.38		
A13	1329	3.1235	32714	32.50		
A12	949.3	2.9774	31442	44.87	0.000617	-
A11	749.8	2.8750	30836	51.12		

Run 14 - Rubber Hydrochloride $w_2 = 0.414$.

A24	21100	4.3243	42496	-37.9		
A23	15480	4.1897	41384	-31.5		
A22	10100	4.0043	39794	-21.9		
A21	8450	3.9269	38921	-16.3		
A20	6614	3.8205	38248	-11.7	0.000581	

(Continued on page xviii).

Run 14 (continued).

Float	R	Log R	1/T	Temp.	dV/dT	θ
A19	3804 ohms	3.5803	0.0036253	2.66	0.000581	
A18	2718	3.4343	35112	11.62		
A17	2405	3.3811	34702	14.99		
A16	1941	3.2880	33985	21.07		
A15	1308	3.1165	32643	33.16		
A14	1020	3.0086	31856	40.73		

Run 15 - Rubber Hydrochloride $w_2 = 0.419$.

B1	51150	4.7088	45632	-54.0		
A24	39900	4.6010	44756	-49.8		
A23	30200	4.4800	43791	-44.8		
A22	16980	4.2300	41730	-33.5		
A21	14520	4.1620	41189	-30.4	0.000574	-49°C
A20	11810	4.0723	40358	-25.4	0.000213	
A19	6545	3.8159	38212	-11.5		
A18	4395	3.6430	36871	-1.9		
A17	3862	3.5868	36364	1.82		
A16	3110	3.4928	35568	7.97		

Run 15a- Rubber Hydrochloride $w_2 = 0.419$ (points added to Run 15 by interpolation of density).

Specific Volume Deduced	R	Log R	1/T	Temp.
0.9714	43700 ohms	4.6405	0.0045098	-51.4
0.9729	35560	4.5509	44354	-47.7
0.9783	21100	4.3243	42496	-37.9
0.9802	17900	4.2529	42009	-35.1
0.9825	15120	4.1796	41313	-31.1
0.9842	13050	4.1155	40723	-27.6
0.9914	7285	3.8623	38574	-13.9
0.9952	5738	3.7588	37775	-8.5
0.9977	4828	3.6837	37158	-4.1

Run 16 - Rubber Hydrochloride $w_2 = 0.453$.

B9	44200	4.6454	45141	-51.56
B8	24900	4.3962	43105	-41.2
B6	15600	4.1931	41267	-30.9
B5	10400	4.0170	39898	-22.5

(Continued on page xix).

Run 16 (continued).

Float	R	Log R	1/T	Temp.	dV/dT	θ
B3	9400 ohms	3.9731	0.0039622	-20.8		
A24	6300	3.7993	38080	-10.6	0.000567	
A23	4980	3.6972	37262	-4.8		
A22	3360	3.5263	35829	5.92		
A21	2930	3.4669	35366	9.62		
A20	2530	3.4031	34871	13.59		

Run 17 - Rubber Hydrochloride $w_2 = 0.453$.

B4	17600	4.2455	41937	-34.7		
A24	11800	4.0719	40355	-25.4		
A23	9200	3.9638	39462	-19.8		
A22	6100	3.7853	37998	-10.0	0.000574	-
A21	5270	3.7218	37462	-6.2		
A20	4443	3.6477	36889	-2.1		

Run 18 - Rubber Hydrochloride $w_2 = 0.560$.

B11	12050	4.0809	40434	-59.5		
B10	7975	3.9018	38785	-15.4		
B9	6570	3.8176	38226	-11.6		
B8	5337	3.7273	37509	-6.6		
B7	4504	3.6536	35931	-2.4		
B6	3070	3.4871	35523	8.33	0.000541	-21°C
B5	2355	3.3720	34631	15.58		
B4	2107	3,3236	34266	18.65		
B3	2050	3.3118	34172	19.46		
B2	1884	3.2751	33893	21.87		
B1	1730	3.2380	33599	24.45		
A24	1578	3.1981	33287	27.24		

Run 19 - Rubber Hydrochloride $w_2 = 0.620$.

B16	69420	4.8415	46801	-59.5		
B15	19330	4.2863	42229	-36.4		
B14	12800	4.1072	40653	-27.3		
B13	7198	3.8572	38542	-13.7		
B12	6290	3.7987	38076	-10.6		
B11	5537	3.7432	37643	-7.6		
B10	4110	3.6138	36583	0.17	0.000542	
B9	3760	3.5752	36211	2.98	0.000218	-22°C
B8	3135	3.4962	35595	7.76		
B7	2602	3.4153	34987	12.64		

(continued on page xx).

Run 19 (continued).

Float	R	Log R	1/T	Temp.	dV/dT	θ
B6	1874 ohms	3.2727	0.0033868	22.08		
B5	1506	3.1776	33131	28.65		
B3	1299	3.1135	32613	33.45		
B2	1198	3.0785	32383	35.62		
B1	1122	3.0500	32108	38.27		

Run 20 - Rubber Hydrochloride $w_2 = 0.652$.

B13	6091	3.7847	37963	-9.8		
B12	5152	3.7120	37379	-5.7		
B11	4733	3.6752	37094	-3.6		
B10	3401	3.5316	35871	5.60		
B9	3091	3.4901	35546	8.15		
B8	2632	3.4203	35018	12.39	0.000523	-
B7	2170	3.3365	34354	17.91		
B6	1538	3.1869	33200	28.02		
B5	1221	3.0867	32445	35.03		
B3	1047	3.0198	31940	39.91		
B2	932.0	2.9694	31560	43.68		
B1	850.0	2.9294	31255	46.77		

Run 21 - Rubber Hydrochloride $W_2 = 0.774$.

B22	1672	3.2232	33482	25.49		
B21	1220	3.0864	32348	35.96		
B20	1113	3.0464	32141	37.95		
B19	1018	3.0076	31848	40.81	0.000526	
B18	925.0	2.9661	31536	43.92		
B17	717.0	2.8555	30660	52.98		
B16	698.0	2.8439	30535	54.31		
B15	575.0	2.7597	29976	60.42		

Run 22 - Rubber Hydrochloride $W_2 = 0.774$.

B24	10580	4.0245	39904	-22.6		
B23	4633	3.6659	37023	-3.1		
B22	1994	3.2998	34097	20.10		
B21	1533	3.1855	33191	28.11		
B20	1335	3.1253	32734	32.31		
B19	1226	3.0885	32457	34.92	0.000520	
B18	1113	3.0464	32141	37.95	0.000280	5°C
B17	856.7	2.9329	31283	46.48		
B16	822.4	2.9151	31136	47.99		
B15	678.9	2.8318	30427	55.48		

Run 23 - Rubber Hydrochloride $W_2 = 0.822$.

Float	R	Log R	1/T	Temp.	dV/dT	θ
B28	3040 ohms	3.4829	0.0035490	- 8.59		
B27	2475	3.3936	34799	14.18		
B26	2049	313115	34169	19.48	0.000507	12°C
B25	1440	3.1584	32987	29.97		
B24	1299	3.1137	32615	33.43		
B23	918.4	2.9630	31513	44.15		

Run 24 - Rubber Hydrochloride $W_2 = 0.935$.

C12	1776	3.2495	33687	23.67		
C11	1751	3.2432	33636	24.12		
C10	1593	3.2022	33319	26.95		
C9	1522	3.1824	33166	28.33		
C8	1300	3.1139	32617	33.41	0.000495	-
C7	1211	3.0831	32418	35.29		
C6	1112	3.0461	32138	37.98		
C5	1088	3.0367	32069	38.65		
C4	1051	3.0216	31951	39.79		

APPENDIX 15.

Second Order Transition Temperatures of Rubber/Rubber Hydrochloride Copolymers by the Height Variation Method.

Height	R	Log R	1/T	Temp.	W_2
20.057	3404 ohms	3.5320	0.0035874	5.57	0.935
19.914	3051	3.4844	35503	8.49	
19.883	2986	3.4751	35430	9.07	
19.836	2914	3.4645	35347	9.73	
19.793	2829	3.4517	35246	10.54	
19.745	2748	3.4391	35149	11.32	
19.687	2682	3.4284	35068	11.98	
19.638	2629	3.4198	35015	12.41	
19.591	2571	3.4101	34955	12.90	
19.567	2533	3.4036	34882	13.50	
19.516	2488	3.3959	34817	14.04	
19.385	2375	3.3756	34659	15.35	
19.334	2307	3.3630	34561	16.16	
19.249	2204	3.3432	34406	17.47	
19.194	2117	3.3257	34282	18.52	
19.117	2017	3.3047	34115	19.95	

Appendix 15 (continued) $w_2 = 0.935$.

Height	R	Log R	1/T	Temp.	w_2
19.089	1979 ohms	3.2965	0.0034051	20.50	0.935
19.043	1905	3.2799	33923	21.61	
19.014	1839	3.2646	33806	22.63	
19.023	1813	3.2584	33759	23.04	
19.042	1774	3.2490	33685	23.69	
19.056	1751	3.2432	33640	24.09	
19.073	1723	3.2362	33584	24.58	
19.089	1691	3.2282	33521	25.14	
19.108	1656	3.2191	33441	25.85	
19.134	1599	3.2039	33332	26.83	
19.213	1550	3.1906	33230	27.75	
19.279	1531	3.1850	33191	28.11	
19.363	1505	3.1775	33129	28.67	

Measured θ at $w_2 = 0.935$ is 22.2°C. Run 24a

(b) Run 24b at $w_2 = 0.935$ (repeat of 24a after 24 hr.)

19.075	2203	3.3430	34405	17.48	0.935
19.058	2122	3.3267	34288	18.47	
19.053	2071	3.3162	34206	19.17	
18.975	1985	3.2978	34061	20.41	
18.965	1943	3.2885	33989	21.03	
18.953	1887	3.2758	33892	21.87	
18.940	1838	3.2644	33805	22.63	
18.936	1728	3.2375	33579	24.63	
18.950	1675	3.2240	33499	25.34	
18.973	1623	3.2104	33382	26.38	
18.987	1577	3.1979	33286	27.25	
19.025	1537	3.1867	33199	28.03	

Measured θ at $w_2 = 0.935$ is 23.6°C.

(c) Run 23a at $w_2 = 0.822$.

22.218	2850	3.4548	35272	10.33	0.822
22.064	2815	3.4495	35230	10.67	
21.896	2757	3.4404	35151	11.32	
21.742	2705	3.4322	35096	11.75	
21.610	2653	3.4237	35039	12.22	
21.495	2591	3.4135	34976	12.74	
21.400	2565	3.4091	34948	12.96	
21.367	2498	3.3976	34830	13.93	
21.250	2470	3.3927	34792	14.24	
21.218	2430	3.3856	34737	14.70	

Run 23a (continued).

Height	R	Log R	1/T	Temp.	w_2
21.197	2385 ohms	3.3775	0.0034674	15.22	0.822
21.177	2345	3.3701	34616	15.70	
21.092	2275	3.3570	34514	16.56	
20.989	2212	3.3448	34419	17.36	
20.954	2149	3.3322	34320	18.20	
20.948	2101	3.3224	34256	18.74	
20.948	2055	3.3129	34180	19.39	
20.945	1996	3.3002	34079	20.26	
20.940	1927	3.2849	33962	21.27	
20.940	1881	3.2744	33881	21.97	

APPENDIX 16.

Coefficients of Expansion of Rubber/Rubber Hydrochloride Copolymers by the Dilatometer Method.

(a) Sample A (w_2 = 0.665) - Upward run.

Temp.	Height	Temp.	Height	Temp.	Height	Temp.	Height
26.86	20.387	32.48	26.408	38.04	32.904	46.12	41.902
27.113	20.667	32.94	26.882	38.60	33.529	46.59	42.395
27.44	20.884	33.47	27.501	39.14	34.152	47.17	43.046
27.91	21.414	34.31	28.551	39.67	34.761		
29.29	22.524	34.77	29.081	42,55	38.104		
29.85	23.234	35.27	29.646	43.01	38.583		
30.37	23.846	35.84	30.277	44.15	39.753		
30.90	24.482	36.39	30.948	44.68	40.282		
31.41	25.079	36.92	31.587	45.20	40.898		
31.90	25.655	37.47	32.262	45.66	41.366		

(b) Sample A (w_2 = 0.665) - Downward run.

46.24	42.086	41.11	36.200	35.51	29.805	29.54	22.860
45.93	41.733	40.77	35.992	34.54	28.788	28.87	22.138
45.47	41.203	40.04	35.187	34.04	28.203	28.39	21.618
44.93	40.598	39.56	34.591	33.22	27.157	27.76	21.202
44.52	40.133	39.22	34.187	32.67	26.662	27.15	20.315
43.99	39.598	38.50	33.380	32.17	26.011		
43.56	39.150	37.82	32.579	31.66	25.355		
43.08	38.612	37.23	31.856	31.12	24.767		
42.27	37.681	36.71	31.312	30.68	24.220		
41.78	37.110	36.05	30.547	30.04	23.418		

(c) Sample B (w_2 = 0.875) - Upward run.

Temp.	Height	Temp.	Height	Temp.	Height	Temp.	Height
21.12	20.141	26.76	27.175	31.85	33.451	36.50	38.634
21.73	20.897	27164	28;267	32.29	34.002	37.73	39.783
22.20	21.475	28.11	28.867	32.74	34.551	38.08	40.136
23.08	22.568	28.60	29.449	33.17	35.052	38.53	40.548
23.66	23.306	29.02	30.024	33.63	35.579	38.97	40.991
24.02	23.748	29.51	30.613	33.92	35.842	39.40	41.423
24.42	24.234	29.98	31.208	34.52	36.508	39.85	41.875
24.98	24.941	30.46	31.795	35.09	37.021	40.33	42.336
25.53	25.621	30.90	32.353	35.55	37.601	40.82	42.757
26.13	26.383	31.38	32.936	35.95	38.072	41.26	43.088

(d) Sample B (w_2 = 0.875) - Downward run.

41.04	42.910	35.72	37.731	30.23	31.479	23.39	22.913
40.52	42.472	35.28	37.286	29.74	30.904	22.84	22.210
39.96	42.010	34.71	36.731	29.26	30.266	22.36	21.620
39.70	41.703	34.21	36.176	28.70	29.598	21.87	21.067
39.15	41.142	33.42	35.341	27.87	28.553	21.38	20.511
38.73	40.738	32.94	34.810	27.33	27.899		
38.29	40.302	32.48	34.331	26.39	26.800		
37.46	39.498	31.64	33.198	25.78	26.021		
36.95	38.891	31.12	32.607	25.26	25.241		
36.10	38.123	30.66	32.033	24.53	24.356		

(e) Sample C (w_2 = 0.728) - Upward run.

2.64	18.780	5.18	21.874	7.61	25.009	10.07	28.324
3.12	19.324	5.77	22.646	8.29	25.951	10.50	28.990
3.54	19.834	6.16	23.157	8.73	26.534	11.41	30.173
3.93	20.324	6.76	23.933	9.19	27.149	10.96	29.553
4.69	21.258	7.21	24.564	9.61	27.731	11.92	30.892
12.31	31.492	14.73	34.898	17.28	38.738	18.82	41.038
12.72	32.046	15.23	35.673	17.600	39.226	19.16	41.550
13.20	32.521	15.53	36.085	17.89	39.632	19.42	41.912
13.74	33.500	16.13	37.042	18.20	40.112		
14.20	34.173	16.53	37.678	18.53	40.600		

(f) Sample D (w_2 = 0.00) - Upward run.

Temp.	Height	Temp	Height	Temp.	Height	Temp.	Height
23.15	20.103	24.88	22.995	27.25	27.010	29.66	31.111
23.47	20.615	25.37	23.804	27.77	27.920	30.02	31.715
23.83	21.216	25.80	24.592	28.29	28.791	30.50	32.509
24.51	22.441	26.39	25.481	28.75	29.598	31.07	33.326
24.72	22.750	26.81	26.202	29.23	30.402	31.36	34.007
31.55	34.262	33.48	37.632				
31.92	34.811	33.91	38.251				
32.42	35.663	34.49	39.256				
32.89	36.471	34.86	39.915				
33.17	37.043						

(g) Sample E (w_2 = 0.233) - Upward run.

18.21	21.514	19.83	24.111	21.69	27.010	23.30	29.725
18.46	21.920	20.17	24.700	21.91	27.460	23.70	30.311
18.82	22.507	20.55	25.321	22.22	28.012	24.13	30.991
19.11	22.988	20.96	25.908	22.58	28.523	24.52	31.705
19.48	23.612	21.28	26.514	22.87	29.103	24.78	32.063
25.10	32.566	26.87	25.312	28.69	38.222	30.61	41.115
25.51	33.120	27.29	35.915	29.15	38.883	30.90	41.604
25.79	33.646	27.71	36.606	29.63	39.715		
26.19	34.266	28.05	37.127	29.98	40.195		
26.57	34.865	28.45	37.773	30.22	40.553		

(h) Sample F (w_2 = 0.144) - Upward run.

10.05	18.511	12.10	21.903	14.17	25.556	16.03	28.715
10.49	19.208	12.57	22.652	14.51	26.010	16.47	29.543
10.84	19.819	12.75	22.995	14.90	26.710	16.92	30.244
11.22	20.530	13.26	23.898	15.32	27.450	17.12	30.551
11.68	21.211	13.63	24.572	15.68	28.117	17.28	30.996
17.70	31.542	19.45	34.491	21.41	37.960	22.43	39.672
17.94	31.880	19.77	35.121	21.67	38.404		
18.28	32.581	20.33	36.016	21.94	38.868		
18.65	33.199	20.61	36.522	22.21	39.362		
18.98	33.688	20.99	37.215	22.39	39.595		

----------ooOoo----------

REFERENCES.

REFERENCES.

(1) Weber, Ber., 1900, 33, 779.

(2) News Edition, Ind. Eng. Chem., 1934, 12, 444.

(3) Blow, Proc. Rubber Technol. Conf., 1938, 186.

(4) Hassels, Chem. Weekblad, 1948, 37, 467.

(5) van Veersen, Proc. 2nd Rubber Technol. Conf., 1948, 87.

(6) Gordon and Taylor, J. Appl. Chem., 1953, 3, 537.

(7) Gordon and Taylor, J. Appl. Chem., 1954, 5, 62.

(8) Crampsey, Gordon, and Sharpe, J. Colloid Sci., 1954, 3, 185.

(9) Gordon and Taylor, Proc. 3rd Rubber Technol. Conf., 1954, 241.

(10) Bunn, Proc. Roy. Soc., 1942, 180, 40; 1942, 67; 1942, 82.

(11) Gordon, Proc. Roy. Soc., 1955, 228, 397.

(12) Crampsey, Gordon, and Taylor, J. C. S., 1953, 3925.

(13) Smith, J. Amer. Chem. Soc., 1948, 70, 3695.

(14) Harkins, J. Amer. Chem. Soc., 1947, 69, 1428.

(15) Bunn and Garner, J. C. S., 1942, 2, 654.

(16) Gordon and McNab, Trans. Faraday Soc., 1953, 49, 31.

(17) International Critical Tables, Vol. III, 301.

(18) Schoon and van der Bie, J. Polymer Sci., 1955, 16, 3.

(19) Gordon, Proc. Roy. Soc., 1951, 204, 569.

(20) Hill, Proc. Roy. Soc., 1928, 104, 39.

(21) Hermans, J. Colloid Sci., 1947, 2, 387.

(22) Collins, J. Colloid Sci., 1950, 5, 499.

(23) Grun, Experientia, 1947, 3, 491.

(24) Wolfenden, Ann. Reports, 1932, 29, 21.

(25) Bloomfield, J. C. S., 1944, 114.

(26) Tiemann, Ber., 1900, 33, 3710.

(27) Hielbron, Kamm, and Owens, J. C. S., 1926, 1630.

(28) Staudinger and Bondy, Annalen, 1929, 1, 468.

(29) Staudinger and Geiger, Helv. Chim. Acta, 1926, 9, 549.

(30) Staudinger and Widmer, Helv. Chim. Acta, 1926, 9, 529.

(31) Bruson, Sebrell, and Calvert, Ind. Eng. Chem., 1927, 19, 1033.

(32) Gordon, Ind. Eng. Chem., 1951, 43, 386.

(33) Fischer, Ind. Eng. Chem., 1927, 19, 1325.

(34) Fischer and McColm, Ind. Eng. Chem., 1927, 19, 1328.

(35) Farmer and Sundralingham, J. C. S., 1942, 1, 121.

(36) Evans and Polanyi, J. C. S., 1947, 1, 252.

(37) D'Ianni, Naples, Marsh, and Zarney, Ind. Eng. Chem., 1946, 27, 1171.

(38) Flory, J. Amer. Chem. Soc., 1939, 61, 1518.

(39) Papadopoulos, Thesis (Glasgow University), June 1954.

(40) Gehman and Field, J. Appl. Phys., 1944, 15, 371.

(41) Alfrey, Goldfinger, and Mark, J. Appl. Phys., 1943, 14, 700.

(42) Parks, J. Chem. Phys., 1936, 4, 459.

(43) Bekkedahl and Wood, J. Appl. Phys., 1946, 17, 362.

(44) Bekkedahl, J. Res. Nat. Bur. Stand., 1934, 13, 411.

(45) Bekkedahl, J. Res. Nat. Bur. Stand., 1935, 15, 503.

(46) Wood, Bekkedahl, and Peters, J. Res. Nat. Bur. Stand., 1939, 23, 571.

(47) Ruhemann and Simon, Z. physical Chem., 1928, 138, 1.

(48) Bekkedahl and Matheson, J. Res. Nat. Bur. Stand., 1935, 15, 503.

(49) Schallamach, Proc. Phys. Soc., 1941, 53, 214.

(50) Ueberreiter, Z. angew. Chem., 1946, 53, 247.

(51) Jenkel, Z. physical Chem., 1941, 190, 24.

(52) Tucket, Trans. Faraday Soc., 1942, 38, 310.

(53) Boyer and Spenser, "Advances in Colloid Science", Interscience, New York, 1946, 2, 2.

(54) Solomon, J. Polymer Sci., 1948, 3, 647.

(55) Wiley and Brauer, J. Polymer Sci., 1948, 3, 647.

(56) Gerke, J. Polymer Sci., 1954, 13, 295.

(57) Edgar and Hill, J. Polymer Sci., 1954, 8, 1.

(58) Coleman, J. Polymer Sci., 1954, 14, 15.

(59) Catsiff and Tobolsky, ONR Report RTL-9.

(60) Gordon and Taylor, J. Appl. Chem., 1952, 2, 493.

(61) Loshaek, J. Polymer Sci., 1955, 15, 391.

(62) Dunlop, Thesis (Glasgow University), June 1954.

(63) Gerke, private communication.